DEVELOPMENT OF A MATHEMATICAL MODEL, VUMP (VINASSE UTILIZATION FOR METHANE PRODUCTION)

by

LUCINA MÁRCIA-DE-MELLO KUUSISTO

Presented to the Faculty of the Graduate School of

The University of Texas at Arlington in Partial Fulfillment

of the Requirements

for the Degree of

DOCTOR OF PHILOSOPHY

THE UNIVERSITY OF TEXAS AT ARLINGTON

May 2013

"I Can Do All Things Through Christ Who Strengthens Me" (Philippians 4:13)

ACKNOWLEDGEMENTS

I would like to express my unending gratitude to God for His love, forgiveness and salvation.

Additionally, I would like to express my gratitude to my advisor Dr. Melanie Sattler, P.E., for her continuous guidance and support throughout the research. This research would not have been possible without her continuous technical guidance and encouragement. Furthermore, I would like to thank Dr. Victoria Chen for her prompt and intelligent help throughout the experimental design phase as well as during the modeling phase. I would also like to thank my committee members Drs. Sahadat Hossain, P.E., Andrew Hunt, Jorge Rodrigues, and Dr. Weatherton, P.E., for their academic support. I also take this opportunity to thank Dr. Max Spindler, P.E., for his intelligent engineering instruction.

I would like to extend my gratitude to Dr. Ana Peña, P.E., BCEE, and Mr. Aaron Long, P.E., for providing material used in the experiments. Additionally, I am grateful to Shammi Rahman for her politeness. I am also grateful to my friends for their friendship.

Last, but not least, I would like to thank Gary, Eric, Karin, and the other members of my family for their continuous love, patience, and support.

April 12, 2013

ABSTRACT

DEVELOPMENT OF A MATHEMATICAL MODEL, VUMP (VINASSE UTILIZATION FOR METHANE PRODUCTION)

Lucina Márcia-de-Mello Kuusisto, PhD

The University of Texas at Arlington, 2013

Supervising Professor: Melanie L. Sattler

Environmental pollution causes ongoing problems. Many countries are faced with the dilemma of finding alternative energy sources that are cost-effective and environmentally friendly. Biofuels have received much attention of late as potential alternative fuels. Although biofuels are indeed attractive energy sources, their manufacturing also brings environmental pollution. One of the most prominent biofuels is ethanol. In the US, the main feedstock for ethanol manufacturing is corn. In Brazil, as well as in some other countries, the main raw material is sugarcane. Although ethanol presents many advantages as a biofuel, including the fact that it is manufactured from renewable resources, there are several disadvantages associated with its waste disposal, including the uncontrolled disposal of 'raw' vinasse (or stillage) onto agricultural fields in some countries.

This work includes development of one treatment solution for the aforementioned problems. The main goal of this research is to develop a mathematical model for predicting methane production rates from the anaerobic digestion of ethanol vinasse. This model is named VUMP (Vinasse Utilization for Methane Production). The effects of six parameters (temperature

in the mesophilic range, COD, N, P, K, and S) on methane generation in a batch bioreactor have been studied.

Methane generation vs. time was measured, and used to develop a multiple linear regression model for predicting methane generation rate as a function of the 6 parameters. VUMP model estimates were then compared with CH_4 generation rates from actual vinasse.

TABLE OF CONTENTS

LIST OF ILLUSTRATIONS

Figure Page

LIST OF TABLES

CHAPTER 1

INTRODUCTION

1.1 Biofuels

Environmental pollution causes ongoing problems. Many countries are faced with the dilemma of finding alternative energy sources with reduced environmental impact. Biofuels are one potential solution. According to Earley et al (2009), the ethanol and biodiesel production increased from about 4.8 billion gallons in 2000 to about 21 billion gallons in 2008, in the world.

Biofuels are obtained from several feedstocks through different technologies. Currently, the primary feedstocks fall into three main categories of agricultural crops:

1. Sugar crops, including sugar cane, sugar beets, and sweet sorghum;
2. Starch crops, including corn, wheat, barley, cassava, and milo (grain sorghum);
3. Oil seed crops, including rapeseed, canola, soybean, sunflower, and mustard.

Current emphasis is on advanced biofuels, which are high-energy liquid fuels made from non-feed, non-food feed stocks that can be sustainably grown. One of the best examples of this is a biofuel made from cellulose or plant fiber. Grasses, fast growing trees and even algae are being dedicated as energy crops with the idea of using them for fuel. More thorough studies are needed on the economic and environmental effects of producing these fuels in a commercial scale.

Currently, the main biofuels being produced at a commercial scale are:

- Corn-based, cane-based ethanol, and cellulose-based ethanol;
- Biodiesel;
- Biobutanol;
- Biogas.

Typically, when used for transportation, biofuels are blended into conventional fuel sources, such as gasoline and petroleum diesel.

Advantages of biofuels include the following:

- Made from renewable resources,
- Biodegradable,
- Produced from domestic feedstocks, and thus able to help countries reduce dependence on foreign petroleum,
- Potentially lower life-cycle emissions of traditional air pollutants,
- Potentially lower life-cycle emissions of greenhouse gases.

Theoretically, an energy source with “zero-carbon” because many potential feedstocks, such as grasses and trees, store carbon in the soil and root systems. However, U.S. biofuel production depends on fossil fuel, which releases greenhouse gases, during several phases and operations, including:

- When fertilizers and pesticides are manufactured, transported, and applied;
- Running farm and refineries machinery;
- Transporting biofuels;
- Using biofuel blends with conventional gasoline and petroleum.

Other environmental concerns include: changing land use for feedstock cultivation, water supply demands, soil erosion, wildlife habitat and watershed misuse.

Currently, in the US, many policies promote the production and use of biofuels. According to Earley et al. (2009), the revised Renewable Fuel Standard (RFS) promotes blending of biofuels in conventional motor fuels. The RFS supports the production of 36 billion gallons of biofuels per year, derived from a mixture of conventional biofuels as well as second generation biofuels, by 2022. The RFS requires that the biofuels meet greenhouse gas reduction targets. When compare to fossil fuels the following life-cycle emissions reductions must be achieved: > 20% for corn ethanol; 50% for biodiesel and advanced biofuels; >60% for

cellulosic biofuels. Nevertheless, in view of the fact that the current capacity of the U.S. ethanol plants is approximately 12 billion gallons per year, another target of 15 billion gallons of renewable fuels to be produced by 2015 will probably be met mainly by corn ethanol from "grandfathered" industries, without much of the required emissions reductions (Earley et al, 2009).

1.2 Vinasse: Liquid Waste from Ethanol Production

A prominent biofuel in the world is ethanol. In the US, the main feedstock for ethanol manufacturing is corn. In Brazil, as well as in some other countries, the main raw material is sugarcane. Although ethanol presents many advantages as biofuel, there are several disadvantages with its production and waste disposal, including the uncontrolled disposal of 'raw' vinasse onto the agricultural fields.

Vinasse is the effluent from the distillation columns of ethanol industries. Vinasse is also known as mosto, stillage, thin stillage, distillery wastewater, distillery spent wash, and distillery slops. The production of ethanol from biomass, whether from sugar crops (sugar beets, sugar cane, molasses, etc.), starch crops (corn, wheat, rice, cassava, etc.), dairy products (whey) or cellulosic materials (crop residues, herbaceous energy crops, bagasse, wood, or municipal solid waste), results in the production of vinasse (A.C. Wilkie et al., 2000). Almeida (1952) described vinasse as an organic liquid residue comprised of about 93% water, 5% organic matter (mainly unfermented sugars and other carbohydrates) and about 2% of inorganic dissolved solids. Vinasse is a viscous dark brown acidic liquid. Its pH is about 4.8, its temperature is about 107 ºC and its smell goes from astringent to nauseating (Silva et al., 1981). Its BOD is high, ranging from 30 to 40 g/L (Polack et al., 1981), which is associated with the putrefaction process that takes place as soon as it is discharged, releasing foul gases that make its environment unbearable (Nadir et al., 1977). According to Glória (1975), some of these characteristics are related to the high content of residual sugar. Another problem with vinasse is its high water content (Goldemberg et al., 1980). Typically, an ethanol distillery produces 12 liters of vinasse

per liter of ethanol. Its solids content vary between 2 and 7%, if derived from sugarcane juice (Cortez and Pérez, 1997). Table 1.1 presents physical/chemical characteristics of Brazilian vinasse from ethanol produced from different feedstocks**.** Table 1.2 compares percent weight composition of vinasse from different countries.

Table 1.1 Brazilian Vinasse Characteristics Resulting from Different Types of Broth

Parameter	**Units**	**Molasses**	**Cane juice**	**Mixture of molasses and juice**
pH	-	4.2-5.0	3.7-4.6	4.4-4.6
COD	g O_2/L	65	15.00-33.00	45
Total solids	g/L	81.5	23.7	52.7
Volatiles solids	g/L	60	20	40
Fixed solids	g/L	21.5	3.7	12.7
Nitrogen	g N/L	0.45-1.60	0.15-0.70	0.48-0.71
Phosphorous	g P_2O_5/L	0.10-0.29	0.01-0.21	0.01-0.20
Potassium	g K_2O/L	3.74-7.83	1.20-2.10	3.34-4.60
Calcium	g CaO/L	0.45-5.18	0.13-1.54	1.33-4.57
Magnesium	g MgO/L	0.42-1.52	0.20-0.49	0.58-0.70
Sulphates	g SO_4/L	6.4	0.60-0.76	3.70-3.73
Carbon	g C/L	11.20-22.9	5.70-13.40	8.70-12.10
C/N ratio	-	16.00-16.27	19.70-21.07	16.40-16.43
Organic Matter	g/L	63.4	19.5	38
Reducing sugars	g/L	9.5	7.9	8.3

Source: Camhi, 1979

Table 1.2 Comparative Vinasse Composition for Different Countries (% weight)

Vinasse Origin	Source	Composition, wt %						Total Solids	Organic Solids
		K	P	N	Ca	Mg	Ash	%	%
Brazil	Molasses	0.48	0.01	0.04	0.07	0.02	1.95	46.47	4.63
Brazil	Juice	0.17	0.007	0.01	0.04	0.01	1.5	6.69	5.14
Australia	Molasses	0.86	0.002	0.31	0.11	0.15	3.2	n.a.	n.a.
Australia	Molasses	1.05	0.012	0.18	0.2	0.13	n.a.	9	n.a.
India	Molasses	0.4-1.2	0.5-1.5	0.1-0.12	n.a.	n.a.	n.a.	8-Jun	n.a.
Louisiana	Molasses	0.89	0.0001	0.015	0.014	0.006	5	n.a.	n.a.

Source: Cortez, L. et al., 1997, extracted from Polack et al., 1981

Vinasse contains potassium, traces of calcium and magnesium, which are among the main elements needed in fertilizers (Glória, 1975). Australia, Brazil and other countries have been applying untreated vinasse to fertilize sugarcane fields for many years (Korndorfer and Anderson, 1997). According to Turner et al. (2002), the irrigation of sugarcane fields with vinasse started in the 1920s. However, using vinasse for fertilizer generates water quality problems, due to its high COD, low pH, and high concentrations of various constituents. A better way of treating and disposing vinasse is needed.

1.3 Research Purpose and Significance

Nowdays, solutions that convert industrial waste into products are important opportunities for recycling valuable substances and generating energy, as well as combating environmental pollution. This work presents a mathematical model for predicting methane production rates (*k* values) from the anaerobic digestion used to decrease the high organic content of vinasse. This model is named VUMP (Vinasse Utilization for Methane Production). The effects of six parameters (temperature, COD, N, P, K, and S) on methane generation in a batch bioreactor have been studied. Methane generation vs. time has been measured, and used to develop a multiple linear regression model for predicting methane generation as a function of the 6 parameters. Many researchers have developed *k* values for solid waste decay, but none for vinasse decomposition. Therefore, studies for estimating *k* values from the

anaerobic digestion of vinasse are needed, particularly as function of composition and temperature.

This research has the potential for broad impacts in many countries because it promotes treatment of vinasse, instead of disposed '*in natura'* [as is] on agricultural fields. The model enables methane generation to be estimated from a variety of vinasse compositions. It will be the first such widely applicable model, to our knowledge.

CHAPTER 2

LITERATURE REVIEW

2.1 Ethanol Production

Although there are some differences in the processing of sugar, starch and lingo-cellulosic feedstocks for ethanol production, many process aspects are the same (Wilkie et al., 2000). As mentioned above, in Brazil, a major sugarcane-based ethanol producing country, the prevalent practice of uncontrolled disposal of 'raw' vinasse onto the agricultural fields is widespread. The statistics data show that the sugarcane industry represents roughly 22% of the total agricultural production in Brazil. Carvalho-Assan (2006) reported that, in 2003, the revenue generated by this type of industry was about US$ 2.4 billion. Currently, Brazil produces 200 billions of liters of alcohol per harvest. Current plans from the Brazilian Energy Ministry predict an increase of ethanol production. Barros de Mello (2008), commercial director of a prominent Brazilian Industry (COSAN), has stated recently that the production of ethanol in Brazil is expected to increase to 35 million cubic meters of ethanol per year by 2013. These figures reveal that there is an emerging necessity to increase the alternatives of treatment available for vinasse.

The juice (and sometimes molasses) is diluted, sent to fermentation tanks, and then inoculated with cream of yeast, in order to promote the fermentation process. The yeast decomposes the disaccharides and then the monosaccharides into alcohol and carbon dioxide. Sugar (sucrose) is transformed into alcohol, according to the Gay-Lussac simplified reaction:

$$C_{12}H_{22}O_{11} + H_2O \rightarrow C_6H_{12}O_6 + C_6H_{12}O_6$$

$$C_6H_{12}O_6 \rightarrow 2CO_2 + 2CH_3CH_2OH + 23.5 \text{ kcal}$$

The generation of carbon dioxide is substantial. This is an exothermic reaction and secondary products are also formed such as higher alcohols, glycerol, and aldehydes.

2.2 Wastewater from Ethanol Production

The sugar mills and the alcohol distilleries use an enormous amount of water in their processes. The classification of the wastewater from these industries is as follows:

- First Group: The wastewater in this group is derived from the washing of the sugarcane as it arrives from the fields;
- Second Group: This industrial effluent is also called vinasse. This wastewater is derived from the distillation process. The vinasse is the effluent of main concern because of its overall physical, chemical and biological characteristics, as well as because of its enormous volume generated. Each liter of alcohol generates about 13 L of vinasse.
- Third Group: This group contains the wastewater derived from the other sources of effluent throughout the industry, such as the effluent generated from the evaporators; from the barometric columns; from the washing of equipment and floor; from the refrigeration processes; from the discharge of caldrons.

2.3 Characterization of Vinasse

Many researchers have studied the characteristics, in terms of its organic strength and nutrient content, of vinasse generated from several types of ethanol-producing feedstocks. Table 2.1 presents the characterization of vinasse from sugar beet molasses feedstocks. Table 2.2 presents the characterization of vinasse from sugar cane juice and mixed cane juice/cane molasses feedstocks. Table 2.3 presents the characterization of vinasse from cane molasses feedstocks. Table 2.4 presents the characterization of vinasse from other sugar and starch feedstocks. Table 2.5 presents the characterization of vinasse from cellulosic feedstocks. Table 2.6 presents a summary of the data published by the year 2000.

Table 2.1 Vinasse Characterization for Sugar Beet Molasses Feedstocks (values are calculated from data in literature sources)[a]

Feedstock	Vinasse yield, L/L etOH	BOD (COD, g/L)	N total, mg/L	P total, mg/L	K, mg/L	Total S as SO4, mg/L	pH	References
Beet molasses	11.8	27.5 (55.5)	4750	Nd	5560	3500	4.3	Vlissidis and Zouboulis (1993)
Beet molasses	Nd	Nd (115.8)	56	175	Nd	1042	6.69	Boopathy and Tilche (1991)
Beet molasses	Nd	69.3 (147)	2700	222	14500	5800	5.5	Basu (1975)
Beet molasses	11.8	Nd (72)	7340	91	Nd	4520	Nd	Vlyssides et al. (1997)
Fresh beets + Molasses	11.3	38 (65)	3000	Nd	Nd	Nd	4.9	Holmes and Sane (1986)

[a] Nd = no data

Source: Wilkie et al., 2000

Table 2.2 Vinasse Characterization for Sugar Cane Juice and Mixed Cane Juice/Cane Molasses Feedstocks (values are calculated from data in literature sources)[a]

Feedstock	Vinasse yield, L/L etOH	BOD (COD, g/L)	N total, mg/L	P total, mg/L	K, mg/L	Total S as SO4, mg/L	pH	References
Cane juice	20	12 (25)	400	200	800	Nd	3.5	van Haandel and Catunda (1994)
Cane juice	Nd	15 (22)	400	58	Nd	400	3.5	Driessen et al. (1994)
Cane juice	Nd	16.5 (33)	700	91	1742	760	3.7-4.6	Costa et al. (1986)
Cane juice	Nd	20 (Nd)	Nd	Nd	Nd	Nd	3.7-5.9	Barnes and Halbert, (1979) Willington and Marten (1982)
Cane juice	Nd	20 (Nd)	1190	329	2100	1470	3.9	Callander and Barford (1983)
Cane juice + Molasses	Nd	19.8 (45)	710	87	3817	3730	4.4-4.6	Costa et al. (1986)
Cane juice + Molasses	12.5	Nd (31.5)	370	24	420	420	3.9	Souza et al. (1992)

[a] Nd = no data

Source: Wilkie et al., 2000

Table 2.3 Vinasse Characterization for Cane Molasses Feedstocks (values are calculated from data in literature sources)[a]

Feedstock	Vinasse yield, L/L etOH	BOD (COD, g/L)	N total, mg/L	P total, mg/L	K, mg/L	Total S as SO4, mg/L	pH	References
Cane molasses	Nd	25 (65)	1610	127	6497	6400	4.2-5.0	Costa et al. (1986)
Cane molasses	16	25.8 (48)	820	157	Nd	Nd	4.4	de Menezes (1989)
Cane molasses	Nd	27 (88)	2000	Nd	Nd	4000	4.3-4.6	Shrihari and Tare (1989)
Cane molasses	Nd	30 (120)	1600	61	1920	4600	4.1	Harada et al. (1996)
Cane molasses	Nd	32 (Nd)	205	6.8	Nd	Nd	4.6	Sahai et al. (1983)
Cane molasses	Nd	35.7 (77.7)	1780	168	8904	4360	4.2	Sheehan and Greenfield (1980)
Cane molasses	13-15	39 (100)	1030	33	7000	9500	3.4-4.5	Driessen et al. (1994)
Cane molasses	Nd	40 (Nd)	345	38.8	Nd	69.5	4.4	Srivastava and Sahai (1985)
Cane molasses	Nd	40 (80)	Nd	45	4013	Nd	4.5-5.0	Silverio et al. (1986)
Cane molasses	12	45 (113)	Nd	Nd	Nd	Nd	4.8	Barnes and Halbert, Willington and Marten (1979)
Cane molasses	12	45 (130)	1000	130	Nd	Nd	4.5	Yeoh (1997)
Cane molasses	Nd	48 (Nd)	382	10.4	Nd	67	4.1	Sahai et al. (1985)
Cane molasses	15	50 (108)	Nd	Nd	8298	4700	4.5	Lele et al. (1989)
Cane molasses	20	60 (130)	2500	200	Nd	3000	4.8	Halbert and Barnes (1998)
Cane molasses	Nd	60 (98)	1200	1500	1200	5000	3.8-4.4	Goyal et al. (1996)
Cane molasses	Nd	Nd (68.9)	Nd	Nd	4484	1640	4.72	Espinosa et al. (1995)

Table 2.3-Continued

Cane molasses	10	Nd (75)	975	20	Nd	Nd	4.4	Garcia Garcia et al. (1985)
Cane molasses	Nd	Nd (100)	2500	300	1750	700	4.6-5.1	Sanchez Riera et al. (1985)
Cane molasses	13	Nd (22.5)	1192	247	Nd	Nd	5.2	Cho (1983)
Cane molasses	Nd	27.5 (65)	750	Nd	10370	Nd	4.2-4.5	Sen and Bhaskaran (1962)
Cane molasses	Nd	41 (118)	1135	Nd	5070	4200	3.5-3.7	Damodara Rao and Viraraghavan (1985)
Cane molasses	Nd	Nd (24.6)	812	29	1980	607	4.17	Casarini et al. (1987)
Cane molasses (rum)	Nd	42 (105)	1450	100	Nd	4000	4.0-5.0	Szendrey (1983), Szendrey (1983) and Dorion (1984)
Cane molasses, (stored)	Nd	27.5 (64.0)	1300	Nd	Nd	2800	4.5-5.5	de Bazua et al. (1991)
Cane molasses	Nd	Nd (66)	Nd	Nd	Nd	Nd	4.5	Calzada et al. (1991)

[a] Nd = no data.

Source: Wilkie et al., 2000

Table 2.4 Vinasse Characterization for Other Sugar and Starch Feedstocks (values are calculated from data in literature sources)[a]

Feedstock	Vinasse yield, L/L etOH	BOD (COD, g/L)	N total, mg/L	P total, mg/L	K, mg/L	Total S as SO4, mg/L	pH	References
Agave tequilana (tequila)	10	Nd (66.3)	Nd	Nd	290	880	3.4	Ilangovan et al. (1997)
Apple/pear	Nd	22 (48.9)	380	62	Nd	Nd	3.4	Robertiello (1982)
Banana	Nd	Nd (53.7)	1530	150	3830	Nd	Nd	Hammond et al. (1996)
Barley spirits (shochu)	1.5	83 (97)	6000	Nd	Nd	Nd	3.7-4.1	Kitamura et al. (1996)
Barley and sweet potato	Nd	Nd (29.5)	Nd	9.1	Nd	1370	4.2	Shin et al. (1992)
Cassava	16	31.4 (81.1)	650	124	Nd	Nd	3.5	de Menezes (1989)
Cherry (morello)	Nd	Nd (80.0)	Nd	Nd	Nd	34	3.5-4.0	Stadlbauer et al. (1992)
Cherry/raspberry	Nd	Nd (60)	Nd	Nd	Nd	1975	2.7-2.9	Stadlbauer et al. (1992)
Corn (thin stillage)	Nd	26.9 (64.5)	755	1170	Nd	Nd	3.3-4.0	Ganapathi (1984)
Corn (thin stillage)	Nd	43.1 (59.4)	546	228	Nd	299	Nd	Dahab and Young (1981)
Figs	Nd	20.4 (35.4)	880	170	Nd	900	3.6	Vlissidis and Zouboulis (1993)
Grapes (cognac)	Nd	Nd (26)	Nd	Nd	800	Nd	3.0-3.2	Henry et al. (1988)
Grapes (wine)	Nd	Nd (30)	450	65	Nd	250	3.5-4	Driessen et al. (1994)
Pear	Nd	Nd (47.5)	Nd	Nd	Nd	157	3.4-3.8	Stadlbauer et al. (1992)
Grapes (wine)	Nd	Nd (40)	Nd	130	Nd	Nd	3.8	Borja et al. (1993)

Table 2.4-Continued

Grapes (wine)	Nd	16.3 (27.5)	650	Nd	Nd	120	4.2	Vlissidis and Zouboulis (1993)
Potato	Nd	Nd (52.0)	2100	Nd	Nd	Nd	4.8	Temper et al. (1985)
Potato	Nd	Nd (39.0)	1000	430	4000	Nd	Nd	Wulfert and Weiland (1985)
Milo (thin stillage)	Nd	34.9 (75.7)	Nd	1280	Nd	Nd	2.5-4.0	Stover et al, (1984) Ganapathi (1984)
Milo (thin stillage)	Nd	40.4 (45.5)	Nd	Nd	Nd	Nd	4.1	Hunter (1988)
Raisins	Nd	30 (57.5)	750	220	Nd	480	3.2	Vlissidis and Zouboulis (1993)
Raisins (raki)	Nd	Nd (14.0)	250	50	Nd	Nd	3.9	Eremektar et al. (1999)
Raspberry	Nd	Nd (70.0)	Nd	Nd	Nd	37	2.9-3.8	Stadlbauer et al.(1992)
Rice spirits (shochu)	Nd	25 (50.9)	Nd	129	Nd	Nd	3.5	Yang and Tung, Yang (1996)
Rice spirits (shochu)	1.5	84 (Nd)	Nd	389	Nd	Nd	4.26	Kida et al. (1995)
Sweet sorghum	16	46.0 (79.9)	800	1990	Nd	Nd	4.5	de Menezes (1989)
Wheat (shochu)	Nd	25.9 (50.1)	1500	170	Nd	Nd	4.6	Nagano et al. (1992)
Whey	1.7	5.4 (Nd)	Nd	Nd	Nd	Nd	Nd	Barry (1982)
Whey	Nd (0.21 L/kg Feddstock)	15 (Nd)	Nd	Nd	Nd	Nd	Nd	Singh et al. (1983)

[a] Nd=no data.

Source: A.C. Wilkie et al., 2000

Table 2.5 Vinasse Characterization for Cellulosic Feedstocks (values are calculated from data in literature sources)[a]

Feedstock	Vinasse yield, L/L etOH	BOD (COD, g/L)	N total, mg/L	P total, mg/L	K, mg/L	Total S as SO4, mg/L	pH	References
Eucalyptus/DA	Nd	Nd (22.5)	200	40	Nd	260-360	5.8-6.3	Good et al. (1982)
Hardwood/TS-DA	Nd	Nd (19.1)	2800	74	Nd	900	Nd	Strickland et al. (1986)
Hardwood (willow)/ SE-Enz	Nd	19.8 (33.3)	Nd	Nd	Nd	Nd	Nd	Larsson et al. (1997)
Mixed (herbaceous)/ nd	Nd	56.2 (140)	Nd	Nd	Nd	60.2	Nd	CH2M Hill[b] (1991)
Mixed (biomass)/nd	Nd	46.8 (119)	Nd	Nd	Nd	61.7	Nd	CH2M Hill[b] (1991)
Mixed (softwood)/nd	Nd	26.7 (72.0)	Nd	Nd	Nd	58.9	Nd	CH2M Hill[b] (1991)
MSW/TS-DA-SF	Nd	32.1 (72.0)	140	Nd	Nd	Nd	5.5	Broder (1999)
MSW/Nd	Nd	20.9 (61)	Nd	Nd	Nd	599	Nd	Larsson et al. (1997)
Pinus radiata/DA-SF	16.7	13.2 (25.5)	95.3	10.3	38.5	600	4.5-5.0	LFTB (1985), Callander et al. (1986)
RDF/CA	Nd	37.7 (104)	13760	14	Nd	Nd	5	Broder (1999)
RDF/DA	Nd	31.1 (110)	2100	0.68	Nd	Nd	5.9	Broder (1999)
RDF/TS-DA-SF	Nd	Nd (38.1)	Nd	Nd	Nd	Nd	5.5	Broder and Henson (1993)
RDF/Nd	6.7	6.5 (Nd)	Nd	Nd	Nd	Nd	Nd	DiNovo et al.
Softwood (spruce and pine)/SE-Enz	Nd	12.8 (26.5)	Nd	Nd	Nd	Nd	Nd	Larsson et al. (1997)

Table 2.5 - Continued

Timothy grass/AFEX	15-Jun	Nd (26)	1100	Nd	Nd	Nd	Nd	Belkacemi et al. (1997)

[a] Nd = no data; AFEX=Ammonia freeze explosion; CA=Concentrated acid; DA=Dilute acid; MSW=Municipal solid waste;
RDF = Refuse derived fuel; SE=Steam explosion; SE-Enz=Steam explosion and enzymatic hydrolysis; SF=Saccharomyces fermentation; TS=Two stage.
[b] CH2M HILL (1991) values are predicted estimates.
Source: A.C. Wilkie et al., 2000

Table 2.6 Summary of Vinasse Characterization for Beet Molasses, Cane Juice, Cane Molasses, and Cellulosic Feedstocks[a]

Feedstock	Vinasse Yield L/L etOH	BOD g/L	COD g/L	COD/ BOD	N, Total, mg/L	P, Total, mg/L	K, mg/L	Total S as SO_4, mg/L	pH
Beet molasses									
Avg.	11.6	44.9	1.95	3569	163	10030	3716	5.35	5.35
Std. dev.	0.3	21.7	0.21	2694	66	6322	2015	1.02	1.02
n	3	3	5	3	5	3	2	4	4
Cane Juice									
Avg.	16.3	16.7	30.4	1.96	628	130	1952	1356	4.04
Std. dev.	5.3	3.4	8.2	0.35	316	110	1151	1396	0.49
n	2	5	6	4	6	6	5	5	7
Cane molasses									
Avg.	14	39	84.9	2.49	1229	187	5124	3478	4.46
Std. dev.	3.3	10.8	30.6	0.57	639	350	3102	2517	0.35
n	7	19	22	16	20	17	12	16	25
Cellulosic									
Avg.	11.1	27.6	61.3	2.49	2787	28	39	651	5.35
Std. dev.	4.14	15.2	40	0.54	4554	30	nd	122	0.53
n	4	11	15	10	8	5	1	6	7

[a]Nd = no data; std dev = standard deviation; n = number of literature values used.
Source: A.C. Wilkie et al., 2000

2.4 Treatment Alternatives for Vinasse

In order to choose an appropriate wastewater treatment method, one must consider whether the wastewater is domestic or industrial. For industrial wastewater, one must consider what type of industry generates the wastewater. Other considerations should be determined, such as the quality and quantity of the wastewater being discharged, the geographic and climatic conditions of the location, as well as the cost-benefit evaluation. In addition, the designer needs to determine the quality of the water body in the vicinity that will be receiving the treated wastewater, as well as the final purpose that the treated wastewater or sludge would serve. Moreover, the environmental rules and regulations need to be applied for designing purposes.

Generally, the following wastewater treatment methods are utilized: physical; physicochemical; and biological methods. Alpina (2005) lists the main levels of wastewater treatment as:

- Primary: Removal of large material, floating material and the sediment.
- Secondary: Degradation of the carbonic compounds and removal of the biological sludge.
- Tertiary: Removal of nutrients, of non-biodegradable material, and of the sludge, followed by disinfection.

Luksenberg et al. (1980) presented the following alternatives for treating vinasse: physicochemical treatment; reverse osmosis; evaporation; incineration; industrial recycling; wetlands; stabilization lagoons; trickling filters; manufacturing of biomass; anaerobic digestion; irrigation of sugarcane fields. Other vinasse treatment studies include: aerobic processes in ponds (Springer & Goissis, 1988); wetlands (Kerner & Rochard, 2004); sequential batch with activated sludge (Torrijos & Moleta, 1997).

Wilkie et al. (2000) presented a thorough review of different types of vinasse treatment, which included:

(1) Physical/mechanical separation: Removal and recovery of suspended solids containing yeast and other materials. This option is widely used in the United States for the corn-based vinasse. The separated solids are dried and sold as animal feed, known as dried distillers grains (DDG). However, this process is not feasible for sugar crops and cellulosic crops due to the high water content in the vinasse generated by these crops. Other types of treatment technologies may be applied, following the physical separation, such as evaporation and/or membrane separation, anaerobic digestion, and single cell protein production.

(2) Evaporation and membrane separation: The stillage is concentrated in multi-effect evaporators. However, the amount of energy required to evaporate the stillage (equivalent to 10% of the energy content of the ethanol) is a major disadvantage of this process. The concentration of vinasse may also be accomplished by membrane separation. Permeate is

recovered for recycling in cooking and mashing. However, membrane fouling is a major disadvantage of this process. Additionally, organic compounds with low molecular weight pass through the membranes, thus decreasing the potential for 100% water recycling in the ethanol production process.

(3) Single cell protein: In the single cell protein production, a second aerobic culture is employed to remove residual sugars and soluble proteins and lower the COD and nutrient content. According to Srivastave (2008), the advantages of this method include: the microorganisms multiply at a high rate, the dry mass has a high protein content, less area is needed for this type of technology, carbon sources can be found in a variety of raw materials, and it does not depend on weather conditions. The main disadvantage of this method is its high cost.

(4) Algae as well as other bioproducts production: The production of algae for nitrogen and phosphorus removal in surface water resources has been studied. Furthermore, studies have been made on the utilization of vinasse to produce practical biological products, such as enzymes, chitosan, astaxanthin, plant hormones and the biopolymers, alternan and pullulan. The main advantage of algae production includes the fact that algae requires carbon dioxide to grow, thus contributing to lower CO_2 levels in its surroundings. On the other hand, from the life cycle analysis point of view, the production of algae requires more energy and water than other biofuel sources. In addition, the production of algae requires the utilization of fertilizer, thus contributing to the eutrophication of lakes and other water systems by the fertilizer-contaminated runoff.

(5) Calcium magnesium acetate production: Vinasse may also be utilized to produce organic acids. Calcium magnesium acetate (CMA), as well as potassium acetate, may be used for deicing roads and bridges, during the winter in North America, as they are less corrosive and produce less environmental damage than sodium chloride (NaCl). CMA may be produced through the fermentation of carbohydrates by *Clostridium thermoaceticum.* The precipitation

and recovery of the organic acids are the subsequent stages. Acetic acid is one of the main products.

(6) Color removal: There are several physico-chemical and biological processes for color removal from wastewater. The traditional coagulation and flocculation process is a convenient and easy method. Typically, the coagulants are salts of a strong acid and a weak base. Typically, $Al_2(OH)_3$ is the base utilized. The main disadvantage is the fact that, according to Souza et al (2013), recent studies have reported a correlation between the onset of Alzheimer's disease and the utilization of aluminum salts in water treatment.

(7) Thermal and electrochemical processes: Research on the use of thermal direct wet air oxidation of vinasse followed by char recovery and incineration for steam production has shown to recover more energy than vinasse evaporation followed by syrup incineration. In addition, research has shown that the supercritical water oxidation of vinasse, using H_2O_2 at elevated temperatures of 673±773 K, results in a rapid reduction of organic strength. Another process researched was the electrochemical treatment of vinasse using NaCl. This treatment resulted in chlorine and other oxidants production, which destructively oxidized the COD. However, at this time, these processes are not considered economical treatment methods for vinasse.

(8) Anaerobic treatment of vinasse: This process is the subject of this research will be discussed in more detail in another section.

Pérez et al. (1998) investigated and developed the basic technology of on-site disposal of vinasse by combustion. His research consisted of determining heating values, composition, and flame characteristics through combustion tests. Initially, he used only vinasse with different solid concentrations and, later, he used emulsions of vinasse and #6-fuel oil. He stated that the purpose of his research was to evaluate the technical feasibility of vinasse combustion via atomization. He derived his conclusions from two different perspectives: (1) Rheological; and (2) Combustion. (1) From the rheological perspective, he stated that for both categories of his trials, i.e., the vinasse by itself and the emulsions of vinasse combined with #6-fuel oil, had rheological

behavior close to the #6-fuel oil alone, when tested in the Brookfield Rotary Viscometer. After the right temperature and shear rate were obtained, he did not have any problems obtaining atomization and combustion. He used vinasse with the solids concentration below 50% for the combustion tests. (2) From the combustion perspective, he stated that the combustion of the emulsions prepared with vinasse plus #6-fuel oil is feasible in the range from 95% of #6-fuel oil and 5% of vinasse to 50% of #6-fuel oil to 50% of vinasse. He stated that, beyond that range, the flame was unstable and not compact. He found out that the best results were obtained when 95 to 75% #6 fuel oil were used together with 5 to 25% of vinasse. The drawbacks he listed included: a) The energy needed for the vinasse pre-evaporation was quite high; b) When concentrating to up to 75% of solids, the foaming in the evaporators was another problem; c) The crystallization of salts in the syrup causes difficulties with the operation of certain appurtenances.

Goncalves (2006) performed research for the treatment of the vinasse by utilizing coagulation and flocculation and the factorial planning technique. She evaluated several variables, specially, the COD removal. Then, she developed a statistical model representing the process, neglecting the variables of less significance. The model demonstrated that the COD removal varied as a function of the pH and mixing parameters. The best results were achieved when calcium oxide and ferrous sulfate were used, with the pH values of 12.41; the removal efficiencies were 52 and 44%, respectively. She observed that the resulting sludge could be used as a fertilizer because it was rich in nutrient content. She concluded that the statistical planning technique was very useful in the evaluation of the efficiency of the COD removal, even with the simultaneous variation of more than one variable, in addition to enabling evaluation of the possible interactions among the variables. She recommended a study about the financial feasibility of that type of treatment on an industrial scale.

Fernández et al. (2001) used activated carbon and natural zeolite as support materials in their research for vinasse treatment in an anaerobic fluidized bed reactor. He stated that, in

Cuba, the vinasse is a very strong pollutant. In addition to its high organic load, it has a high content of sulfates. In his research, when he applied the anaerobic technology, most of the biodegradable organic matter turned into biogas, especially methane. The problem he had was the unwanted concentration of sulfides, which was above 1%. In his work, he developed two experiments with anaerobic fluidized bed reactors (AFBR), using raw materials easily available in Cuba as support media: (1) activated carbon and (2) natural zeolite. The purpose of his research was to achieve high removal rates for the organic matter, while maintaining the concentrations of sulfides and ammonium within the permissible ranges. In his research, the reactors were operated during 120 days. His experiment achieved an organic loading rate of 10 kg COD/m^3 day, with COD removal above 70%. The methane production was 2 L/d. He stated that the activated carbon and natural zeolite, used as support materials in the anaerobic fluidized bed reactors, showed good results for waste removal.

2.5 Anaerobic Digestion of Vinasse

In anaerobic degradation of vinasse, microorganisms are used to degrade the organic matter in the fluid in the absence of oxygen. Bacteria, rotifers, and protozoa are the main microorganisms used by this method. After digestion, the following are produced: a clearer liquid, sludge, and methane gas.

The anaerobic digestion encompasses the following stages: (i) Hydrolysis of the large molecules by the bacteria; (ii) Acidogenesis: The acidogenic bacteria convert sugars and amino acids into CO_2, H_2, NH_3, and other organic acids; (iii) The acetogenic bacteria convert carboxylic acids into simpler organic acids, acetic acid, as well as more CO_2, H_2, and NH_3. (iv) Then, the methanogen microbes produce CH_4 and more CO_2.

The following chemical reaction represents hydrolysis of a simple sugar glucose, as an example (Saikkonen, 2006):

$$2\ C_6H_{12}O_6 + H_2O \longrightarrow 2\ CH_3COOH + 2\ CO_2 + 4\ H_2$$

With the formation of acetic acid, carbon dioxide and hydrogen, methane is, then, formed by the two following pathways:

$2\ CH_3COOH \longrightarrow 2\ CH_4 + 2\ CO_2$

$4\ H_2 + CO_2 \longrightarrow CH_4 + 2\ H_2O$

Table 2.7 shows that, generally, the acetogenic biochemical reactions are thermodynamically unfavorable (ΔG0> 0) in standard conditions.

Table 2.7 Important Reactions in Anaerobic Processes

Oxidation	Reactions	Δ G_o, kJ
Propionate → acetate	$CH_3CH_2COO^- + 3H_2O \rightarrow CH_3COO^- + H^+ + HCO_3 + H_2$	76.1
Butirate → acetate	$CH_3CH_2CH_2COO^- + 2\ H_2O \rightarrow 2\ CH_3COO^- + H^+ + 2\ H_2$	48.1
Ethanol → acetate	$CH_3CH_2OH + H_2O \rightarrow CH_3COO^- + H^+ + 2\ H_2$	9.6
Acetate → methane	$CH3COO^- + H_2O \rightarrow HCO_3^- + CH_4$	-31
Reduction		
HCO_3^- → acetate	$2\ HCO_3^- + 4\ H_2 + H^+ \rightarrow CH_3COO^- + 4\ H_2O$	-104.6
HCO_3^- → methane	$HCO_3^- + 4\ H_2 + H \rightarrow CH_4 + 3\ H_2O$	-135.6

Source: EEA, 2005; Salomon, 2007

The chemical reactions, represented on Table 2.7, demonstrate the following: if the chemical species on the right side of the arrow are present in concentrations indicated by the reaction, the reaction forms chemical species on the left (reverse). As methanogenesis depends on the availability of acetate, it is important to balance the acetogenic reactions and shift the direction of the reaction to the right. This can be achieved by the continuous removal of H_2 from the reaction of electrons recipients (Salomon, 2007).

Satyawali et al. (2007) reviewed the existing status and advances of various treatment methods. He stated that anaerobic treatment was the most attractive primary treatment due to the BOD removal rate being over 80%, in addition to the energy recovery in the form of biogas.

His work focused on various: (1) biological methods, and (2) physicochemical methods such as adsorption, coagulation/precipitation, oxidation, and membrane filtration.

Ribas (2006) has stated that the anaerobic reactors have shown to be a promising alternative because they accomplish a high rate of organic load removal and produce biogas. Additionally, this type of treatment has already been tested and used in many countries to treat the effluent from alcohol industries (Ribas, 2006).

Wilkie et al. (2000) advocated the advantages of the anaerobic digestion because of its effective reduction of the organic load and because it produces biogas. He concluded that the thermophilic anaerobic digestion of the vinasse could be achieved in smaller reactors than conventional aerobic treatment, because of higher loading rates. Ahring et al. (1991) concluded that the organic load introduced to a thermophilic anaerobic reactor may be above 30 kg COD/m^3-day. In addition, anaerobic digestion produces less sludge than the conventional aerobic treatment (Speece, 1996). According to Vazzoler (1997), the thermophilic anaerobic digestion of the vinasse presents a higher rate of biogas production than mesophilic digestion. Several authors, including Wiegant et al. (1986), Souza et al. (1992), Vlissidis & Zouboulis (1993), Driessen et al. (1994), and Harada et al. (1996), have evaluated the thermophilic anaerobic digestion of the vinasse in an upflow anaerobic sludge blanket (UASB) reactor, because this type of treatment presented the best performance.

2.6 Anaerobic Reactor Designs

Anaerobic treatment uses reactors which are designed to hold the wastewater for a specific interval, the detention time. These reactors enable the composition and the concentration changes. In the United States, there are several types of anaerobic digesters being used for methane production and recovery. The most common are: plug flow, complete mix, and covered lagoons.

The plug flow digester is a flow-through tank with complete mixing perpendicular to the flow direction but theoretically no mixing in the direction of flow. Generally, the plug flow digester

is a long trough, built below ground, and the cover may be either airtight and inflatable or a hard top type. Plug-flow digesters operate within the mesophilic temperature range (35-40 °C or 95-103 °F). Usually, high-strength waste requires a hydraulic retention time (HRT) of 20 days, depending on the waste characteristics (Lusk, 1999 as referred by Saikkonen, 2006).

A complete mix digester is a tank with complete mixing that theoretically leads to uniform concentrations everywhere in the tank. The digester is designed for methane production and recovery, and connected to a separate waste storage facility.

A covered anaerobic lagoon is a lagoon with constant volume, designed for biogas production and recovery connected to a separate waste storage facility, where the total solids concentration in the influent waste is less than 2% (Wilkie, 2005 as referred by Saikkonen, 2006). The operating volume of the lagoon is designed based on the daily volatile solids (VS) loading rate per 1,000 ft^3/ day or the minimum hydraulic retention time needed for methane production, whichever is greater.

Carvalho-Assan (2006) evaluated the performance of vinasse aerobic digestion using rotating discs or bio-discs. The efficiency of COD and of BOD removal increased with time, as the thickness of the bio film increased and at a hydraulic detention time of 3.5 days. However, the bio-discs did not accomplish much in the effort of raising the pH. Another downside of the treatment with bio-discs is that the treatment showed variation in the volatile suspended solids values.

The popular upflow anaerobic sludge blanket (UASB) reactor was developed in the late seventies by Prof. Gatze Lettinga, the Wageningen University the Netherlands. This type of reactor has been used mainly for treating the wastewater from the following types of industry: sugar refining, breweries, distilleries and fermentation, food, pulp and paper. The technology of the UASB reactor is very effective and economical. This type of digester displays the following main features (Lettinga et al*.,* 1980):

(1) The upward flow regime of the wastewater at the entrance of the apparatus. The wastewater enters the tank from the base and it is directed upwards and passes through a layer of sludge.

(2) The upward motion of the gas bubbles causes additional collisions between the particles. The anaerobic biochemical reactions produce a biogas containing CH_4 and CO_2. These bubbles provide additional opportunities for the mixing of the substrate. Therefore, mechanical parts are not necessary for stirring.

(3) The higher setting velocities of the granules formed by the selected type of microorganisms. The anaerobic microorganisms promote the formation of granules. The approximate diameters of these granules are between 0.5 and 2 mm. The anaerobic microorganisms decompose the organic matter present in the wastewater.

(4) A three-phase separator, at the top of the reactor, facilitates the separation between the gas, solid, and liquid phases (gas-solids-liquid, or GSL, separator). Typically, the three-phase separator comprises of a funnel-like gas cap. The baffles inside the tank deflect the gas into the opening of the gas cap. The gas cap conveys the flow of the bio gas into a settler, right above it. The supernatant flows through the weirs.

Figure 2.1 displays a schematic diagram of an UASB reactor (Ghangrekar, 2008).

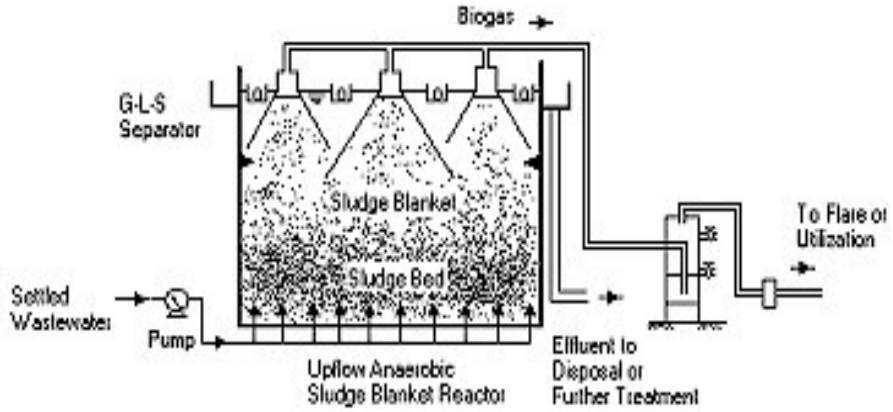

Figure 2.1 Schematic Diagram of an UASB Reactor (Ghangrekar, 2008)

The design of an UASB reactor is dependent upon the average COD concentration of the raw vinasse. Generally, for temperature between 15 and 35 degrees C, the Organic Loading Rate should be between 1.5 to 18 kg COD /(m^3 d) (Lettinga and Hulshoff, 1980). The volume of the reactor is dependent on the Organic Loading Rate (OLR) (Ghangrekar, 2008):

Volume = (Flow Rate x COD concentration) /OLR

Ghangrekar (2008) points out that the GSL separator is better designed when the Solids (microbe) Retention Time (SRT) should be between 50 to 100 days, thus facilitating the treatment with a short liquid waste Hydraulic Residence Time (HRT). Generally, the sludge blanket occupies 20 to 30% of the total volume and the GSL separator occupies 15 to 30% of the total volume. The volume of biogas produced varies in accordance to the content of biodegradable organic matter of the vinasse.

Riera et al. (1985) utilized a 100-liter-UASB reactor for the digestion of vinasse in Argentina and achieved COD removal rates above 75% and good sludge precipitation.

Driessen et al. (1994) conducted a study on the vinasse digestion using UASB, with data collected from representatives in Brazil, India, Venezuela and the Netherlands. They showed the importance of the correct choice of parameters for each type of treated effluent for different geographic locations. The rate of COD removal varied between 65 and 95%, with feeding rates up to 22 kg/m^3 day.

In 1981, the IPT (Institute for Technological Research of São Paulo, Brazil) conducted an experiment in Penedo Agro Distillery (PAISA), in Penedo, Brazil, which investigated the anaerobic digestion of vinasse at 32° C, utilizing two UASB reactors with 11 and 24 m^3. The results included an average biogas production of 13.1 liters per liter of vinasse, with 65% CH_4. In addition, with a retention time of 1.5 days, the COD removal rate accomplished was 95% (CNI, 1982). Figure 2.2 presents the framework with typical values of vinasse anaerobic digestion from an ethanol distillery producing 120,000 liters of ethanol per day.

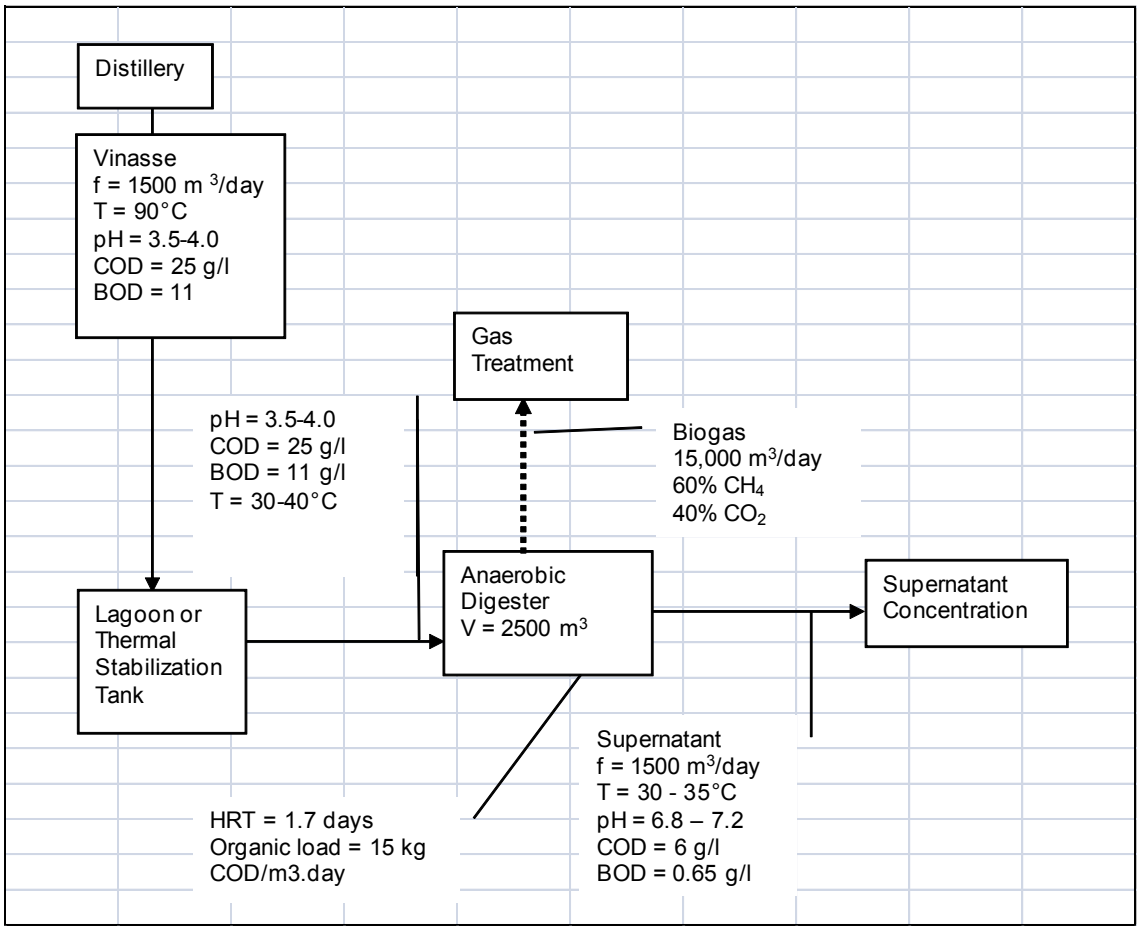

Figure 2.2 Flowchart Example of Vinasse Biodigestion on an Industrial Scale (IPT, 1990)

According to De Paula et al. (2008), the treatment capacity of the conventional UASB reactor is low and limited by the retention capacity of the anaerobic sludge inside the reactor. In order to increase the contact time of the sludge, an expansion or fluidization of the granular sludge bed has been added to the original design. This more modern concept is named Expanded Granular Sludge Bed (EGSB). De Paula et al. (2008) rationalized that the optimization of the conventional UASB reactor may be accomplished by increasing the height/diameter ratio and by recycling a portion of the treated effluent. Among the various designs of EGSB reactors, the Internal Circulation (IC) reactor is preferred. The IC reactor is based on the installation of two UASB reactors. De Paula et al. (2008) point out that the main advantage of the IC reactor is the segregation of the biogas in one of the sections inside the

reactor. Its main disadvantage is that it takes approximately one year to get the sludge acclimated with the vinasse, before treatment is applied.

2.7 Biogas Composition

Biogas consists mainly of methane (CH_4) and carbon dioxide (CO_2), smaller amounts of nitrogen (N_2), water vapor, hydrogen sulfide (H_2S) and ammonia (NH_3). Table 2.8 presents the typical biogas composition. Table 2.9 presents other relevant characteristics of the biogas. Table 2.10 presents a more detailed description of the typical biogas composition.

Table 2.8 Typical Biogas Composition in % (CENBIO, 2003)

Methane (CH_4)	Carbon Dioxide (CO_2)	Oxygen (O_2) + nitrogen (N_2)	Moisture (H_2O)
66.5%	30.5%	0.5%	2.5%

Source: Coelho *et al* (2006)

Table 2.9 Some Biogas Characteristics (CENBIO, 2003 and SABESP, 2001)

Relative Density	0.86 at 15 °C 101.325 kPa
Pressure	250 mm water column

Source: Coelho *et al* (2006)

Table 2.10 Detailed Typical Biogas Composition

Component	Typical Analysis (%)
Methane	50-60
Carbon Dioxide	38-48
Trace Components	2
Trace Components	
Moisture	
Hydrogen Sulfide (H_2S)	134 ppm or 0.01%
Hydrogen with Halo-carbons	
Volatile Organic Carbons (VOCs)	

Source: Wilson (2005), Coelho et al. (2006)

2.8 Biogas Utilization

Generally speaking, biogas may be used directly for heating or cooling, or in household appliances; used for generation of electricity; or upgraded and used as motor vehicle fuel. There

are several technologies for converting the chemical energy contained in the biogas into a useful type of energy. Internal combustion engines, including gas turbines, are the technologies most frequently used for this type of energy conversion (Coelho et al., 2006). The biogas is burned, or combined with oxygen, which releases heat energy that had been stored in the chemical bonds of the methane. The expansion of the high-temperature/high-pressure gases applies direct force to a piston, turbine blade, or nozzle, thus transforming chemical energy into useful mechanical energy. In a gas turbine, the mechanical energy of the turbine turns a generator, which produces electricity.

In order to use biogas in diesel engines, having ignition by compression, it is necessary, in addition to the mixture of air and biogas, to inject a quantity of diesel fuel to start the combustion. These motors are robust and generate greater power. In addition, these motors can operate with biogas having CO_2 concentrations of up to 45% (Pinto, 1999).

2.9 Biogas Purification

Before its utilization, it is important to treat the biogas. The degree to which the gas must be processed depends on the intended use for the biogas. Using the gas in a boiler or in an internal combustion engine requires minimal gas processing. Other applications such as using the gas to power a fuel cell or upgrading the biogas to natural gas quality require more rigorous processing (Saikkonen, 2006).

The main problems posed by the biogas impurities include:

- CO_2: inert gas that lowers the biogas calorific value. This means that biogas of a certain energy content occupies more space, which is particularly an issue in the case of motor vehicles. Anders (2005) suggests that the methane content has to be increased to at least 96–97 % for motor vehicle applications. However, some engines, such as micro-turbines, are designed to operate with CO_2 levels between 30% and 50% (Coelho et al., 2006).

- Moisture: It can compromise the proper functioning of the internal parts of the engine (nozzles, combustion chamber, turbine palettes), and reduce the biogas calorific value;
- Hydrogen sulfide (H_2S): It is corrosive and can also undermine the proper functioning of the internal parts of engines. Most anaerobic digesters produce a biogas that contains between 0.3 and 2% H_2S (Costa et al, 2001);
- Presence of air: reduces the biogas calorific value;

Typically, the purification of biogas consists of removing the majority of the contaminants, except much of CO_2, thus producing a gas with medium calorific value (4000kcal/kg to 6000 kcal / kg) that feeds some adapted equipment (CENBIO, 2000). Moisture may be removed from the biogas through coalescing filters and refrigeration dryers. Due to the H_2S affinity with iron oxide, H_2S removal may be accomplished by simply making the biogas flow through an iron sponge. Higher temperatures will increase the absorption efficiency of the hydrogen sulfide (Pinto, 1999). Another way of removing H_2S is by directing the biogas flow through an activated carbon filter (Coelho et al., 2006).

In view of the fact that CO_2 is acidic, it may be absorbed by alkaline solutions, such as calcium or sodium hydroxide, or calcium or potassium carbonate. These chemical reactions yield carbonates and bicarbonates possessing different solubility indexes. Another method for removing CO_2 is by making it flow through cool pure water, which is an ancient process that uses water as an adsorbent. Due to Henry's law, the equilibrium pressure of CO_2 dissolved in water is a direct function of temperature, i.e., the hot water holds less quantity of CO_2, compared to cold water (Nogueira, 1986).

The techniques usually employed for the purification of biogas are shown in Table 2.11.

Table 2.11 Techniques for Removal of Impurities from Biogas

Impurity	General Description	Details
Moisture	Adsorption	Silica gel Molecular Sieve Alumina
	Absorption	Ethylene glycol (temperature -6.7 ° C) Selexol
	Cooling to 2°C	
Hydrocarbons	Adsorption	Activated carbon
	Absorption	Light oil Ethylene Glycol Selexol (Temperature between -6.7° C and -33.9° C)
	Combination	Cooling with ethylene glycol and activated Carbon adsorption
CO_2 and H_2S	Absorption	Organic Solvents Selexol Fluorine Rectisol Solutions of alkali salts Potassium at high temperature Alkanolamines Mono, di - tri - ethanol amine De-glicolamina Ucarsol-CR
	Adsorption	Molecular Sieves Activated Carbon
	Membrane separation	Hollow fiber membrane
Siloxina	Adsorption	Activated Carbon

Source: Alves (2000) and CAPSTONE (2001)

2.10 Storage of Purified Biogas

The storage of purified biogas presents a major challenge: it does not liquefy at low pressure and ambient temperature. This biogas characteristic demands large reservoirs for storage. According to Pinto (1999), there are three forms of methane storage, as shown in

Table 2.12. In the first, the liquefaction is achieved cryogenically, in which methane is stored in the liquid state in thermally insulated cylinders, at a temperature of -161 ° C. Another storage method is to apply high pressure in order to compress the methane in the vessel, while still in the gaseous state. The third methane storage alternative is to maintain the methane also in the gaseous state, but adsorbed onto activated carbon. This third process is relatively simple and lower cost than the other two.

Table 2.12 Methane Storage Alternatives

Type	Storage Features			
	Pressure (atm)	Temp. (° C)	Density (kg/m^3)	Energy (kJ/L)
Liquefaction	2	161	1.0	22300
High pressure	200	ambient	6.5	9800
Adsorption	20	ambient	7.0	2640

Source: Lucas, 1990

2.11 Case Study: Biogas Production from the Anaerobic Digestion of Vinasse

In 1984, CODISTL, a manufacturer of industrial equipment, that had bought the Dutch UASB reactor technology, namely METHAX BIOPAQ, installed this type of digester at two different locations, the São Luís Sugar Mill and the St. John Distillery, in Brazil. The capacity of the St. John Distillery is 300 m^3 of alcohol per day, producing 300 million liters of vinasse. The vinasse anaerobic digestion plant remained in operation until the end of 1997. The nominal vinasse processing was 1500 m^3 /day, with an effective load of about 1000 m^3/day, 85% COD removal and mesophilic (35° C) operating temperatures. The effluent was used as fertilizer in the sugarcane fields. A gas tank was installed and collected 600 Nm^3 of biogas, which had a content of 70% methane. Then, the biogas was purified to 98% methane, compressed to 220 atm and stored in 400 Nm^3 cylinders. Table 2.13 shows results of biogas production. The average total production, considering the entire operating time, was 4274 Nm^3/day.

Table 2.13 Biogas Production from Anaerobic Digestion of Vinasse at the St. John Distillery

Harvest	Duration (days)	Biogas Production, 60% CH_4 (Nm^3)	Methane Production, 98% CH_4 (Nm^3)	Avg. Methane Production, CH_4 (Nm^3/day)
86/87	197	319282	234704	1191
87/88	197	918514	593544	3012
88/89	169	1112453	687274	4067
89/90	176	1032683	656374	3729
90/91	213	1751904	1035200	4860
91/92	196	1848320	1126181	5743
92/93	207	2371946	1488396	7190
93/94	186	1778486	1085053	5834
94/95	204	1228496	804665	3944
95/96	147	514798	337502	2296

Source: Barbeli, 1998

2.12 Novel Research: Methane Generation Rates from Vinasse

Many researchers have developed *k* values for solid waste decay, but none for vinasse decomposition. Therefore, studies for estimating *k* values for the anaerobic digestion of vinasse are needed, particularly as function of composition and temperature.

CHAPTER 3

MATERIALS AND METHODS

3.1 Introduction

The main purpose of this research was to develop a model, VUMP (Vinasse Utilization for Methane Production), for predicting methane generation rates from ethanol-distillery vinasse. The methodology for this research encompassed the following steps:

Step #1: Vinasse composition experimental design development to study the effect of Chemical Oxygen Demand (COD), nitrogen (N), phosphorus (P), potassium (K), sulfur (S), and temperature on methane generation.

Step #2: Setting up laboratory-scale bioreactors.

This stage encompassed selecting the bioreactors with their fitted appurtenances, designing and setting up air tight laboratory-scale bioreactors, connected to gas collecting devices.

Step #3: Operating and monitoring laboratory-scale bioreactors. This stage included the preparation of various batches, each batch having a different vinasse composition/temperature combination, and measuring parameters such as biogas volume, percentage of methane (CH_4), carbon dioxide (CO_2) and oxygen (O_2) in the biogas.

Step #4: Analysis and Development of the VUMP model. A comprehensive multiple linear regression (MLR) model was developed to predict first-order methane generation rate constants as functions of temperature and vinasse composition i.e., COD, N, P, K, and S.

3.2. Vinasse Composition Experimental Design Development and Preparation

The primary vinasse constituents of environmental interest are Chemical Oxygen Demand, nitrogen, phosphorous, potassium, and sulfate. All are present at substantial concentrations in vinasse, and are water quality parameters of interest.

Initially, we wanted to develop a model that could estimate methane generation for vinasse from any feedstock; we thus developed an experimental design regarding vinasse composition with this in mind. A review paper on anaerobic treatment of vinasse, published by Wilkie et al. (2000), assimilated information from dozens of studies of composition of vinasse from a wide variety of feedstocks. From this paper, we determined the maximum, minimum, and intermediate values of the vinasse constituents of interest: Chemical Oxygen Demand (COD), nitrogen (N), phosphorus (P), potassium (K), sulfur (S). We wanted our experimental design to cover the ranges of these constituent values, from minimum to maximum, given in Wilkie's paper; then, our methane generation model would be applicable to any vinasse of any composition from any feedstock. However, maximum ammonia, potassium, and sulfate were limited to levels that previous studies have been shown to be toxic to the methanogens, as shown in Table 3.1. The resulting experimental design, a strength 2 orthogonal array (V. Chen, 2011), is shown in Appendix A. The resulting 18 batches, representing 18 synthetic vinasse compositions, to be run at 3 temperatures (30, 35, and 40C), are also shown in Appendix A.

Table 3.1 Compounds Affecting Methane Production: Toxic Substance Concentration (adapted from OLGPB, 1976)

Constituent	Maximum Recommended Concentration
Ammonia (NH_3)	1500-3000 mg/L
Calcium (Ca)	2500-4500 mg/L
Chromium (Cr)	200 mg/L
Copper (Cu)	100 mg/L
Cyanide (CN^-)	<25 mg/L
Magnesium (Mg)	1000-1500 mg/L
Nickel (Ni)	200-500 mg/L
Potassium (K)	2500-4500 mg/L
Sodium (Na)	3500-5500 mg/L
Sodium chloride (NaCl)	40,000 ppm (~40 mg/L)
Sulfate (SO_4^{2-})	5000 ppm (~5mg/L)
Oxygen	

Initial experimental runs were conducted using the experimental design shown in Appendix A. Unfortunately, only 3 of 18 batches produced significant methane. The vinasse compositions may have contained unsuitable constituent combinations of COD, N, P, K, and S; for example: the following formula, run at 40°C, did not produce any biogas: (COD= 2.6; N= 0.550; P= 0.007; K= 0.400; S= 0.034)g/Liter of vinasse. An example of another formula, run at 30°C, that did not produce any biogas was the following: (COD= 147; N= 1.200; P= 0.007; K= 0.400; S= 1.470)g/L of vinasse.

The initial experimental design was thus abandoned. The actual experimental design used is shown in Table 3.2. Runs were conducted using the 4 compositions from the original design that had produced significant methane. Each of the 4 compositions, as shown in Table 3.2, was operated at 3 mesophilic temperatures (30, 35, and 40°C), for a total of 12 runs.

Table 3.2 Final Experimental Design of Vinasse Composition

Composition Number	Vinasse Composition (g of constituents per L of vinasse)				
	COD	N	P	K	S
	$C_6H_{12}O_6$	NH_3	H_3PO_4	KOH	$CaSO_4$
1	2.6	0.06	0.007	0.039	0.034
4	75	1.2	0.09	1.742	0.034
9	147	0.55	0.09	0.039	0.58
12	75	1.2	0.007	0.039	0.58

The synthetic vinasse was prepared using glucose, ammonia, phosphoric acid, potassium hydroxide, and calcium sulfate as sources of COD, N, P, K, and S, respectively. First, the glucose was weighed and dissolved in deionized water. The Chemical Oxygen Demand was estimated by calculating the amount (in g/L) of glucose consumed in an oxidation reaction, represented as follows:

$$C_6H_{12}O_6 + 6O_2 \rightarrow 6CO_2 + 6H_2O$$

Then, separately, the other constituents were combined. Then, the pH was checked and adjusted with either HCl or NaOH. The adjusted pH was between 7.0 and 8.4. Then, a buffer solution was added, within the range of 4.5 and 5.5 g of sodium bicarbonate ($NaHCO_3$)/L of

vinasse (depending on the initial pH, and how much NaOH had been used during the pH adjustment). Afterwards, anaerobic-digested sewage sludge was added (10-15% of the total solution volume, according to Espinoza-Escalante et al., 2008), collected from the City of Fort Worth Village Creek Wastewater Treatment Plant, to inoculate each bioreactor with an initial supply of microbes. Trace mineral solution (TMS) was added to each batch, as shown in Table 3.3, to ensure that microbes had sufficient minor nutrients. The initial trace mineral solution composition was taken from the Revised Anaerobic Mineral Medium (RAMM) (Shelton and Tiedje, 1984), and modified for use with vinasse. Then, the volume was completed to 6 liters of solution with deionized water, and the pH was checked and adjusted again.

Table 3.3 Trace Mineral Solution Composition, Modified for vinasse

Mineral Salt	Concentration (mg/L)
Calcium Chloride ($CaCl_2.2H_2O$)	75
Magnesium Chloride ($MgCl_2.6H_2O$)	100
Ferrous Chloride ($FeCl_2.4H_2O$)	20
Trace Metals	
Manganese (ii) Chloride ($MnCl_2.4H_2O$)	0.5
Boric Acid (H_3BO_3)	0.05
Zinc Chloride ($ZnCl_2$)	0.05
Cupper Chloride ($CuCl_2$)	0.03
Cobalt Chloride ($CoCl_2$. 6 H_2O)	0.5
Nickel Chloride ($NiCl_2$. 6 H_2O)	0.05

3.3 Reactor Experimental Set-Up

A total of 3 6-L lab-scale anaerobic digesters, as shown in Figure 3.1 (VWR part #22877-082), were assembled. The 6-L reactors had one threaded cap with a circular opening. A septum was installed in the threaded cap opening of each reactor to allow insertion of a syringe. The purpose of the syringe was two-fold: (1) Draw vinasse samples for pH monitoring and (2) insert 3 mL of 5N NaOH solution to adjust the vinasse pH, if needed.

Figure 3.1 ProCulture® Glass Spinner Reactor with Angled Side Arms

All joints were tightly fitted with Teflon® tape and sealed with plenty of 100% silicon DAP® sealant. After these joints were tightly fitted and sealed, the sealant was allowed to dry for at least 5 hours. Then, tests were performed for air leakage, i.e., pressure testing through a manometer, searching for bubbles in soap solution, as well as searching for bubbles while dipping the entire system in water. The pressure testing was conducted was by connecting our system to an U-tube manometer for 1 or 2 days. If the head difference was observed to be between 0.5 and 3 inches, then we concluded that the system was air-tight. If more leakage was observed, then more sealant was applied.

Each reactor was connected to an air-tight gas-collecting bag (22-L Cali-5-Bond™ Bag, Calibrated Instruments, Inc.), as shown in Figure 3.2. Each reactor was then filled with synthetic vinasse, re-sealed, and placed in the constant-temperature room. The reactors were located in a constant temperature room with the thermostat set at these specific temperatures. During two months, initial experiments were conducted at 50, 55, and 60°C, in the thermophilic range, since methane generation rates are higher for the thermophilic range. However, low amounts of methane were generated; it was thought that this could have been due to the fact that the sludge had not been adapted to the thermophilic range. Thus, subsequent experiments were conducted in the mesophilic range (30, 35, and 40°C).

Figure 3.2 Experiment Setup

3.4 Analytical Methods for Biogas Measurements

The biogas volume was measured daily by pumping the gas out of the collection bag through a standard air-grab sampler (SKC Air-check pump, model 224-44XR), which pumped the biogas at 1.0 L/min, and was connected to a calibrator (Bios Defender 510M), as shown in Figure 3.3. During the gas pumping period, the time needed to empty the gas bag was recorded. A LANDTEC-GEM 2000 PLUS with infrared gas analyzer (±3% accuracy), shown in Figure 3.4, was used to measure the concentrations of methane, carbon dioxide, and oxygen in percent volume, and hydrogen sulfide and carbon monoxide in parts per million. LANDTEC measurements of methane have previously been compared to those from an SRI gas chromatograph, and found to be within 7% of the GC readings (Karanjekar, 2012).

Figure 3.3 SKC Pump and Calibrator Used for Gas Volume Measurements
(Source: Karanjekar, 2012)

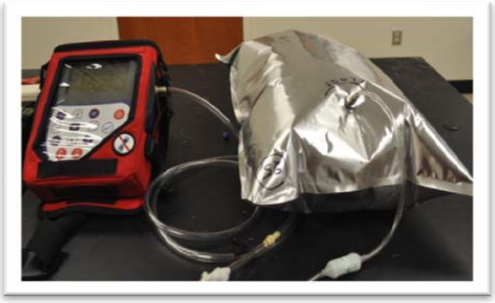

Figure 3.4 Landtec GEM 2000 Used for Gas Composition Measurements
(Source: Karanjekar, 2012)

The amount of biogas generated depended on each specific formulation. If a specific synthetic vinasse formulation generated any biogas at all, then, most of the time, the following pattern was observed: During the initial 12 hours, there was no biogas in the bags. Then, after 12 hours, there was some biogas in the bags, which had to be changed. Occasionally, there was biogas generation after 5 days. In addition to different quantities, each formulation produced biogas at different intervals. Some batches stopped generating biogas after 3 days, while others stopped after 5 to 8 days. As the synthetic vinasse digestion progressed, the rate of gas production decreased and the frequency of biogas measurement was reduced accordingly. Gas production rate was reported at STP.

3.5 Data Analyses

Methane production was recorded versus time for each vinasse formula. Cumulative methane volume can be estimated using the following equation:

$$V = L_o(1-e^{-kt}) \quad (3\text{-}1)$$

where,

V= Cumulative volume of methane per liter of vinasse (mL/L),

L_o = Ultimate methane potential (mL/L),

k = first-order methane generation rate constant (day^{-1}),

t = time (days).

Rearranging Eq. 3-1 and taking the natural log of both sides gives:

$$\ln(1-V/L_o) = -kt$$

If $\ln(1-V/L_o)$ is plotted vs. time, the negative value of the slope gives *k*. L_o was estimated from the horizontal asymptote of the plots of $\ln(1-V/L_o)$ vs. time. When the plot did not clearly reach an asymptote, the value of L_o was chosen which gave the largest R^2 value for a regression line fit to $\ln(1-V/L_o)$ vs. time.

Using the k values, a multiple linear regression model was developed to estimate k as a function of the 5 chemical components of vinasse, along with mesophilic temperature, as shown in Eq. 3.3:

$$k = \beta_0 + \beta_1 COD + \beta_2 N + \beta_3 P + \beta_4 K + \beta_5 S + \beta_6 T + \varepsilon \quad (3.3)$$

where,

k = methane generation rate constant (day^{-1});

β's = parameters to be determined through multiple linear regression, using lab data;

COD = Chemical Oxygen Demand concentration (g/L);

N = nitrogen concentration (g/L);

P = phosphorus concentration (g/L);

K = potassium concentration (g/L);

S = sulfur concentration (g/L);

T = temperature in the mesophilic range (K);

ε = error uncertainty, modeled as a random variable

CHAPTER 4

RESULTS AND DISCUSSION

4.1 Introduction

This chapter presents the results of this research experiments. The initial portion of this chapter presents the volume of methane generated from the anaerobic digestion of different formulations of synthetic vinasse in lab-scale reactors operated at 3 temperatures in the mesophilic range (30, 35, and 40° C). The final portion of this chapter presents specific information about modeling the ultimate methane potential (L_0) and the methane generation rate constant (k).

4.2 Experimental Results

The methane volume generated from the best-methane-yielding formulas, identified in preliminary runs, as described in Ch. 3, ranged between 30 and 78 mL per Liter of vinasse. The best methane-yielding formulations were: formulas #1, #4, #9, and #12. The formulation numbers and compositions are summarized in Table 4.1.

Table 4.1 Independent Variable Parameters for Formulations #s 1, 4, 9, and 12

Synthetic Vinasse Composition (g of constituents per L of vinasse)					
Formula	COD	N	P	K	S as SO_4
1	2.6	0.06	0.007	0.039	0.034
4	75	1.2	0.09	1.742	0.034
9	147	0.55	0.09	0.039	0.58
12	75	1.2	0.007	0.039	0.58

During anaerobic decomposition, there are four phases, which are: (i) the aerobic phase; (ii) acidogenesis (acid formation); (iii) methanogenesis (methane formation); and (iv)

decelerating methane phase. During the aerobic phase, the biogas generated was, mainly, carbon dioxide and other gases (H_2S, CO, H_2, and nitrogen compounds).

The acidogenic phase presented many challenges to this research. It was observed that the vinasse pH started dropping, drastically, approximately 4 hours after the preparation of each batch. Then, after those 4 hours, the pH had to be adjusted. The vinasse samples were collected by inserting a syringe through the septa, which had been installed in one of the mouths of the reactors (please refer to Chapter 3, Figure 3.3). Then, the samples were obtained and the pH was measured. Once the pH decreased to below 5.5, then 5 mL of a 5N sodium hydroxide solution would be added to the vinasse, also through a syringe. Then, the pH was checked again and increments of 3mL of 5N NaOH solution were added until the pH reached the range between 6.0 and 8.0. The syringe was inserted through the septa, which had been installed in one of the mouths of the reactor. The pH was measured and adjusted daily. Then, the pH stabilized in a range between 6.0 and 8.0 for the remainder of the decomposition duration. Each batch lasted between 5 and 10 days. Figure 4.1 shows the results of the pH variation from Formula #12 at 40°C.

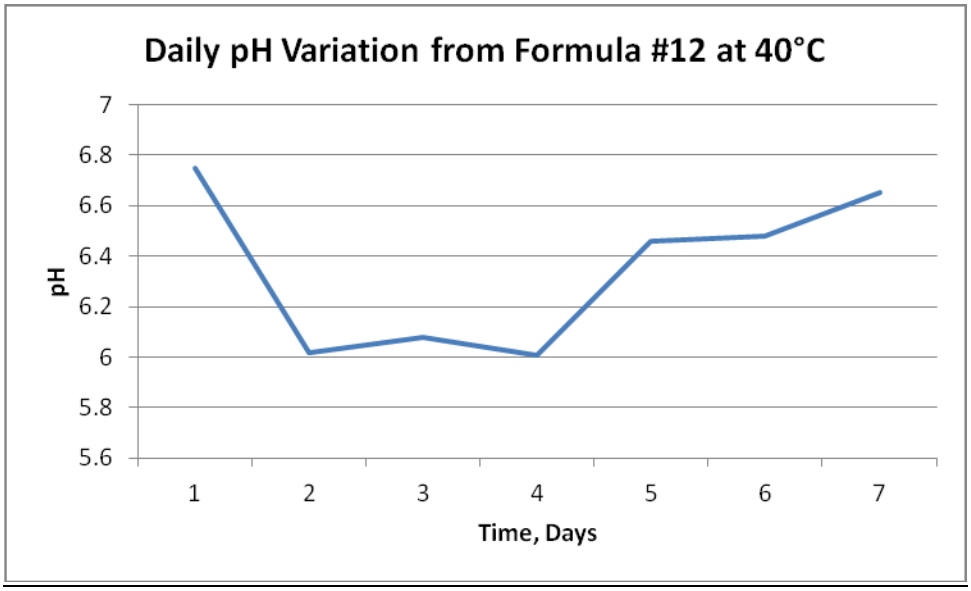

Figure 4.1 Daily pH Variation from Formula #12 at 40°C

4.2.1 Daily Methane Generation

4.2.1.1 Formula #1

Figures 4.2 – 4.4 show the daily methane volume, at STP, per Liter of vinasse (mL/L), generated from Formula #1 at 30, 35, and 40°C, respectively.

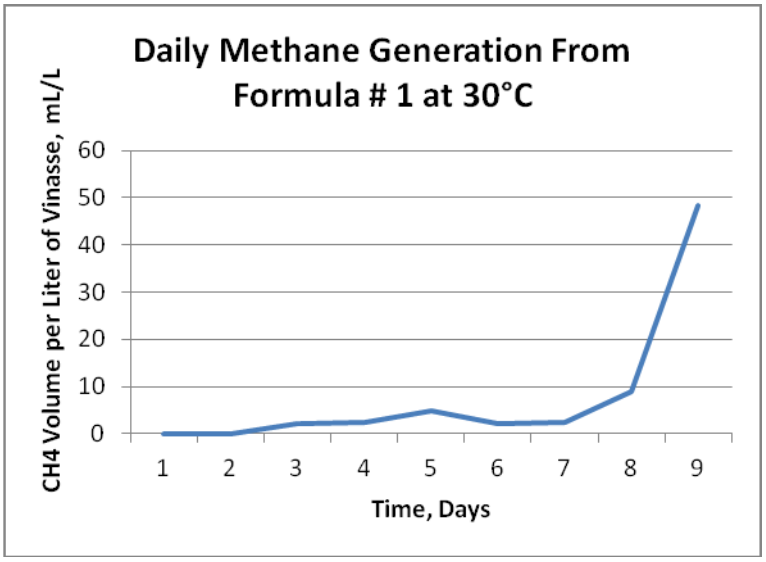

Figure 4.2: Daily Methane Generation from Formula #1 at 30°C

As shown in Figure 4.2, the methanogenesis started on Day 3. As discussed in Ch. 2, the aerobic and acidogenesis phases that precede the methanogenesis phase can take some time. After Day #3, methanogenesis continued at a low pace, generating a very small quantity of methane during the next few days; due to the low COD concentration, the methanogens did not have enough food to grow to significant numbers to start generating substantial volumes of methane. However, on the 9th day, there was a sudden increase of methane level. After the 9th day, the batch stopped generating biogas altogether.

As shown in Figure 4.3, the batch operated at 35°C took less time to start generating methane (beginning on Day #2). This was to be expected, since increased temperatures increase rates of microbial activity. This batch then continued generating methane, at a slightly higher pace than at 30°C, generating a small quantity of methane during the next few days of

decomposition. The pH had to be adjusted more often than it had been required at 30°C. The peak methane volume occurred on Day #6, sooner than it had happened for 30°C. Again, this is not surprising, since increased temperatures increase microbial activity. The height of the peak, however, was lower than that for 30°C. After the 6th day, the batch stopped generating biogas altogether.

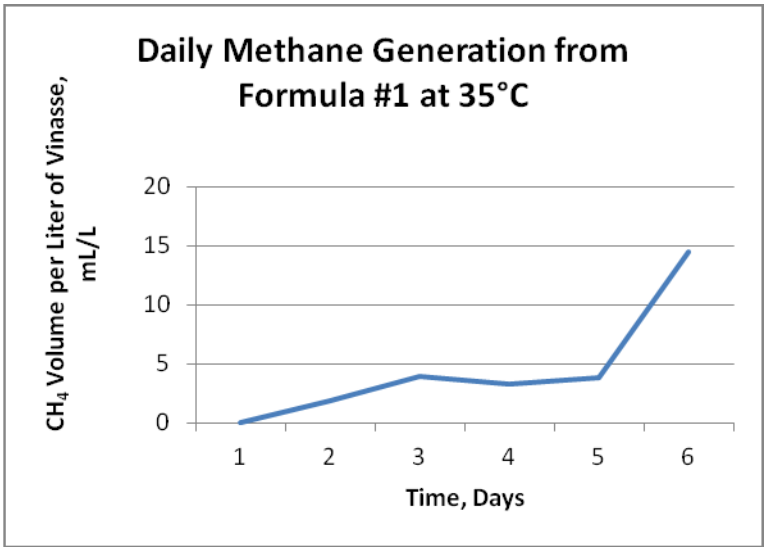

Figure 4.3 Daily Methane Generation from Formula #1 at 35°C

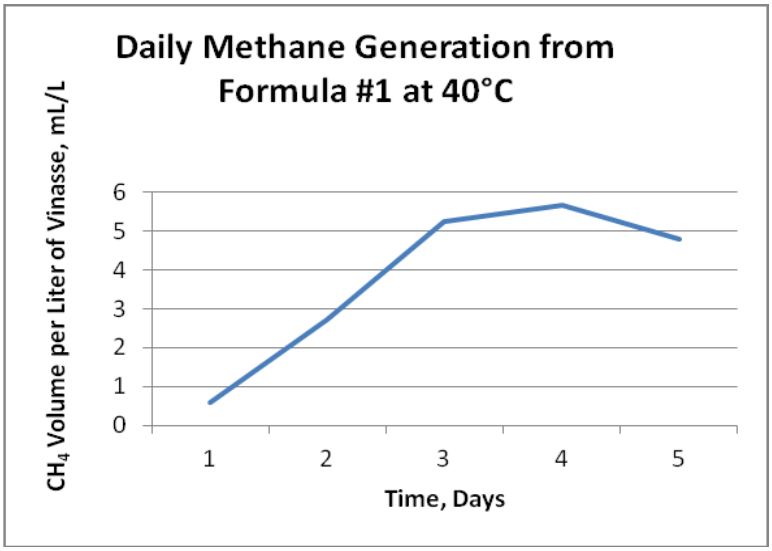

Figure 4.4 Daily Methane Generation from Formula #1 at 40°C

As shown in Figure 4.4, the batch operated at 40°C took less time to start generating methane (beginning on Day 1); the higher temperature was thus observed to accelerate methane production due to increased rates of microbial activity. Following Day 4, the methane generation dropped on the following day. The pH had to be adjusted more frequently than it had been required at 30°C. It is interesting to notice that the peak methane volume occurred on Day #4. In addition, the height of the peak was lower than for the lower temperature batches. The reason for this is not clear. After 5 days, the batch stopped generating biogas altogether. This was one day sooner than for the 35°C batch, which again is consistent with greater microbial activity depleting the glucose faster.

It can be observed that the methane generation from Formula #1 was significantly influenced by the temperature. It was observed that the duration of the lag phase (before methane production started) was longer at 30°C than at 40°C. These batches contained the same amount of glucose; since microbial activity was greater at 40°C, the microbes used all of the glucose sooner.

4.2.1.2 Formula #4

Figures 4.5 – 4.7 show the daily methane volume, at STP, per Liter of vinasse (mL/L), generated from Formula #4 at 30, 35, and 40°C, respectively.

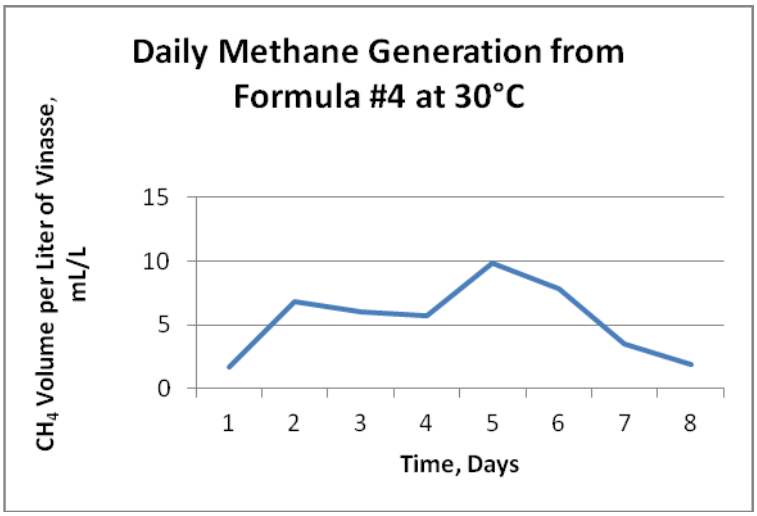

Figure 4.5 Daily Methane Generation from Formula #4 at 30°C

For Formula #4, all batches started generating methane on Day #1. The batch operated at 30°C generated the lowest volume on Day #1 (less than 2 mL/L), the 35°C batch generated an intermediate amount (around 2.3 mL/L), and the 40°C batch generated the most (around 2.5 mL/L). This indicates a faster start to methane production with higher temperature, which is consistent with increased microbial activity.

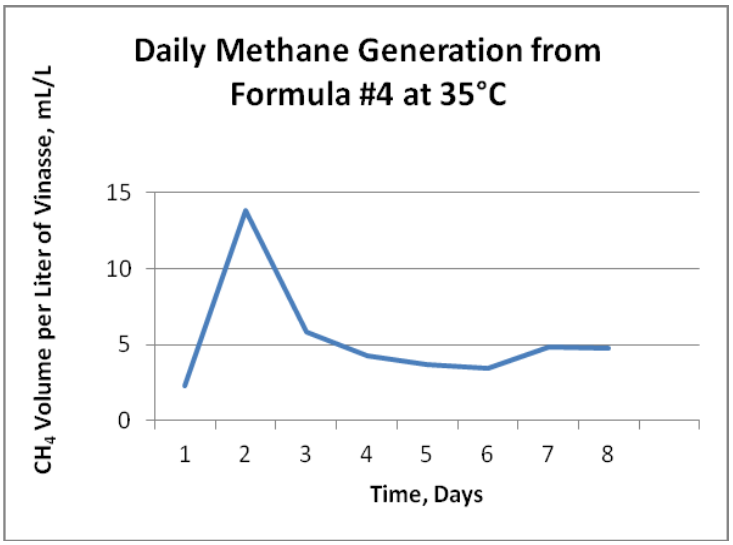

Figure 4.6 Daily Methane Generation from Formula #4 at 35°C

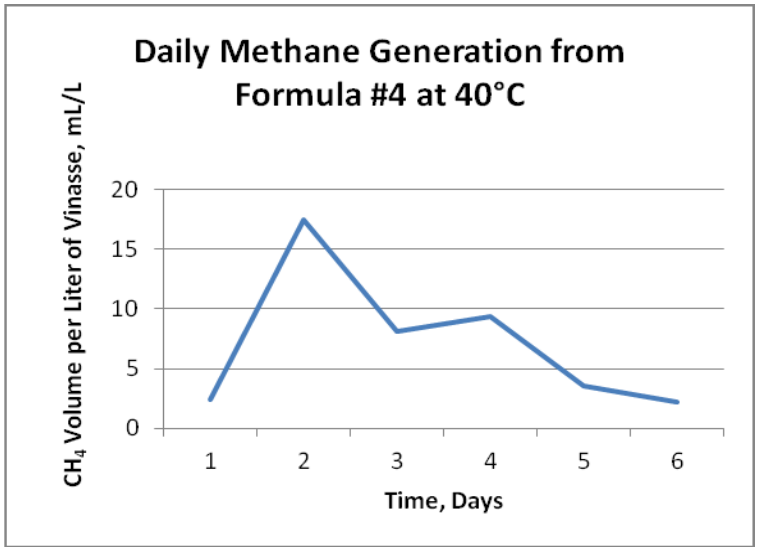

Figure 4.7 Daily Methane Generation from Formula #4 at 40°C

The 30, 35, and 40°C batches reached peak methane volume on Days #5, #2, and #2, respectively. The height of the peak was lowest for 30°C and highest for 40°C. The 30, 35, and 40°C batches stopped generating methane on Days #8, 8, and 6, respectively.

4.2.1.3 Formula #9

Figures 4.8 – 4.10 show the daily methane volume, at STP, per Liter of vinasse (mL/L), generated from Formula #9 at 30, 35, and 40°C, respectively.

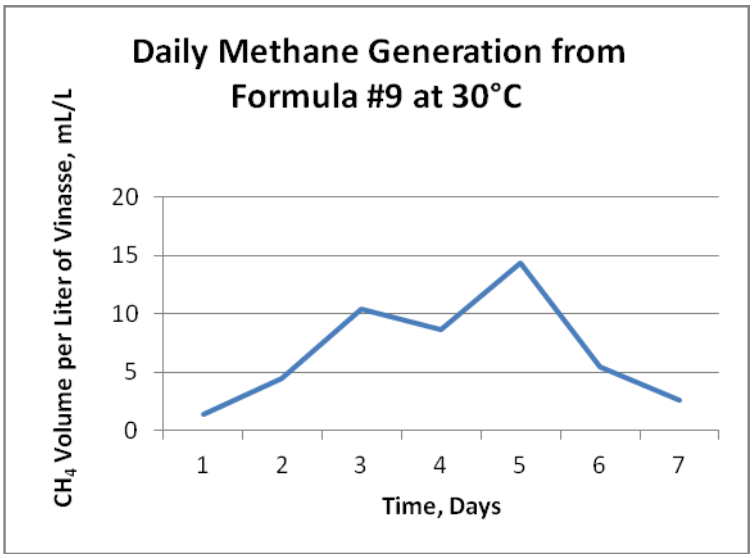

Figure 4.8 Daily Methane Generation from Formula #9 at 30°C

For Formula #9, all batches started generating methane on Day #1. The batch operated at 30°C generated the lowest volume on Day #1 (around 1.3 mL/L), and the 40°C batch generated the most (around 3 mL/L). This indicates a faster start to methane production with higher temperature, which is consistent with increased microbial activity. The plots from Formula #9 at 30 and 35°C display two peaks. For both batches, the peaks occur on Days #3 and #5. The 40°C batch had only one peak, and it was reached on the second day of anaerobic decomposition. The peak heights were lowest for the 30°C batch, and highest for the 40°C batch. The 30, 35, and 40°C batches stopped generating methane on Days #7, 7, and 6, respectively. This again is generally consistent with the trend of increased temperature accelerating methane production.

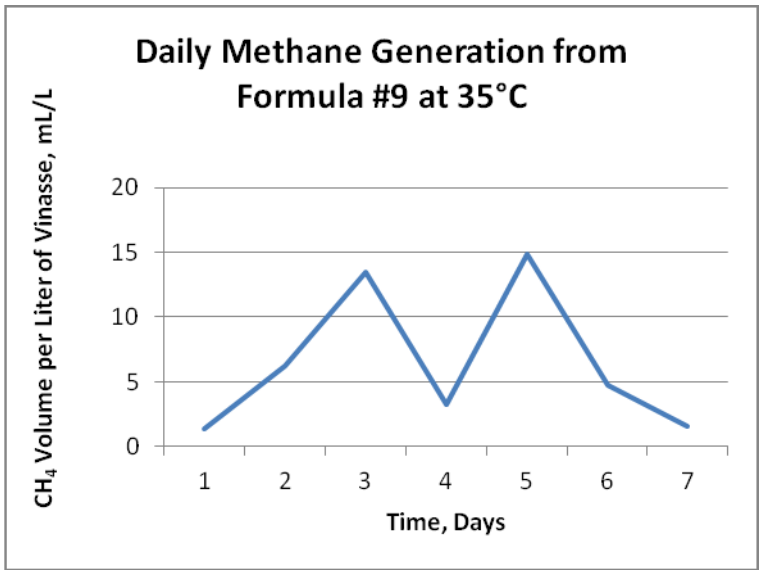

Figure 4.9 Daily Methane Generation from Formula #9 at 35°C

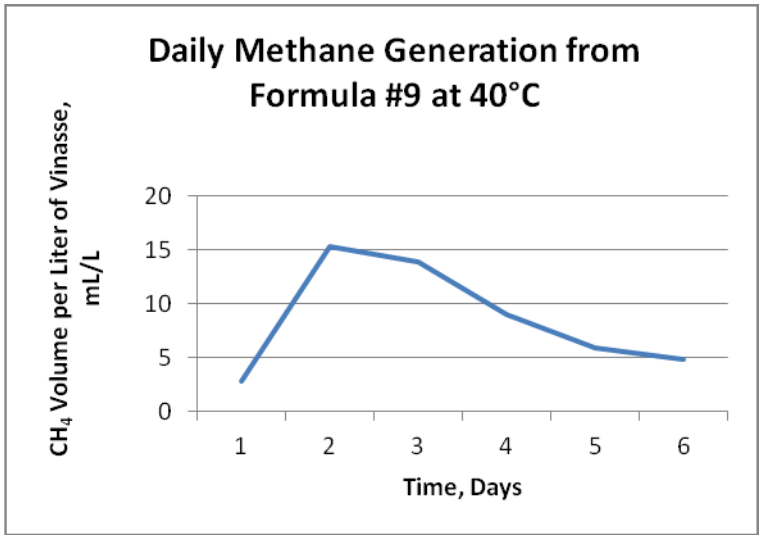

Figure 4.10 Daily Methane Generation from Formula #9 at 40°C

4.2.1.4 Formula #12

Figures 4.11 – 4.13 show the daily methane volume, at STP, per Liter of vinasse (mL/L), generated from Formula #12 at 30, 35, and 40°C, respectively.

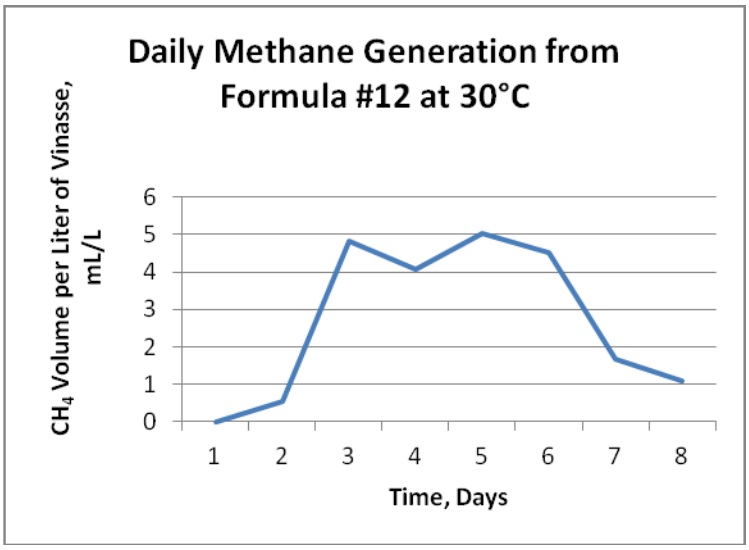

Figure 4.11 Daily Methane Generation from Formula #12 at 30°C

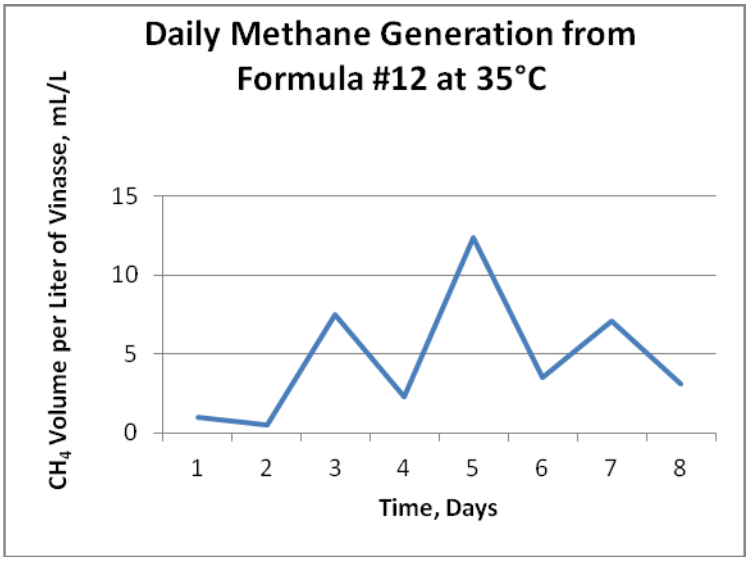

Figure 4.12 Daily Methane Generation from Formula #12 at 35°C

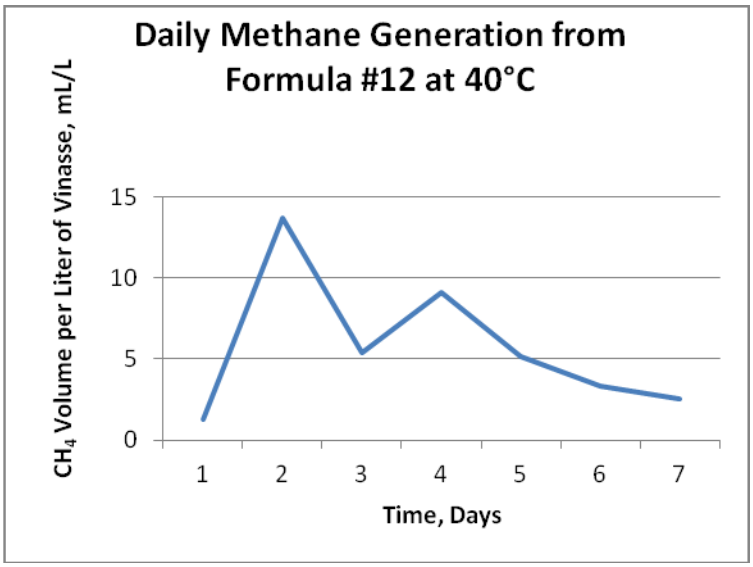

Figure 4.13 Daily Methane Generation from Formula #12 at 40°C

For Formula #12, the 35 and 40°C batches started generating methane on Day #1. This indicates a faster start to methane production with higher temperature, which is consistent with increased microbial activity. The plot from Formula #12 at 35°C displayed three peaks. The plots for the 30 and 40°C batches displayed two peaks. The earliest peak occurred on Day #2 for the 40°C batch, and on Day #3 for the 30 and 35°C batches. The highest peak for the 30 and 35°C batches occurred on Day #5; the highest peak for the 40°C batch occurred on the second day of decomposition. The dates of peak occurrence are generally consistent with the trend of increased temperature accelerating methane production. The highest peak for 40°C was higher than the highest peaks for the batches at 30°C and 35°C. The 30, 35, and 40°C batches stopped generating methane on Days #8, 8, and 7, respectively.

4.2.2 *Cumulative Methane Generation*

Figure 4.14 compares the cumulative methane volume at STP per Liter of vinasse (mL/L) generated from all formulas decomposed at 30°C.

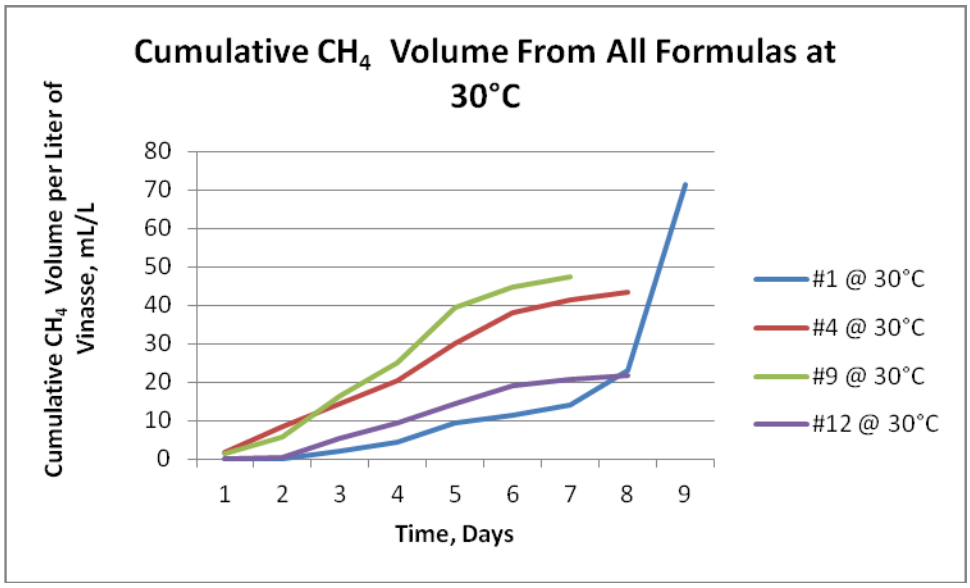

Figure 4.14: Comparison of the Cumulative Methane Volume, Generated from All Formulas at 30°C

As shown in Figure 4.14, Formulas #4 and #9 began generating methane on Day #1; the other two formulas did not. At 30°C, Formula #1 generated the highest ultimate methane volume. The total quantity of methane produced would be anticipated to be a function of the COD value of the formula. Since Formula #1 had the lowest COD value, its generating the highest quantity of methane was very surprising. The high methane volumes associated with Formula #1 may be attributed to the fact that the quantity of ammonia, which had been added to the vinasse solution as the nitrogen source, was within the recommended range. High concentrations of ammonia can inhibit the methanogenic activities. Table 3.1 shows the maximum recommended concentration of ammonia. All the constituents in Formula #1 had the minimum values reported by Wilkie et al. (2000). The low quantity of H_3PO_4 resulted in less need for NaOH to keep the pH in the optimum range of 7-8.0, meaning less potential sodium toxicity for microbes. On the other hand, the lower quantities of KOH resulted in no need to

decrease the pH with HCl. This reduced potential chloride toxicity for the methanogenic microorganisms. The small quantity of sulfur also meant less potential sulfate toxicity.

The fact that Formula #9, which had twice as much glucose as Formulas #4 and #12 (147 g/L vs. 75 g/L), did not generate exceptionally high volumes of methane was also unexpected. One explanation for these results may be due to the fact that the higher quantity of glucose, added as the COD source, enabled the uncontrollable multiplication of several different microbiological species, which may have consumed the methanogens at a faster pace. Another reason for the mediocre methane volumes from Formula #9 may be due to the fact that the carboxylic acids, produced by the increased microbiological activities, caused the pH to drop to below the recommended range. Formula #4 generated more cumulative methane than Formula #12 at all temperatures. Although Formulas #4 and #12 had the same COD quantities, the quantities of phosphorus and potassium were higher for Formula #4. Perhaps the higher quantity of phosphorous and potassium had a better nutrition value than that from Formula #12.

Figure 4.15 compares the cumulative methane volume at STP per Liter of vinasse (mL/L) generated from all formulas decomposed at 35°C. Similar to 30°C, Formulas #4 and #9 began generating methane on Day #1; the other two formulas did not. During the runs at 35°C, Formula #1 did not generate as much methane as it had been generating at 30°C. This may have been due to methanogens for Formula #1 functioning more optimally at 30°C. The ultimate methane production (asymptotic cumulative value) for the other 3 formulas was comparable (only slightly higher) than for 30°C. This is to be expected, since the change in temperature would be anticipated to affect how fast the methane is produced, but not the total quantity produced.

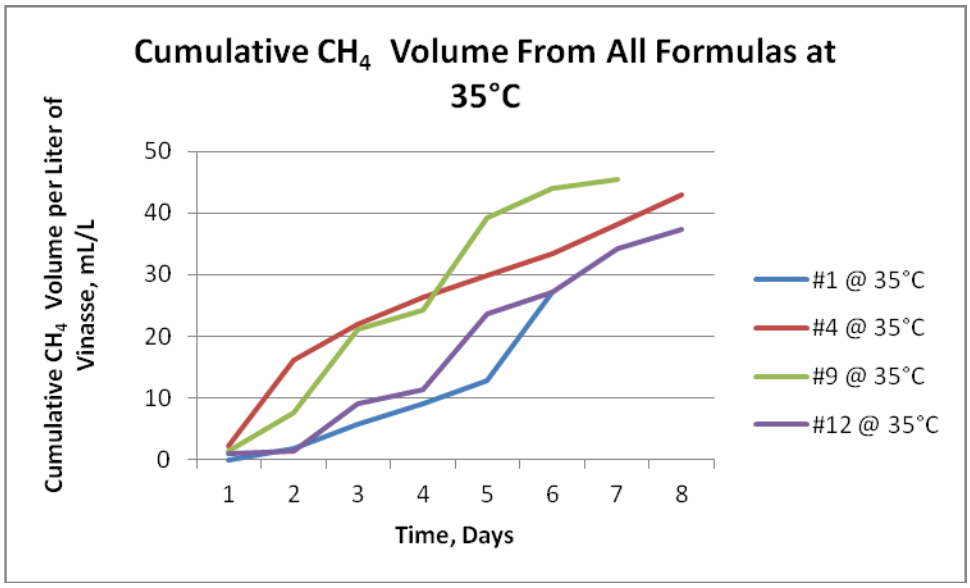

Figure 4.15: Comparison of the Cumulative Methane Volume, Generated from All Formulas at 35°C

Figure 4.16 compares the cumulative methane volume, at STP, per Liter of vinasse (mL/L), generated from all formulas decomposed at 40°C. Formulas #4 and #9 began generating gas on Day #1. During the runs at 40°C, Formula #9 had the highest ultimate methane potential, which was approximately 52mL CH_4/L vinasse. This was slightly higher than the ultimate methane potential for Formula #9 for 35°C. Similarly, the ultimate methane potential for Formulas #4 and #12 were slightly higher than their potentials at 35°C. The ultimate methane potential for Formula #1, however, was substantially lower than its value for 30°C. The reason for this is unknown.

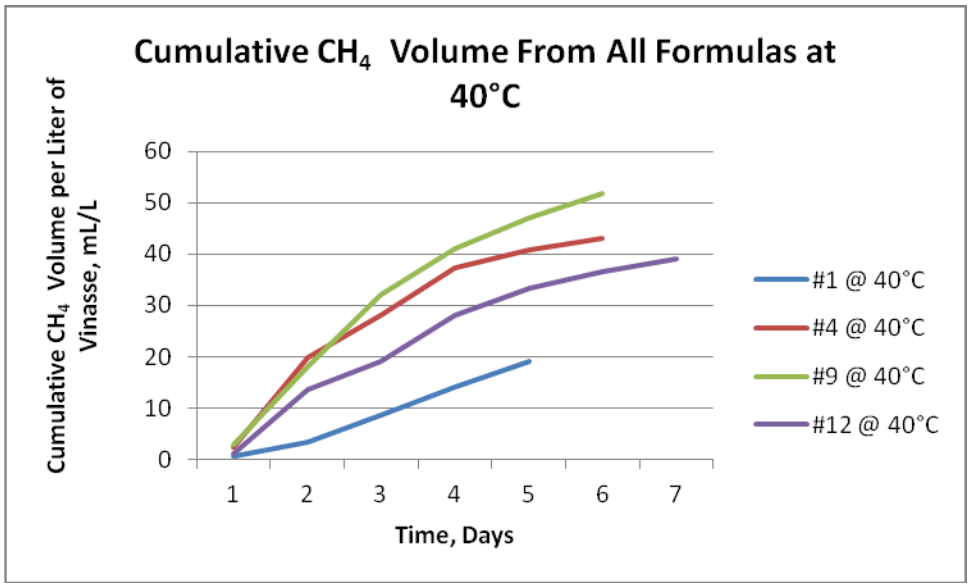

Figure 4.16: Comparison of the Cumulative Methane Volume, Generated from All Formulas at 40°C

An interesting observation was the fact that all formulas had their shortest duration at 40°C. As expected, the higher temperature promoted rapid microbiological activities as well as rapid nutrient consumption.

Figures 4.17-4.20 compare directly the cumulative methane volumes at the 3 different temperatures for each of the vinasse formulas.

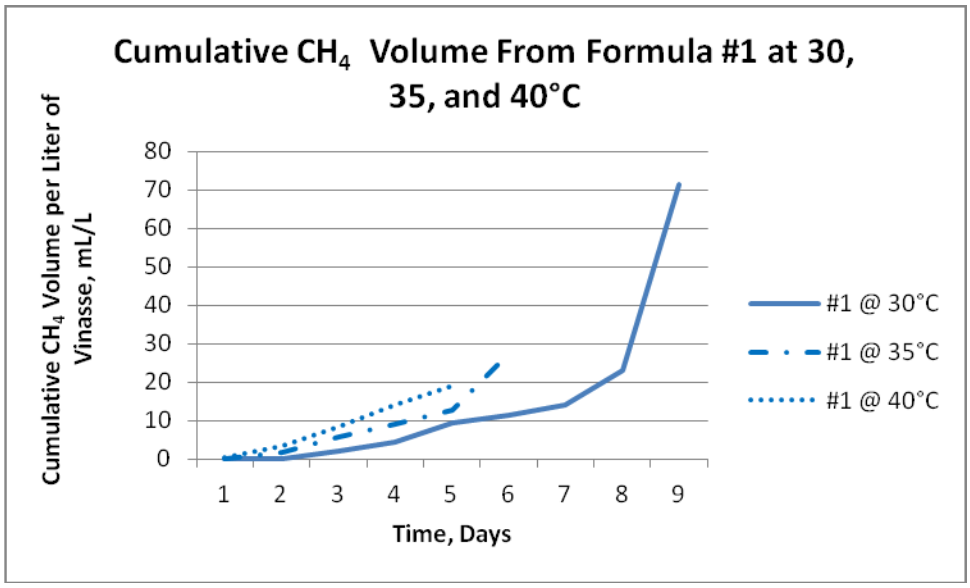

Figure 4.17: Comparison of the Cumulative Methane Volume, Generated from Formula #1 at 3 Temperatures

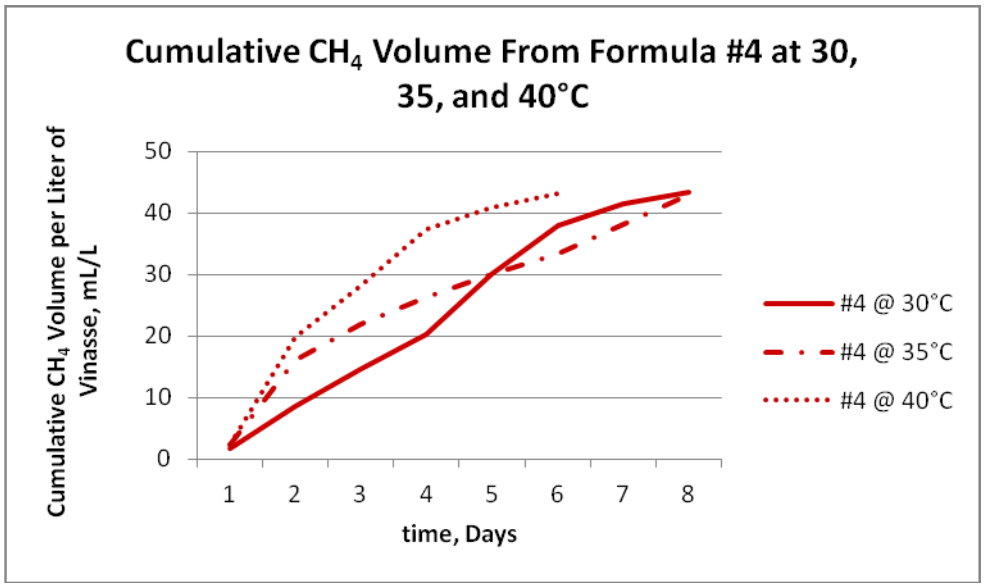

Figure 4.18: Comparison of the Cumulative Methane Volume, Generated from Formula #4 at 3 Temperatures

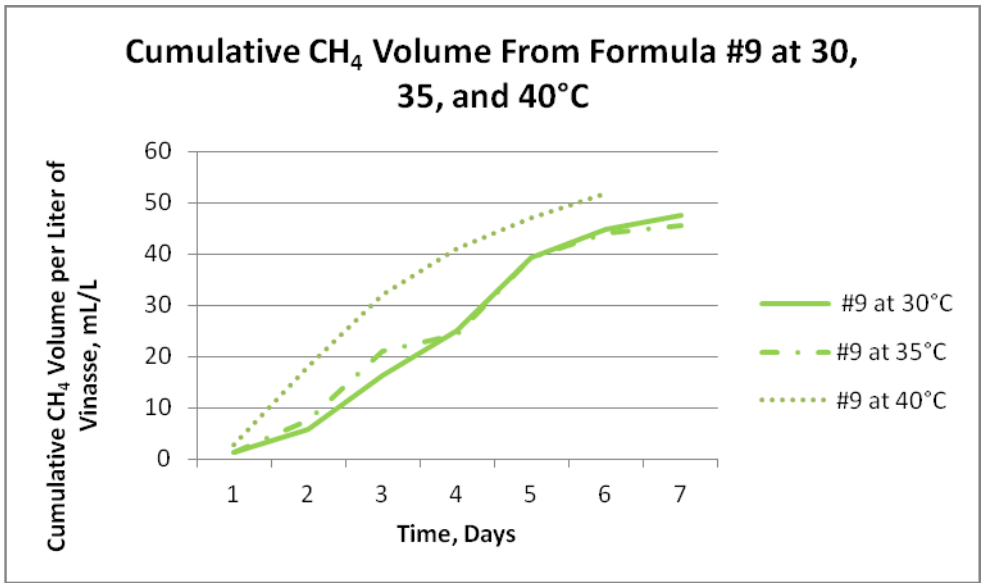

Figure 4.19: Comparison of the Cumulative Methane Volume, Generated from Formula #9 at 3 Temperatures

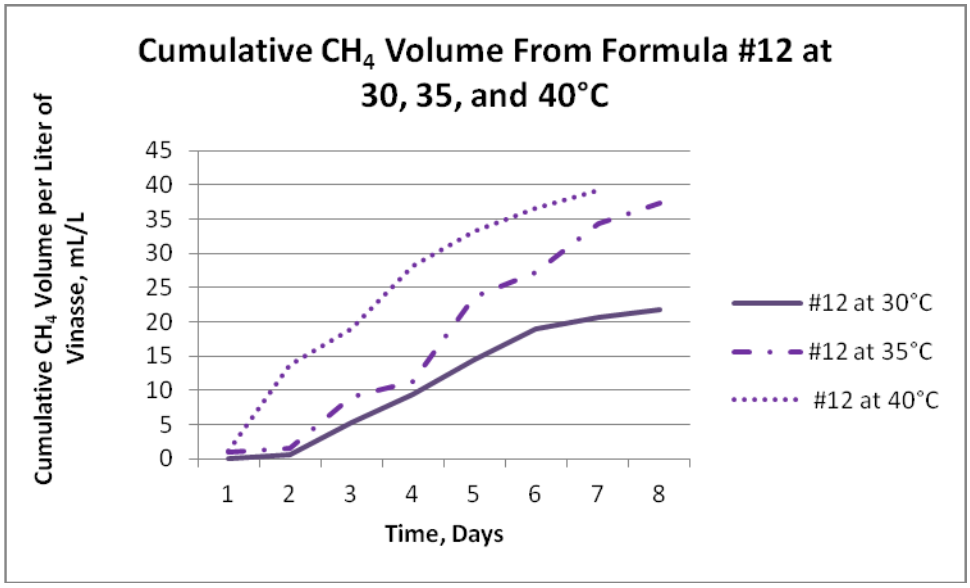

Figure 4.20: Comparison of the Cumulative Methane Volume, Generated from Formula #12 at 3 Temperatures

As shown in Figure 4.17, the cumulative methane volume generated by Formula #1 varied between 19.02 mL/L of vinasse for 40°C and 71.3 mL/L of vinasse for 30°C. As stated

previously, this large difference was surprising, and the reasons for it are not clear, unless the methanogens for Formula #1 functioned better at 30°C. The cumulative methane volume generated by Formula #4 hovered around 43 mL/L of vinasse at all three temperatures. The cumulative methane volume generated by Formula #9 varied between 45.5 mL/L of vinasse (35°C) and 52 mL/L of vinasse (40°C). At 30°C, the cumulative methane volume generated by Formula #9 was about 47.4 mL/L of vinasse. The cumulative methane volume generated by Formula #12 varied between 21.75 mL/L of vinasse (30°C) and 39.15 mL/L of vinasse (40°C). As shown in Figure 4.20, Formula #12 at 40°C did not generate similar cumulative methane volume as it had generated at 30 and 35°C. This difference in the total volume generated by the same formula was probably due to operational difficulties in maintaining the pH within the recommended range for the methanogens.

4.3 Computations to Determine the Methane Generation Rate Constant (k)

4.3.1 Lag Phase

During the lag phase, the microorganisms become acclimatized to the wastewater, hydrolyzing the matter and converting the larger substances into smaller and simpler substrates. According to Karanjekar (2012), during the calculations to determine the methane generation rate constant (k) from solid waste, the lag phase needs to be eliminated while curve fitting the data. However, for this research, in view of the fact that the duration of the entire synthetic vinasse decomposition process lasted only between five to 10 days, it was decided that the whole duration of the vinasse decomposition process would be included in the computations of the *k* value for each batch. In addition, the lag phase from the decomposition of vinasse lasted, often, only a few hours (in only one batch, the lag phase lasted 2 days). Formula #1 at 30°C produced the longest lag phase, which lasted 2 days. At 35°C, the lag phase of the same Formula (#1), lasted one day. Formula #12 had a lag phase of one day, during its decomposition at 35°C. The fact that Formula #1 had lag phases of one to two days at lower temperatures may be due to its low carbon content. However, the same reasoning does not

explain the fact that Formula #12 had such a slow start at 30°C. Maybe the explanation for the slow performance of Formula #12 lies in the fact that it had fewer hydroxide ions in its solution than Formula #4, although they both had the same quantity of sugar. In addition, Formula #12 had more sulfates than Formula #4.

4.3.2 Linear Regression

Linear regression to determine *k* values for each experiment was performed using MS Excel software. Plots of ln(1-V/Lo) versus time were drawn for each batch. The *k* value of each batch was the slope from each equation. As explained previously, V represented the cumulative volume of methane per Liter of vinasse, generated from each formula (mL/L), and L_o represented the ultimate methane potential (mL/L) of each batch. In this study, L_o was the asymptote of the curve, which was determined visually.

The biochemical reactions in the batches from Formula #1 at 30 and 35°C were such that the curves drawn from their cumulative volume versus time did not follow a first-order equation curve. Therefore, the *k* values of these formulas were not included in this model. Figures 4.2 and 4.3 show the results from Formula #1 at 30 and 35°C. Table 5.1 in the next chapter shows the *k* values used in this model. The *k* values are of similar order of magnitude as those developed from solid waste in lab-scale reactors (Karanjekar, 2012). This indicates that vinasse would produce methane at rates sufficient for use.

CHAPTER 5

MODEL DEVELOPMENT: MULTIPLE-LINEAR REGRESSION

5.1 Introduction

Using the collected data, a mathematical model (the VUMP Model) was developed to predict the methane generation rate constant, commonly known as *k*, for vinasse. The multiple linear regression (MLR) equation for predicting *k* values used 6 predictor variables, as shown in Eq. 5.1:

$$k = \beta_0 + \beta_1 COD + \beta_2 N + \beta_3 P + \beta_4 K + \beta_5 S + \beta_6 T + \varepsilon \quad (5.1)$$

where,

k = methane generation rate, in terms of first order decomposition constant (day^{-1});

β's = parameters to be determined through multiple linear regression, using lab data;

COD = Chemical Oxygen Demand concentration (g/L);

N = Nitrogen concentration (g/L);

P = Phosphorus concentration (g/L);

K = Potassium concentration (g/L);

S = Sulfur concentration (g/L);

T = Temperature of vinasse, in the mesophilic range (K);

ε = error uncertainty, modeled as a random variable.

5.2 Multiple Linear Regression Analyses: Statistical Modeling to Develop VUMP

The main software tool utilized in this study was statistical regression software, SAS® (Statistical Analysis System). According to Rodriguez, 2004, SAS has a complete data access, management, analyses and presentation system. SAS allows easy storage and efficient retrieval of a large array of data from varying sources. It can be used to collect and manipulate

large statistical analyses on data and create time-based comparisons, trend analyses, and predictions.

The raw data used for developing the MLR equation is presented in Table 5.1

Table 5.1 Raw Data for Developing the MLR Equation

Computed k value	COD	N	P	K	S	Temperature	Formula #
day^{-1}	g/L vinasse	g/L vinasse	g/L vinasse	g/L vinasse	g/L vinasse	K	
0.67	2.6	0.06	0.007	0.039	0.034	313	1
0.56	75	1.2	0.09	1.742	0.034	303	4
0.57	75	1.2	0.09	1.742	0.034	308	4
0.79	75	1.2	0.09	1.742	0.034	313	4
0.7	147	0.55	0.09	0.039	0.58	303	9
0.74	147	0.55	0.09	0.039	0.58	308	9
0.88	147	0.55	0.09	0.039	0.58	313	9
0.52	75	1.2	0.007	0.039	0.58	303	12
0.61	75	1.2	0.007	0.039	0.58	308	12
0.62	75	1.2	0.007	0.039	0.58	313	12

A matrix scatter plot was generated showing the relationship of each of these variables with every other, in a 7x7 plot-matrix. These plots are presented in Figure 5.1. The plots of the first row are basically the XY scatter plots. The response vs. predictor and predictor vs. predictor matrix plots are used for evaluating the overall appropriateness of a MLR form. Figure 5.1 shows an increasing linear trend between *k* and COD, *k* and phosphorous, and *k* and temperature. The plot between *k* and nitrogen shows a concave curve trend.

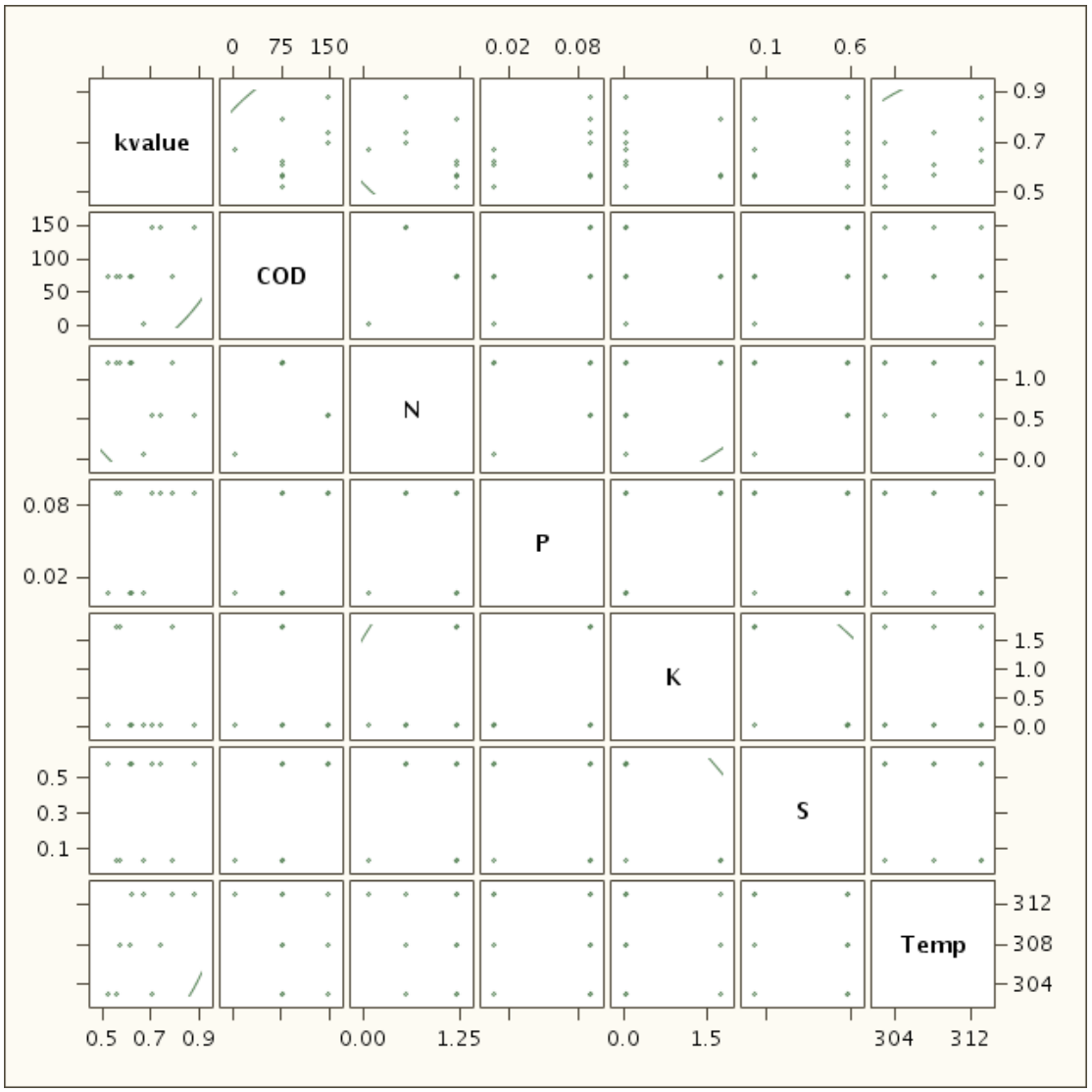

Figure 5.1 Response vs. Predictor and Predictor vs. Predictor Matrix Plot

SAS computed pair-wise correlations between response-predictor and predictor-predictor. The simple statistics are presented in Table 5.2, and the correlation matrix is presented in Table 5.3. The purpose of the correlation analysis is to quantify the linear association between two variables.

Table 5.2 SAS Output: Simple statistics of the Variables

Simple Statistics						
Variable	N	Mean	Std Dev	Sum	Minimum	Maximum
k	10	0.666	0.11296	6.66	0.52	0.88
COD	10	89.36	45.6212	893.6	2.6	147
N	10	0.891	0.42325	8.91	0.06	1.2
P	10	0.0568	0.04286	0.568	0.007	0.09
K	10	0.5499	0.82263	5.499	0.039	1.742
S	10	0.3616	0.28195	3.616	0.034	0.58
Temp	10	308.5	4.37798	3085	303	313

Table 5.3 Pearson's Correlation Coefficients

Pearson Correlation Coefficients, N = 10							
Prob > |r| under H0: Rho=0							
	kvalue	COD	N	P	K	S	Temp
kvalue	1	0.49362	-0.49701	0.46477	-0.15883	0.14095	0.57742
		0.1471	0.1439	0.1759	0.6612	0.6977	0.0805
COD	0.49362	1	-0.07763	0.61237	-0.21721	0.61237	-0.24133
	0.1471		0.8312	0.0598	0.5466	0.0598	0.5018
N	-0.49701	-0.07763	1	-0.0488	0.50379	-0.0488	-0.24915
	0.1439	0.8312		0.8935	0.1376	0.8935	0.4876
P	0.46477	0.61237	-0.0488	1	0.53452	-0.25	-0.14744
	0.1759	0.0598	0.8935		0.1114	0.486	0.6844
K	-0.15883	-0.21721	0.50379	0.53452	1	-0.80178	-0.07881
	0.6612	0.5466	0.1376	0.1114		0.0053	0.8287
S	0.14095	0.61237	-0.0488	-0.25	-0.80178	1	-0.14744
	0.6977	0.0598	0.8935	0.486	0.0053		0.6844
Temp	0.57742	-0.24133	-0.24915	-0.14744	-0.07881	-0.14744	1
	0.0805	0.5018	0.4876	0.6844	0.8287	0.6844	

The Pearson's correlation coefficient (*r*) ranges from -1 to +1. The high magnitude values of *r* are an indication of strong linear relationships between the pair of variables. When *r* is nearly zero, it means that there is little correlation between the variables. It can be observed on Table 5.3 that *k* value and Temperature were highly correlated, with a correlation coefficient

of 0.577. The correlation coefficients of *k* value and Nitrogen, and *k* value and COD were 0.497 and 0.494, respectively.

The presence of a non-zero value between predictor variables indicates the presence of multicollinearity between the predictors, which can adversely affect the analysis. If, however, $r < |0.7|$, it can be assumed that the multicollinearity problems are not very serious. Table 5.3 shows that the correlations between COD and Nitrogen, Nitrogen and Phosphorus, Nitrogen and Sulfur, Potassium and Sulfur, and Temperature and Potassium have numeric values greater than |0.7|. Therefore, these variables exhibit multicollinearity that should be further investigated. Due to the mixture design of this experiment, multicollinearity of the data was unavoidable. Using the collected data, the initial equation had the following form:

$$k = \beta_0 + \beta_1 COD + \beta_2 N + \beta_3 P + \beta_4 K + \beta_5 S + \beta_6 T + \varepsilon$$

SAS was used to calculate the least square estimators. Table 5.4 presents a summary of the calculation results. The calculations presented the following preliminary fitted regression function:

$$k = -4.6543 + 0.00117COD - 0.0757N + 0.68273P + 0K + 0S + 0.017T$$

Table 5.4 displays the SAS output of the preliminary model parameter estimates.

Table 5.4 Preliminary Parameter Estimates

Parameter Estimates							
Variable	DF	Parameter Estimate	Standard Error	t Value	Pr > |t|	Type I SS	Variance Inflation
Intercept	B	-4.6543	1.37287	-3.39	0.0195	4.43556	0
COD	B	0.00117	0.00051	2.3	0.07	0.02798	1.68496
N	B	-0.0757	0.04409	-1.72	0.1467	0.02431	1.08959
P	B	0.68273	0.52762	1.29	0.2522	0.00482	1.6
K	0	0	.	.	.	.	.
S	0	0	.	.	.	.	.
Temp	1	0.017	0.00438	3.88	0.0116	0.04335	1.15

The 0 values for DF for K and S are due to the mixture structure design which directly relates the K and S variables to the other predictors via mixture formulas. For the initial experimental design (refer to Appendix A), the mixture of all Formulas sums to 1 (or 100%). The repetition of the "Best-Methane-Producing" Formulas (refer to Table 4,1) yielded the *k* values used in this model. The preliminary model had the following form:

$$k = \beta_0 + \beta_1 COD + \beta_2 N + \beta_3 P + \beta_4 T + \varepsilon$$

SAS was used to calculate the least square estimators. Table 5.5 presents a summary of the calculation results.

Table 5.5 Parameter Estimated for the Preliminary Fitted Regression Function

Parameter Estimates							
Variable	DF	Parameter Estimate	Standard Error	t Value	Pr > |t|	Type I SS	Variance Inflation
Intercept	1	-4.65428	1.37287	-3.39	0.0195	4.43556	0
COD	1	0.00117	0.00051	2.3	0.07	0.02798	1.68496
N	1	-0.07568	0.04409	-1.72	0.1467	0.02431	1.08959
P	1	0.68273	0.52762	1.29	0.2522	0.00482	1.6
Temp	1	0.017	0.00438	3.88	0.0116	0.04335	1.15

The calculations presented the following fitted regression function:

$$k = -4.65428 + 0.00117COD - 0.07568N + 0.68273P + 0.01700T$$

In order to find out if the model is significant, an F test was performed. The ANOVA calculations, presented in Table 5.6, show that F* = 8.73 and the investigation of F(0.1, 4, 5) = 3.52. In view of the fact that F* = 8.73 > F(0.1, 4, 5) = 3.52, we may conclude that this model is significant. This model *p*-value = 0.0177 < α = 0.05, which also indicates that this model is significant to a 95% level of confidence.

Table 5.6 Analysis of Variance

Analysis of Variance					
Source	DF	Sum of Squares	Mean Square	F Value	Pr > F
Model	4	0.10046	0.02511	8.73	0.0177
Error	5	0.01438	0.00288		
Corrected	9	0.11484			

Root MSE	0.05363	R- Square	0.8748
Dependent Mean	0.666	Adj R-Sq	0.7746
Coeff Var	8.05324		

5.2.1 Model Assumptions

In order to verify if the preliminary model satisfies regression model assumptions, a residual analysis is performed. This verification is achieved by checking if the following assumptions are satisfied:

a) The current model form is reasonable (no curvature)

b) The residuals are normally distributed

c) The residuals have constant variance

d) The residuals are uncorrelated

e) There are no outliers

f) The predictors are not highly correlated with each other

These assumptions are tested as described below.

5.2.1.1 Reasonability of Model Form

In order to assess the reasonableness of the current model form, the following plots are displayed. Each plot represents the residuals versus each of the variables. Figure 5.2 represents the variation of the residuals with each of the predictive variables.

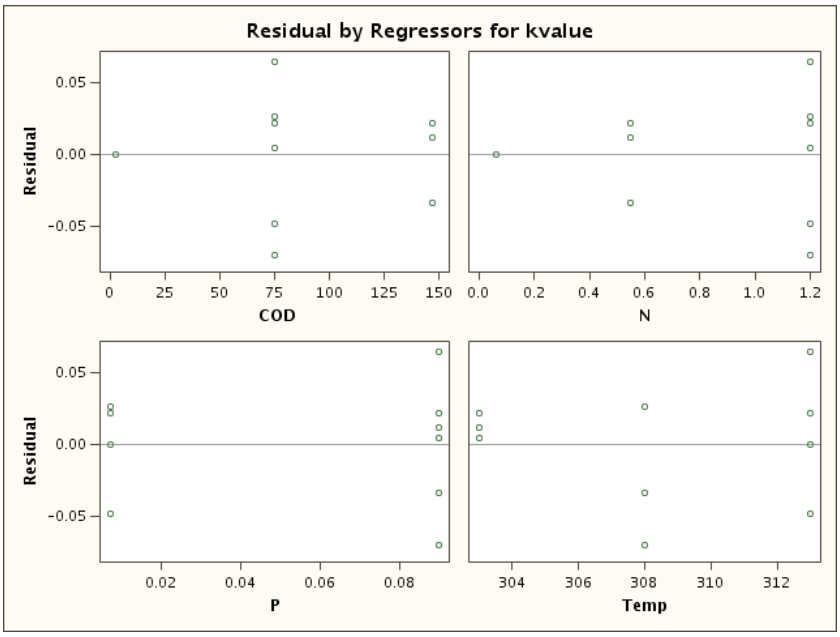

Figure 5.2 Variation of Residuals with each Predictive Variable

After performing a sight analysis of the plots, it was concluded that the model is adequate in respect of form because no curvature was identified in the plots.

Conclusion: Since there is no curvature in the plots, shown in Figure 5.2, the current MLR model form is acceptable.

5.2.1.2 Normally Distributed Residuals

In order to test whether the residuals are normally distributed or not, one may first take a look at the residuals versus normal scores plot. This plot is also known as the Normal Probability Plot (NPP). The SAS output for normal probability plot is shown in Figure 5.3. After that, a hypothesis test on normality is conducted.

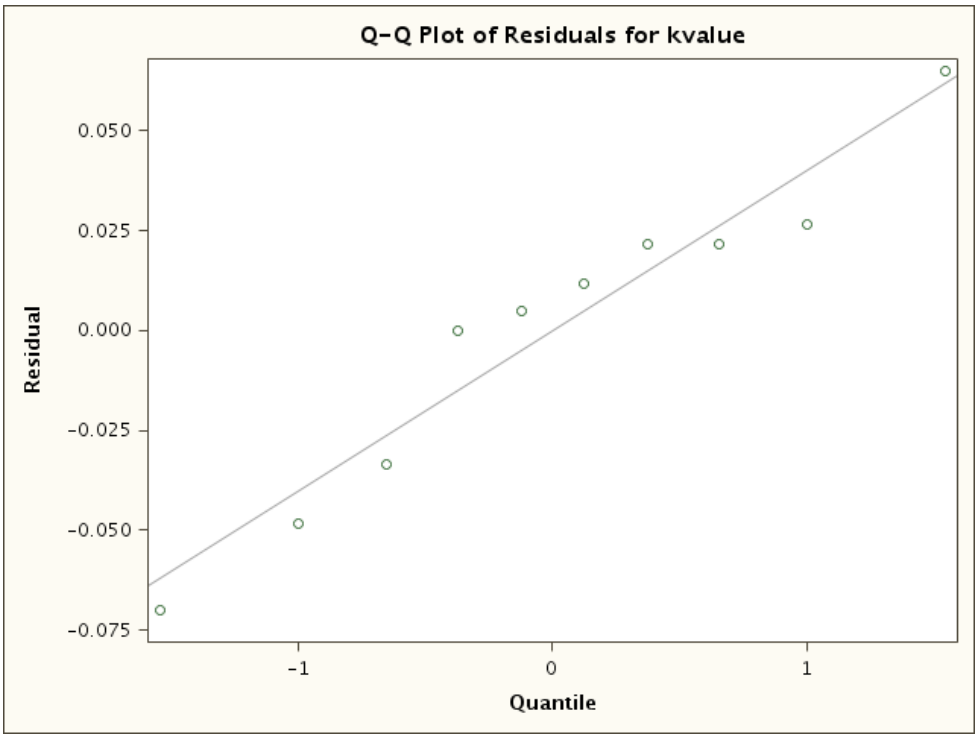

Figure 5.3 Normal Probability Plot (NPP): Residuals versus Normal Scores

In Figure 5.3, one can see that the NPP does not display much curvature. Therefore, from visual analysis, the following conclusion is reached: The residuals are almost normally distributed.

The Normality Test

The normality test was performed. The null and alternate hypotheses are:

H0: Normality is OK.

H1: Normality is violated.

The correlation between residuals and normal scores is shown on table 5.7. The correlation coefficient, ρ = 1.0. The cut-off value for α = 0.10, c(α, n) = c(0.10,10) = 0.952 Since the calculated ρ = 1.0 is greater than the cut-off value of c(0.10,10) = 0.952, we fail to reject the null hypothesis and conclude that normality is OK.

Table 5.7 SAS Output for Normality Test

Simple Statistics						
Variable	N	Mean	Std Dev	Sum	Minimum	Maximum
initial_residual	10	2.00E-07	0.03998	2.00E-06	-0.07	0.065
initial e_normal	10	0.5	0.01594	5.00001	0.4721	0.52591

Pearson Correlation Coefficients, N = 10 Prob > |r| under H0: Rho=0		
	initial_residual	initial e_normal
initial_residual	1	1
		<.0001
initial e_normal	1	1
	<.0001	

5.2.1.3 Constant Variance of Residuals

In order to make a decision about this assumption, the residual analysis was conducted. A linear regression model assumes that the errors have constant variance. Therefore, the plot of the residuals versus the predicted *k* value should present randomly scattered dots. When such plot displays a funnel shape, it means that the errors have non-constant variance.

Figure 5.4 represents the residuals versus the predicted values of methane generation rate constant.

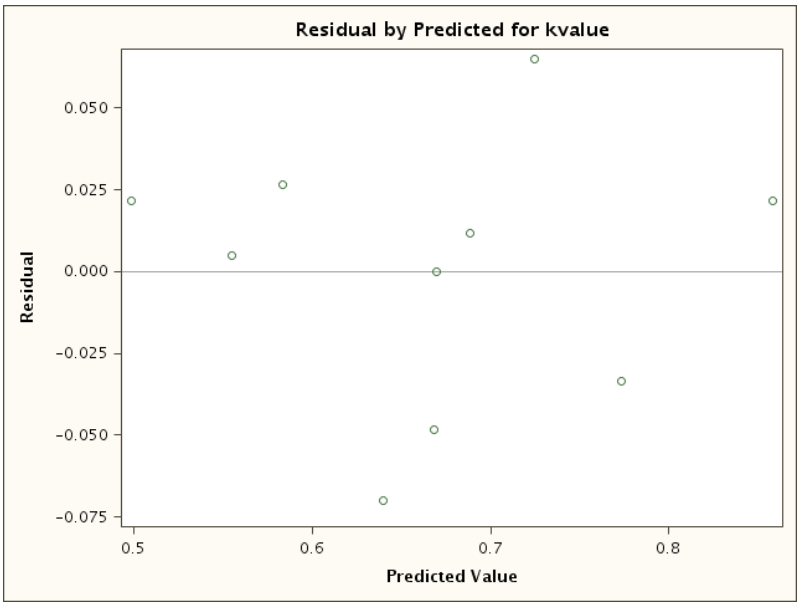

Figure 5.4 Residuals versus Predicted *k* values

After performing a sight analysis of the plot on Figure 5.4, no funnel shape was observed, which means that this model exhibits constant variance.

Modified Levene Test for Constant Variance:

In order to detect non-constant variance, the Modified Levene Test was conducted. In order to perform the Modified Levene Test, the data is divided into two groups, based on the fitted values. For this model, the number of observations in each group was equal to 5. In this case, the dividing point was the median value of *k* value, the predicted methane generation rate, 0.666 (median *k* value). The points with predicted *k* greater than 0.666 were placed in group 1, and the points with predicted *k* less than the median value were placed in group 2. The absolute deviations of residuals around the medians were calculated for each group. The Modified–Levene test was performed through SAS by using the two-sample t-test. Table 5.8 shows the output of the Modified Levene Test.

Table 5.8 SAS Output of Modified Levene Test

Method	Variances	DF	t Value	Pr > |t|
Pooled	Equal	8	-0.1	0.9241
Satterthwaite	Unequal	7.3104	-0.1	0.9244

Equality of Variances				
Method	Num DF	Den DF	F Value	Pr > F
Folded F	4	4	1.89	0.5538

For H_0: Variances of the two groups are equal, the Pr > F = 0.5538. Since the *p*-value > α = 0.05, we fail to reject the null hypothesis and conclude that the variances in two groups are equal. Now an analysis is performed by looking for the "Equal" case in T test. For the "Equal" case, Table 5.18 shows that Pr > |t|=0.9241. This, again, is greater than the value of α = 0.1 (and even when α = 0.05). Therefore, we, again, fail to reject the null hypothesis and conclude that the two groups of absolute deviations have the same mean. This translates to a validation of the constant error variance assumption for the linear regression model.

Conclusion: The constant error variance assumption is satisfied.

5.2.1.4 Uncorrelated Residuals

A multiple linear regression model requires that the errors be uncorrelated or independent from each other. In order to check if the residuals are serially uncorrelated, a time series plot is used. If an increasing or decreasing trend in the time series plot is identified, it indicates that the errors are serially correlated. In this research, all the reactors were operated independently from each other, and the *k* values were computed from these reactors. Therefore, the *k* values were not expected to be correlated and time series plots were not plotted.

5.2.1.5 Diagnostics (Outlier, Leverage, Variance Inflation)

Leverage values (X-outlier): The x-outliers are identified by performing a visual assessment of the diagonal elements of H, h_{ii}, (also known as the leverage values). In order to determine if a specific h_{ii} should be considered large, the following guideline was used: If h_{ii} >

2*hbar* = 2*p*/*n*, then, it is considered large. For these calculations, *p* = number of parameters in the model, and *n* = total number of observations. This model cutoff value (2*p*/*n*) = (2*5/10) = 1.0. Looking at the values, shown in Table 5.9, it can be seen that Observation #1 has the leverage value = 1.0, which is exactly at the limit of this model cutoff value of 1.0. Therefore it has been concluded that Observation #1 may not be considered to be an x-outlier, and it has been decided that Observation #1 is going to remain in this model because it seemed to be barely influential.

Bonferroni Outlier Test (Y-Outlier): The Studentized Deleted Residuals (t_i) are shown in the Table 5.9 as "RStudent." The guideline for the Bonferroni Outlier Test is: If $|t_i| > t(1-\alpha/2n; n-p-1)$, then observation *i* is a y-outlier. This model cutoff values for the Bonferroni Outlier Test were, $t(1-\alpha/2n; n-p-1) = t(0.995; 4) = 4.604$, at $\alpha = 0.1$. Based on the results, shown on Table 5.9, there is no y-outlier in this dataset.

Table 5.9 Diagnostics to Test for Outliers, Leverage and Influence of Outliers

Obs	Residual	Cook d	Hat Hii	R Student	Diffits
1	4.55E-15	.	1	.	.
2	0.005	0.003476	0.5	0.118125	0.118125
3	-0.07	0.255504	0.333333	-2.04453	-1.4457
4	0.065	0.587486	0.5	2.386761	2.386761
5	0.011667	0.018926	0.5	0.277787	0.277787
6	-0.03333	0.057937	0.333333	-0.72405	-0.51198
7	0.021667	0.065276	0.5	0.528525	0.528525
8	0.021667	0.065276	0.5	0.528525	0.528525
9	0.026667	0.03708	0.333333	0.566039	0.40025
10	-0.04833	0.324836	0.5	-1.38726	-1.38726

Variance Inflation: In order to check for variance inflation, the Variance Inflation factor (VIF) values need to be checked. The decision rule is:

$$\overline{VIF} = \frac{\sum_{k=1}^{p-1}(VIF)_k}{p-1}$$

If >> 1 and max $(VIF)_k > 10$, then there is serious multicollinearity. Moreover, we need to avoid any model with any $(VIF)_k > 5$.

The VIF values of this model are presented in Table 5.5. The average VIF = (1.68496+1.08959+1.60000+1.15000)/4 = 1.381138, which is not much greater than 1. In addition, none of the individual VIF values is greater than 5.

Conclusion: There is no serious multicollinearity issue in this model.

5.2.1.6 Correlation of Predictor Variables

The correlation matrix was presented in Table 5.3. For the secondary model (after the exclusion of the parameters representing potassium and sulfur), there are two correlation values greater than the absolute value of |0.7|. These values indicate correlation among the following variables: COD and Nitrogen, and Nitrogen and Phosphorus. The values for the correlation between COD and Nitrogen (0.8312), and between Nitrogen and Phosphorus (0.8935) are greater than |0.7|. Therefore, the multicollinearity among these variables needs to be investigated. However, in view of the fact that the correlation coefficients are not much greater than the absolute value of |0.7|, it has been concluded that the multicollinearity among these variables does not pose a serious issue.

Conclusion: The predictor variables are not highly correlated.

5.2.1.7 Decision About The Model Assumptions:

From the above analysis, it has been concluded that all the model assumptions are reasonably satisfied for this model. Therefore, we accept this secondary model as this research model and conduct further analysis of this model.

5.2.2 Exploration of Interaction Terms

The interactions terms are the results of the multiplication of two predictor variables. Six possible interaction terms were considered in this research. These predictors are named as follows: x1 (= COD), x2 (= Nitrogen), x3 (= Phosphorus), and x4 (= Temperature). The 6

interaction terms are: x1x2, x1x3, x1x4, x2x3, x2x4, x3x4. These interactions may explain some of the variability in the response that may not have been explained by the current model. However, only a few of these interaction terms may be helpful for improving model fit.

5.2.2.1 Interaction Plots

In order to decide whether the addition of these interactions to this model is meaningful or not, an examination of the partial regression plots can be conducted. Another method for detecting interaction is by plotting the standardized interaction term against the residuals. This is done by first standardizing the predictors. Standardization is a procedure where each value is centered to zero and scaled to have a variance of one. This process is useful for numerical stability. If a linear trend is observed in the residuals vs. standardized interaction term plot, then that interaction term may be helpful to the MLR model. If, however, the dots are randomly scattered, then the interaction term will not be helpful. Figures 5.5 through 5.10 display the residuals vs. standardized interaction plots.

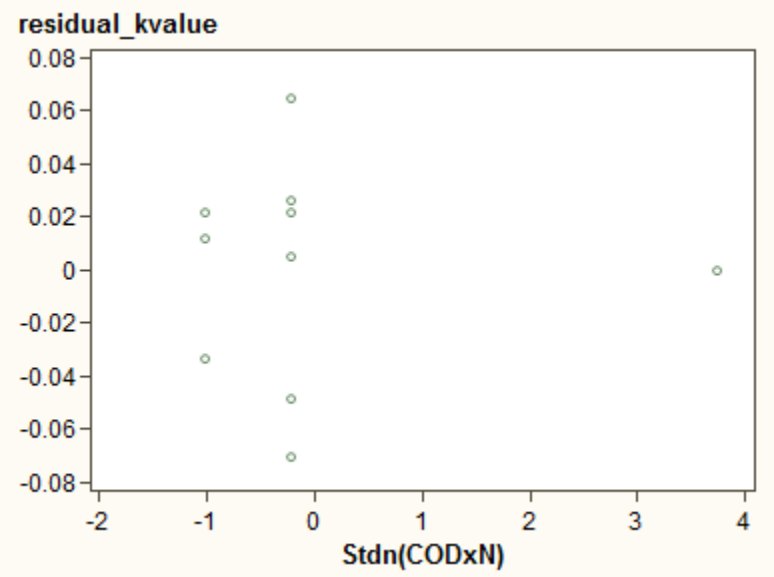

Figure 5.5 Residuals versus Standardized (CODxN)

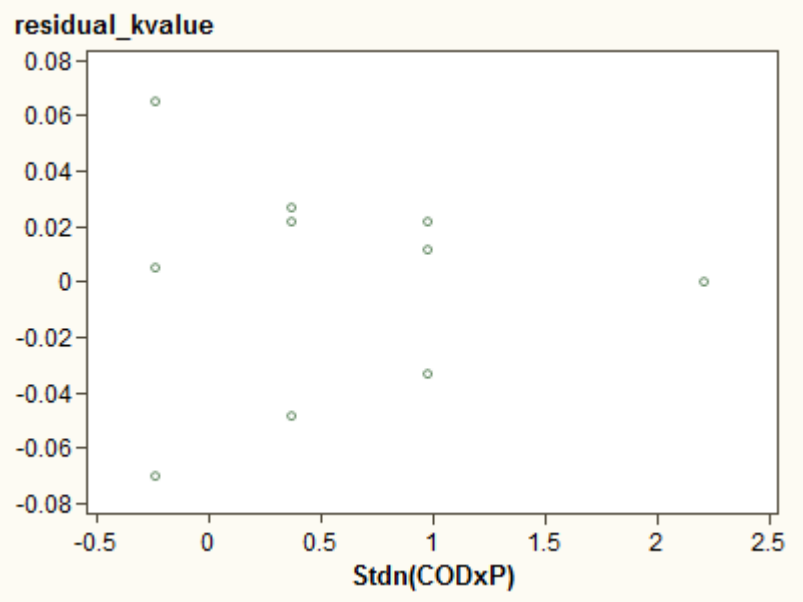

Figure 5.6 Residuals versus Standardized (CODxP)

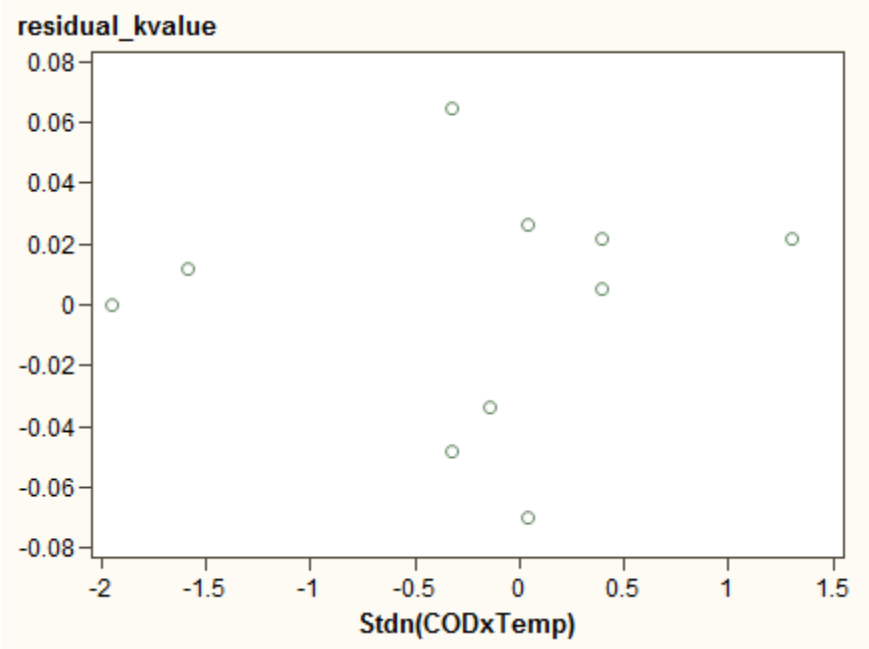

Figure 5.7 Residuals versus Standardized (CODxTemp)

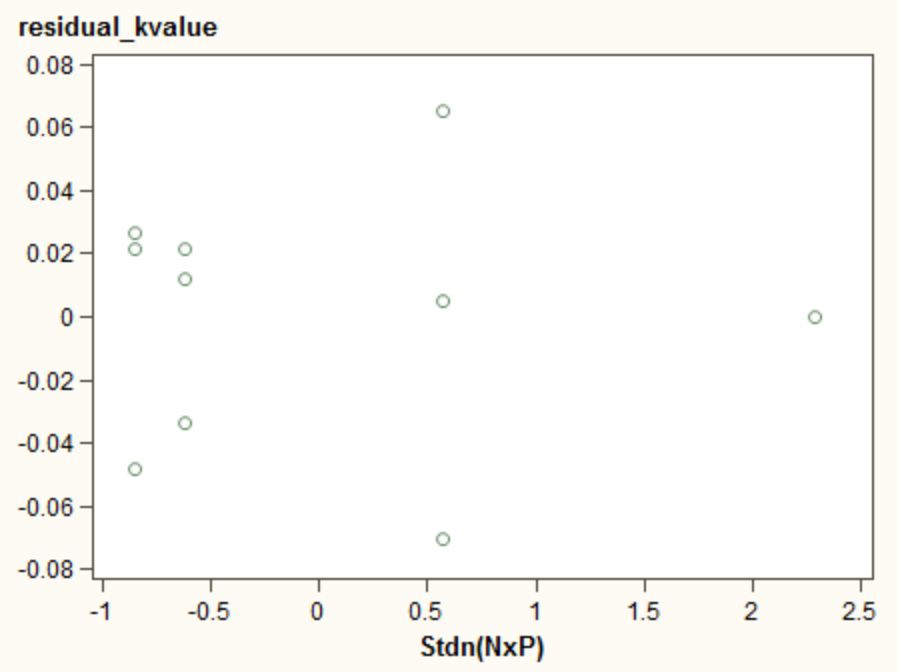

Figure 5.8 Residuals versus Standardized (NxP)

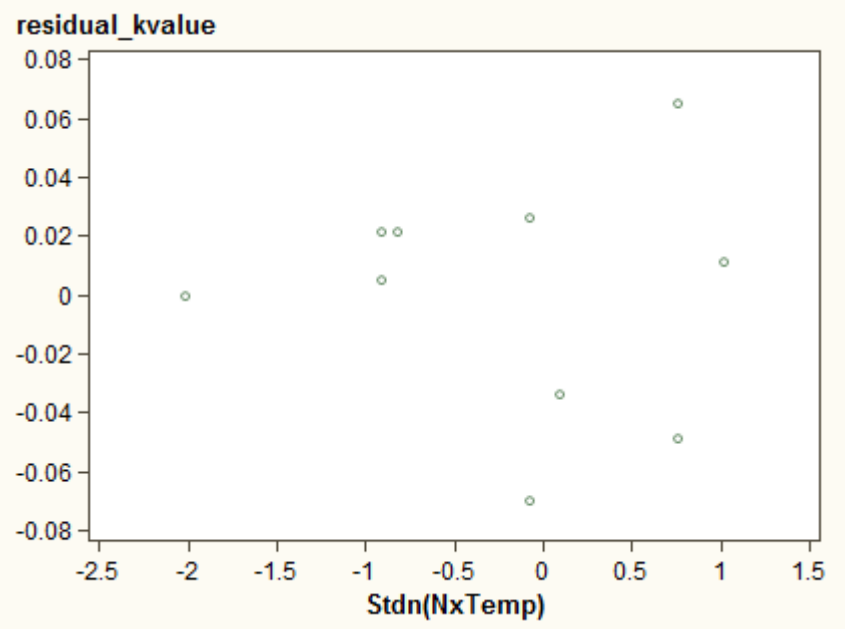

Figure 5.9 Residuals versus Standardized (NxTemp)

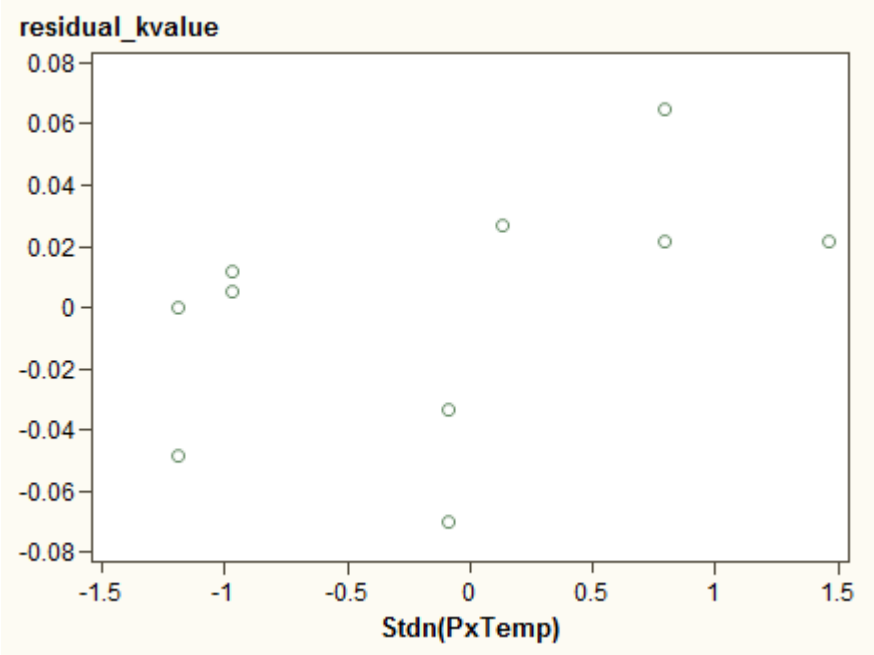

Figure 5.10 Residuals versus Standardized (PxTemp)

Figures 5.5 through 5.10 show that all interaction terms display some kind of a linear trend with the residuals. Therefore, all six interaction terms (Stdn(CODxN), Stdn(CODxP), Stdn(CODxTemp), Stdn(NxP), Stdn(NxTemp), as well as Stdn(PxTemp)) were considered further for addition this model.

5.2.2.2 Correlations of the Added Interactions

In view of the fact that it was decided to include all six interaction terms in this model, it is important to look at how they correlate with the other parameters in the model. Table 5.10 shows the correlation coefficients of the interaction terms with the predictor variables.

Table 5.10 Correlation Coefficients of the Interaction Terms with the Predictive Variables

Pearson Correlation Coefficients, N = 10											
Prob > |r| under H0: Rho=0											
	kvalue	COD	N	P	Temp	Stdn(CODxN)	Stdn(CODxP)	Stdn(CODxTemp)	Stdn(NxP)	Stdn(NxTemp)	Stdn(PxTemp)
kvalue	1	0.49362	-0.49701	0.46477	0.57742	-0.16871	0.32344	0.07786	-0.02451	0.16398	0.17811
		0.1471	0.1439	0.1759	0.0805	0.6413	0.362	0.8307	0.9464	0.6508	0.6225
COD	0.49362	1	-0.07763	0.61237	-0.24133	-0.84305	-0.08802	0.36337	-0.69718	0.50844	0.2232
	0.1471		0.8312	0.0598	0.5018	0.0022	0.8089	0.302	0.025	0.1335	0.5354
N	-0.49701	-0.07763	1	-0.0488	-0.24915	-0.47076	-0.93216	0.50877	-0.38882	0.39497	0.31291
	0.1439	0.8312		0.8935	0.4876	0.1697	<.0001	0.1332	0.2668	0.2586	0.3787
P	0.46477	0.61237	-0.0488	1	-0.14744	-0.51558	-0.30912	0.22183	0.01843	0.3108	0.06056
	0.1759	0.0598	0.8935		0.6844	0.1272	0.3848	0.5379	0.9597	0.3821	0.868
Temp	0.57742	-0.24133	-0.24915	-0.14744	1	0.34796	0.27431	-0.03873	0.28763	-0.04	-0.0238
	0.0805	0.5018	0.4876	0.6844		0.3245	0.4431	0.9154	0.4203	0.9127	0.9479
Stdn(CODxN)	-0.16871	-0.84305	-0.47076	-0.51558	0.34796	1	0.58076	-0.59601	0.82671	-0.663	-0.3663
	0.6413	0.0022	0.1697	0.1272	0.3245		0.0783	0.069	0.0032	0.0367	0.2978
Stdn(CODxP)	0.32344	-0.08802	-0.93216	-0.30912	0.27431	0.58076	1	-0.53926	0.29733	-0.4552	-0.3006
	0.362	0.8089	<.0001	0.3848	0.4431	0.0783		0.1077	0.4041	0.1862	0.3988
Stdn(CODxTemp)	0.07786	0.36337	0.50877	0.22183	-0.03873	-0.59601	-0.53926	1	-0.49263	-0.0561	0.6161
	0.8307	0.302	0.1332	0.5379	0.9154	0.069	0.1077		0.148	0.8778	0.0579
Stdn(NxP)	-0.02451	-0.69718	-0.38882	0.01843	0.28763	0.82671	0.29733	-0.49263	1	-0.5481	-0.3567
	0.9464	0.025	0.2668	0.9597	0.4203	0.0032	0.4041	0.148		0.101	0.3117
Stdn(NxTemp)	0.16398	0.50844	0.39497	0.3108	-0.03996	-0.66301	-0.45517	-0.05605	-0.54808	1	-0.0358
	0.6508	0.1335	0.2586	0.3821	0.9127	0.0367	0.1862	0.8778	0.101		0.9218
Stdn(PxTemp)	0.17811	0.2232	0.31291	0.06056	-0.02381	-0.36632	-0.30056	0.6161	-0.35665	-0.0358	1
	0.6225	0.5354	0.3787	0.868	0.9479	0.2978	0.3988	0.0579	0.3117	0.9218	

The presence of interaction terms in a model usually induces high multicollinearity. Table 5.10 shows that the following predictors were highly correlated with the added interaction terms: COD and Stdn(CODxN); COD and Stdn(CODxP); N and Stdn(CODxP); P and Stdn(NxP); P and Stdn(PxTemp); Temp and Stdn(CODxTemp); Temp and Stdn(NxTemp); Temp and Stdn(PxTemp); Stdn(CODxN) and StdnCODxTemp; Std(CODxTemp and Stdn(NxTemp); as well as Stdn(NxTemp) and Stdn(PxTemp). This indicated that there may be serious multicollinearity if all these terms are included in the model. High multicollinearity in the relationships should be avoided because it can complicate the MLR analysis. Extremely high multicollinearity signifies that two or more predictors are explaining the same variation in the response variable, causing numerical problems in the computations of least squares, used to estimate the parameters of the model. These numerical problems can cause an inability to precisely determine the estimated parameters, i.e., the variance of the least squares estimators

is inflated. Therefore, the concern for all these multicollinearity issues contributed to the exclusion of all these terms from the Final Chosen Model, which is presented through the selection process of the Final Chosen Model in the next section, Section 5.2.3.

5.2.3 Model Search

The model search is a procedure for identifying potential good models. Three algorithms were used to search for the best model: Best Subset Regression, Backward Elimination, and Stepwise Regression (Forward and Backward).

The following ten predictor variables were considered: Chemical Oxygen Demand (COD), Nitrogen (N), Phosphorus (P), Temperature (TEMP), Stdn(CODxN), Stdn(CODxP), Stdn(CODxTemp), Stdn(NxP), Stdn(NxTemp), as well as Stdn(PxTemp).

5.2.3.1 Stepwise Regression

Stepwise regression uses backward elimination and forward selection. The variables are added or deleted using the p-value to test the hypothesis: H0: $\beta_k = 0$. The predictors are either removed (if $p > \alpha_{out}$) or added (if $p < \alpha_{in}$), depending on the predictor p-value. Table 5.11 displays the SAS output for the stepwise regression. In this model, the α_{in} and α_{out} were set at 0.1. The best model suggested by stepwise regression method had three variables.

Table 5.11 Stepwise Regression

Stepwise Selection: Step1

Variable Temp Entered: R-Square = 0.3334 and C(p) = 16.7754 Analysis of Variance					
Source	**DF**	**Sum of Squares**	**Mean Square**	**F Value**	**Pr > F**
Model	1	0.03829	0.03829	4	0.0805
Error	8	0.07655	0.00957		
Corrected	9	0.11484			
Variable	**Parameter Estimate**	**Standard Error**	**Type II SS**	**F Value**	**Pr > F**
Intercept	-3.9302	2.29789	0.02799	2.93	0.1256
Temp	0.0149	0.00745	0.03829	4	0.0805

Bounds on condition number: 1,1

Stepwise Selection: Step2

Variable COD Entered: R-Square = 0.7588 and C(p) = 4.2398

Analysis of Variance					
Source	**DF**	**Sum of Squares**	**Mean Square**	**F Value**	**Pr > F**
Model	2	0.08715	0.04357	11.01	0.0069
Error	7	0.02769	0.00396		
Corrected	9	0.11484			
Variable	**Parameter Estimate**	**Standard Error**	**Type II SS**	**F Value**	**Pr > F**
Intercept	-5.37	1.53333	0.04853	12.27	0.01
COD	0.00166	0.00047	0.04886	12.35	0.0098
Temp	0.01908	0.00493	0.05916	14.95	0.0062

Bounds on condition number: 1.0618, 4.2474

All variables left in the model are significant at the 0.1000 level.

No other variable met the 0.1000 significance level for entry into the model

Table 5.11-Continued

Summary of Stepwise Selection								
Step	Variable Entered	Variable Removed	Number Vars In	Partial R-Square	Model R-Square	C(p)	F Value	Pr > F
1	Temp		1	0.3334	0.3334	16.7754	4	0.0805
2	COD		2	0.4254	0.7588	4.2398	12.35	0.0098
3	Stdn(NxP)		3	0.1073	0.8661	2.574	4.81	0.0708

5.2.3.2 Backward Deletion or Elimination

The regression in the backward deletion or elimination method is conducted by including all possible variables, then eliminating the predictor variables one by one, if they are not significant at the specified confidence level. In this study, the cut-off value of α is 0.1. Initially, ten predictor variables were considered in the model. From the regression equation obtained from the entire model, *p*-values were calculated for testing the following hypotheses: H_0: $\beta_k = 0$, H_1: $\beta_k \neq 0$. Then, the predictor variable with largest *p*-value (if *p* was greater than α = 0.1) was removed. The remaining parameters were regressed again, until all the remaining predictor variables were significant at α = 0.1. Table 5.12 displays the last five iterations. Table 5.13 shows the summary of the backward elimination method. A model with three predictor variables was chosen by the backward elimination method, which is the same model as the one selected by the stepwise method.

Table 5.12 Last Five Iterations of the Backward Elimination Method

Backward Elimination: Step 7
Variable Stdn(CODxP) Removed: R-Square = 0.8328 and C(p) = 3.7124

Analysis of Variance					
Source	DF	Sum of Squares	Mean Square	F Value	Pr > F
Model	3	0.09564	0.03188	9.96	0.0096
Error	6	0.0192	0.0032		
Corrected	9	0.11484			

Variable	Parameter Estimate	Standard Error	Type II SS	F Value	Pr > F
Intercept	-4.65051	1.44797	0.03301	10.32	0.0183
COD	0.00156	0.000431	0.04208	13.15	0.011
N	-0.07577	0.0465	0.00849	2.65	0.1544
Temp	0.017	0.00462	0.04335	13.55	0.0103

Backward Elimination: Step 8
Variable Stdn(NxP) Entered: R-Square = 0.8748 and C(p) = 4.2793
Note: The variable which previously had small tolerance is now allowed to enter after removal of some variables from the model.

Analysis of Variance					
Source	DF	Sum of Squares	Mean Square	F Value	Pr > F
Model	4	0.10046	0.02511	8.73	0.0177
Error	5	0.01438	0.00288		
Corrected	9	0.11484			

Variable	Parameter Estimate	Standard Error	Type II SS	F Value	Pr > F
Intercept	-4.74626	1.37486	0.03428	11.92	0.0182
COD	0.00222	0.000653	0.03327	11.57	0.0192
N	-0.03248	0.05535	0.00099	0.34	0.5829
Temp	0.017	0.00438	0.04335	15.07	0.0116
Stdn(NxP)	0.04008	0.03098	0.00482	1.67	0.2522

Bounds on condition number: 3.1591, 35.211

Table 5.12-Continued

Backward Elimination: Step 9

Variable N Removed: R-Square = 0.8661 and C(p) = 2.5740 Analysis of Variance					
Source	DF	Sum of Squares	Mean Square	F Value	Pr > F
Model	3	0.09947	0.03316	12.94	0.005
Error	6	0.01537	0.00256		
Corrected Total	9	0.11484			
Variable	Parameter Estimate	Standard Error	Type II SS	F Value	Pr > F
Intercept	-4.96822	1.24749	0.04064	15.86	0.0073
COD	0.00243	0.000517	0.05663	22.1	0.0033
Temp	0.01757	0.00403	0.04866	18.99	0.0048
Stdn(NxP)	0.05107	0.02329	0.01232	4.81	0.0708

Bounds on condition number: 2.0048, 15.154

Backward Elimination: Step 10

Variable Stdn(CODxN) Entered: R-Square = 0.8748 and C(p) = 4.2793

Note: The variable which previously had small tolerance is now allowed to enter after removal of some variables from the model.

Analysis of Variance					
Source	DF	Sum of Squares	Mean Square	F Value	Pr > F
Model	4	0.10046	0.02511	8.73	0.0177
Error	5	0.01438	0.00288		
Corrected	9	0.11484			
Variable	Parameter Estimate	Standard Error	Type II SS	F Value	Pr > F
Intercept	-4.81808	1.34634	0.03684	12.81	0.0159
COD	0.00272	0.000733	0.03952	13.74	0.0139
Temp	0.017	0.00438	0.04335	15.07	0.0116
Stdn(CODxII)	0.01837	0.03131	0.00099	0.34	0.5829
Stdn(NxP)	0.04008	0.03098	0.00482	1.67	0.2522

Bounds on condition number: 5.8998, 54.813

Table 5.12-Continued

Backward Elimination: Step 11

Variable Stdn(CODxN) Removed: R-Square = 0.8661 and C(p) = 2.5740

Analysis of Variance					
Source	DF	Sum of Squares	Mean Square	F Value	Pr > F
Model	3	0.09947	0.03316	12.94	0.005
Error	6	0.01537	0.00256		
Corrected Total	9	0.11484			

Variable	Parameter Estimate	Standard Error	Type II SS	F Value	Pr > F
Intercept	-4.96822	1.24749	0.04064	15.86	0.0073
COD	0.00243	0.000517	0.05663	22.1	0.0033
Temp	0.01757	0.00403	0.04866	18.99	0.0048
Stdn(NxP)	0.05107	0.02329	0.01232	4.81	0.0708

Bounds on condition number: 2.0048, 15.154

All variables left in the model are significant at the 0.1000 level.

Table 5.13 Summary of Backward Elimination

Summary of Backward Elimination								
Step	Variable Entered	Variable Removed	Number Vars In	Partial R-Square	Model R-Square	C(p)	F Value	Pr > F
1		Stdn(CODxTemp)	5	0.0054	0.9068	5.186	0.19	0.6954
2	Stdn(NxTemp)		6	0.0054	0.9122	7	0.19	0.6954
3		Stdn(NxTemp)	5	0.0054	0.9068	5.186	0.19	0.6954
4		Stdn(PxTemp)	4	0.032	0.8748	4.2793	1.37	0.3064
5		P	3	0.0419	0.8328	3.7124	1.67	0.2522
6	Stdn(CODxP)		4	0.0419	0.8748	4.2793	1.67	0.2522
7		Stdn(CODxP)	3	0.0419	0.8328	3.7124	1.67	0.2522
8	Stdn(NxP)		4	0.0419	0.8748	4.2793	1.67	0.2522
9		N	3	0.0086	0.8661	2.574	0.34	0.5829
10	Stdn(CODxN)		4	0.0086	0.8748	4.2793	0.34	0.5829
11		Stdn(CODxN)	3	0.0086	0.8661	2.574	0.34	0.5829

5.2.3.3 Best Subset Method for MLR Model Search

This method provides the specified number of best models with one or more variables. The following criteria were used for selecting the best models: (i) R^2, the coefficient of determination, should be high. R^2 is used to describe how well a particular model fits the data. Usually, R^2 does not decrease as the number of predictors increases. A model having as many predictors as possible may lead to a potentially inaccurate model. The best decision is to have the smallest model with a high R^2. (ii) Adjusted R^2 should also be high. Adjusted coefficient of determination (*Adj RSq*) penalizes the addition of useless variables. Therefore, the best decision is to have the smallest model with a high adjusted R^2. (iii) Mallows' *Cp* value should be small or close to the number of parameters in the model. If the model has no bias or if it has all the significant parameters included in it, the *Cp* value should be small; (iv) Akaike Information Criterion (AIC) and Schwarz Bayesian Criterion (SBC) should be small. AIC and SBC measure the relative goodness of fit for the model. Table 5.14 displays the results of the best subsets method.

Table 5.14 Best Subsets Method Results

Number in Model	C(p)	R-Square	Adjusted R-Square	AIC	SBC	Variables in Model
1	27.19480	0.02850	-0.09300	-40.95680	-40.35159	Stdn(CODxN)
1	27.24850	0.02690	-0.09470	-40.94060	-40.33541	Stdn(NxTemp)
1	19.84200	0.24370	0.14910	-43.46070	-42.85551	COD
1	16.77540	0.33340	0.25010	-44.72390	-44.11870	Temp
2	21.67600	0.24850	0.03380	-41.52510	-40.61735	COD Stdn(PxTemp)
2	21.49320	0.25390	0.04070	-41.59660	-40.68880	COD Stdn(NxTemp)
2	15.05010	0.44240	0.28310	-44.51000	-43.60221	COD Stdn(NxP)
2	15.08140	0.44150	0.28200	-44.49360	-43.58581	N P
2	4.23980	0.75880	0.68990	-52.89100	-51.98323	COD Temp
3	2.57400	0.86610	0.79920	-56.77680	-55.56645	COD Temp Stdn(NxP)
3	3.71240	0.83280	0.74920	-54.55430	-53.34396	COD Temp Stdn(CODxN)
3	3.71240	0.83280	0.74920	-54.55430	-53.34396	COD N Temp
3	3.71240	0.83280	0.74920	-54.55430	-53.34396	N Temp Stdn(CODxN)
4	3.79200	0.88900	0.80020	-56.65160	-55.13870	COD Temp Stdn(NxP) Stdn(PxTemp)
4	4.27930	0.87480	0.77460	-55.44270	-53.92978	COD Temp Stdn(CODxN) Stdn(CODxP)
4	4.27930	0.87480	0.77460	-55.44270	-53.92978	COD P Temp Stdn(NxP)
4	4.27930	0.87480	0.77460	-55.44270	-53.92978	COD Temp Stdn(CODxN) Stdn(NxP)
4	4.27930	0.87480	0.77460	-55.44270	-53.92978	COD N Temp Stdn(NxP)
5	5.18600	0.90680	0.79020	-56.39320	-54.57767	COD P Temp Stdn(NxP) Stdn(PxTemp)
5	5.18600	0.90680	0.79020	-56.39320	-54.57767	COD Temp Stdn(CODxN) Stdn(NxP) Stdn(PxTemp)
5	5.18600	0.90680	0.79020	-56.39320	-54.57767	COD Temp Stdn(CODxP) Stdn(NxP) Stdn(PxTemp)
5	5.18600	0.90680	0.79020	-56.39320	-54.57767	COD Temp Stdn(CODxN) Stdn(CODxP) Stdn(PxTemp)
5	5.18600	0.90680	0.79020	-56.39320	-54.57767	COD P Temp Stdn(CODxN) Stdn(PxTemp)
5	5.18600	0.90680	0.79020	-56.39320	-54.57767	COD N Temp Stdn(CODxP) Stdn(PxTemp)
5	5.18600	0.90680	0.79020	-56.39320	-54.57767	COD N P Temp Stdn(PxTemp)
6	7.00000	0.91220	0.73660	-54.99460	-52.87647	COD Temp Stdn(CODxP) Stdn(CODxTemp) Stdn(NxTemp) Stdn(PxTemp)
6	7.00000	0.91220	0.73660	-54.99460	-52.87647	P Temp Stdn(CODxTemp) Stdn(NxP) Stdn(NxTemp) Stdn(PxTemp)
6	7.00000	0.91220	0.73660	-54.99460	-52.87647	COD Temp Stdn(CODxTemp) Stdn(NxP) Stdn(NxTemp) Stdn(PxTemp)
6	7.00000	0.91220	0.73660	-54.99460	-52.87647	COD N Temp Stdn(CODxTemp) Stdn(NxP) Stdn(PxTemp)
6	7.00000	0.91220	0.73660	-54.99460	-52.87647	COD P Temp Stdn(CODxN) Stdn(CODxTemp) Stdn(PxTemp)

From Table 5.14, it can be seen how Adjusted R^2 jumps up from the 2-predictor to the 3-predictor models. This indicates that, in this study, the 2-predictor models are clearly inferior. In addition, Table 5.14 shows that the highest Adjusted R^2 drops from the 4-predictor to the 5-predictor models, indicating that the models with 5 or more predictors have useless predictors, so these models were eliminated from consideration.

5.2.3.4 Best Model Selection

Based on all three selection methods mentioned above, the models in Table 5.15 were considered.

Table 5.15 Models considered from the Best Subsets Method

Model	Number of Var. in Model	C(p)	R-Square	Adjusted R-Square	AIC	SBC	Variables in Model
A	3	2.57400	0.86610	0.79920	-56.77680	-55.56645	COD Temp Stdn(NxP)
B	4	3.79200	0.88900	0.80020	-56.65160	-55.13870	COD Temp Stdn(NxP) Stdn(PxTemp)

After the analyses of the results from the Model Selection Processes, the Model A was selected because it most closely met all the previously described criteria. In addition, Model A was the model selected by both selection methods Stepwise and Backward Deletion.

5.3 The Final Model

The following equation represents the selected final model.

$$k = - 4.96822 + 0.00243\text{COD} + 0.01757\text{T} + 0.05107(\text{N x P})$$

where,

k = methane generation rate constant, in terms of first order decomposition constant (day^{-1});

COD = Chemical Oxygen Demand concentration (g/L);

N = Nitrogen concentration (g/L);

P = Phosphorus concentration (g/L);

T = Temperature in the mesophilic range (K);

The parameter estimates of the selected model are presented on Table 5.16. All predictor terms in the model were significant at α = 0.1 level (p-values were less than significance level). All the variance inflation factors were less than five, indicating that there was not much serious multicollinearity. As discussed earlier, the parameters representing sulfur and potassium were excluded from this model because these parameters were inducing biased results. This model shows that the k values increase with COD, temperature, and the interaction between nitrogen and phosphorus.

Table 5.16 Parameter Estimates for the Final Model

Parameter Estimates							
Variable	DF	Parameter Estimate	Standard Error	t Value	Pr > |t|	Type I SS	Variance Inflation
Intercept	1	-4.96822	1.24749	-3.98	0.0073	4.43556	0
COD	1	0.00243	0.000517	4.7	0.0033	0.02798	1.95265
Temp	1	0.01757	0.00403	4.36	0.0048	0.05916	1.09405
Stdn(NxP)	1	0.05107	0.02329	2.19	0.0708	0.01232	2.00478

The ANOVA table for the selected model is presented on Table 5.17. Table 5.18 shows the results of simple statistics calculations. Pearson Correlation Coefficients are shown on Table 5.20.

Table 5.17 ANOVA Table for the Selected Model

Analysis of Variance					
Source	DF	Sum of Squares	Mean Square	F Value	Pr > F
Model	3	0.09947	0.03316	12.94	0.005
Error	6	0.01537	0.00256		
Corrected Total	9	0.11484			

Root MSE	0.05062	R-Square	0.8661
Dependent Mean	0.666	Adj R-Sq	0.7992
Coeff Var	7.60046		

Table 5.18 Final Model Simple Statistics Calculations Results

Simple Statistics						
Variable	N	Mean	Std Dev	Sum	Minimum	Maximum
kvalue	10	0.666	0.11296	6.66	0.52	0.88
COD	10	89.36	45.62122	893.6	2.6	147
Temp	10	308.5	4.37798	3085	303	313
Stdn(NxP)	10	-0.0439	1.02583	-0.4392	-0.8483	2.28122

Table 5.19 Pearson Correlation Coefficients

Pearson Correlation Coefficients, N = 10 Prob > |r| under H0: Rho=0				
	kvalue	**COD**	**Temp**	**Stdn(NxP)**
kvalue	1	0.49362	0.57742	-0.02451
		0.1471	0.0805	0.9464
COD	0.49362	1	-0.24133	-0.69718
	0.1471		0.5018	0.025
Temp	0.57742	-0.24133	1	0.28763
	0.0805	0.5018		0.4203
Stdn(NxP)	-0.02451	-0.69718	0.28763	1
	0.9464	0.025	0.4203	

Table 5.19 shows that there is correlation between the *k* value and the standardized interaction of Nitrogen with Phosphorus because their Pearson Correlation Coefficient numeric value 0f 0.9464 is greater than |0.7|. Therefore, these variables exhibit multicollinearity. Most of the other correlation coefficients were non-zero, which indicated that there was some correlation between all predictors and response variables. As previously discussed, due to the mixture design of this experiment, some multicollinearity of the data was unavoidable

5.3.1 Reasonability of Model Form

In order to view the current model form, the following plots are displayed. Each plot represents the residuals versus each of the variables. Figure 5.11 represents the variation of the residuals with each of the predictive variables.

After performing a sight analysis of the plots, it was concluded that the model is adequate in respect of form because no curvature was identified in the plots.

Conclusion: Since there is no curvature in the plots, shown in Figure 5.11, the current MLR model form is acceptable.

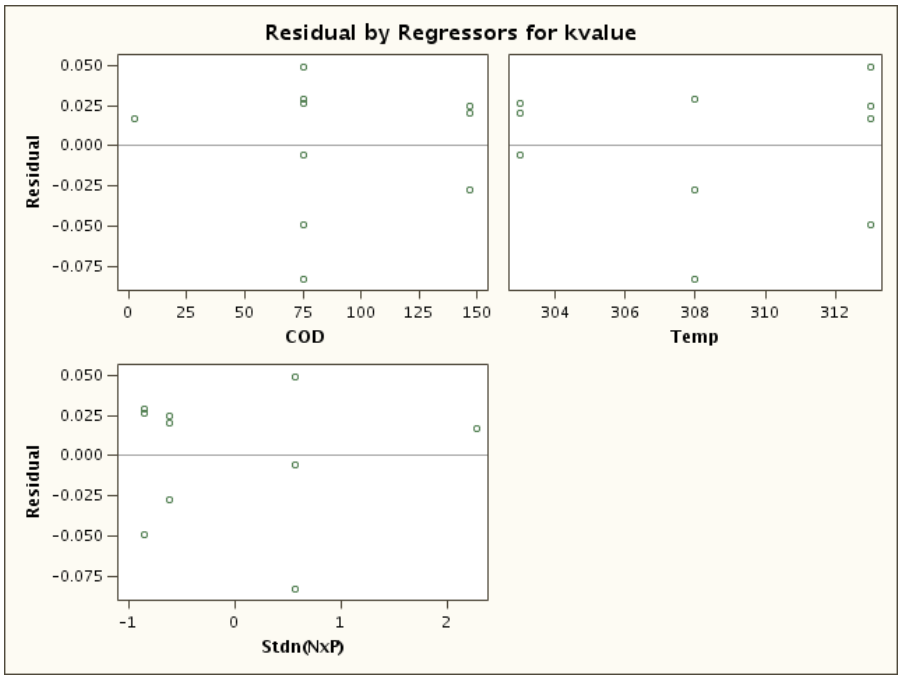

Figure 5.11 Final Model Residuals versus Predictive Variables

5.3.2 Normally Distributed Residuals

In order to test whether the residuals are normally distributed or not, one may, first, take a look at the residuals versus normal scores plot. This plot is also known as the Normal Probability Plot (NPP). The SAS output for normal probability plot is shown in Figure 5.12. After that, a hypothesis test on normality is conducted.

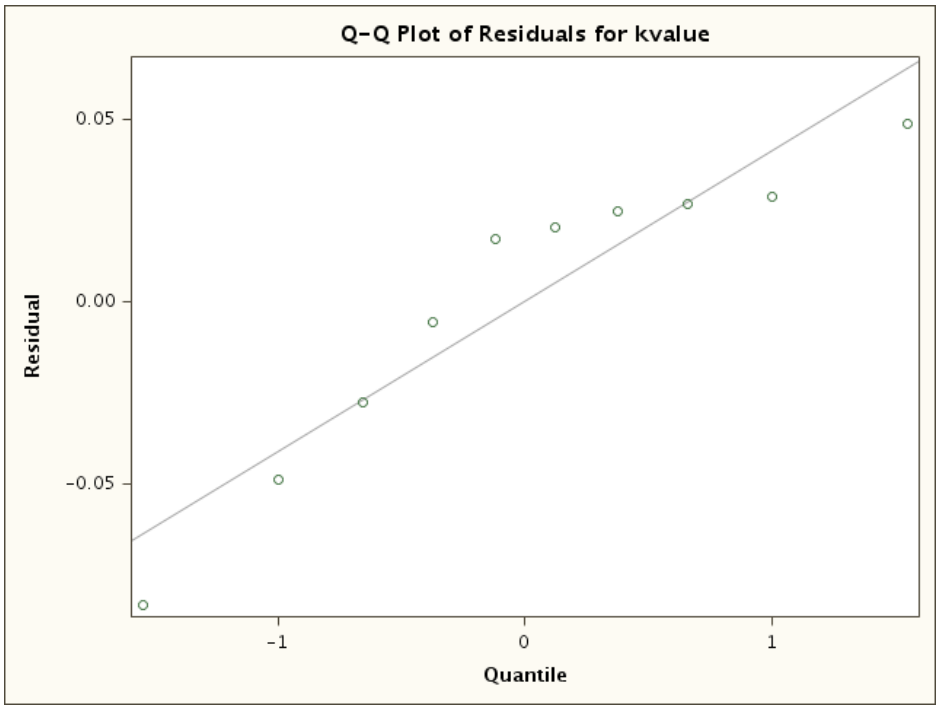

Figure 5.12 Final Model Normal Probability Plot

In the Figure 5.12, one can see that the NPP does not display much curvature. Therefore, from visual analysis, the following conclusion is reached: The residuals are almost normally distributed. In view of the fact that normality is desired, but not required, this issue does not pose as a severe violation.

The Normality Test

The normality test was performed. The null and alternate hypotheses are:

H0: Normality is OK.

H1: Normality is violated.

The correlation between residuals and normal scores is shown on table 5.20. The correlation coefficient, ρ = 1.0. The cut off value for α = 0.10, c(α, n) = c(0.10,10) = 0.952. Since the calculated ρ = 1.0 is greater than the cut off value of c(0.10,10) = 0.952, we fail to reject the null hypothesis and conclude that normality is OK.

Table 5.20: SAS Output for Normality Test

Simple Statistics						
Variable	N	Mean	Std Dev	Sum	Minimum	Maximum
e	10	1.00E-11	0.04133	1.00E-10	-0.0835	0.04872
e_normal	10	0.5	0.01648	5.00004	0.46675	0.51943

Pearson Correlation Coefficients, N = 10 Prob > |r| under H0: Rho=0		
	e	e_normal
e	1	1
		<.0001
e_normal	1	1
	<.0001	

5.3.3 *Constant Variance of Residuals*

In order to make a decision about this assumption, the residual analysis was conducted. A regression-based model assumes that the errors have constant variance. Therefore, the plot of the residuals versus the predicted *k* value should present randomly scattered dots. When such plot displays a funnel shape, it means that the residuals have non-constant variance.

Figure 5.13 represents the residuals versus the predicted values of methane generation rate.

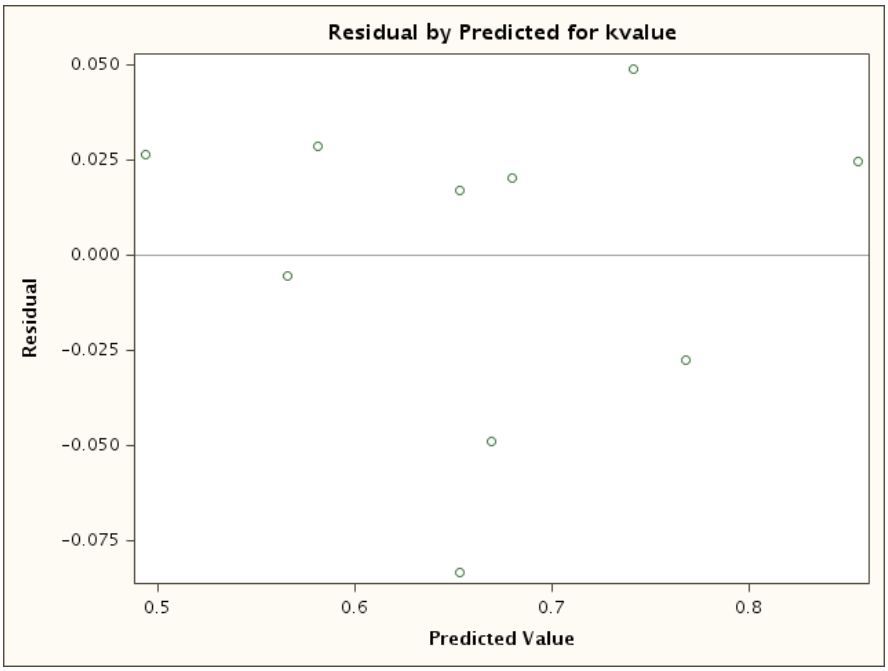

Figure 5.13 Final Model Residuals versus the Predicted *k* Values

After performing a sight analysis of the plot on Figure 5.13, no funnel shape was observed, which means that this model exhibits constant variance.

Modified Levene Test for Constant Variance:

In order to detect non-constant variance, the Modified Levene Test was conducted. In order to perform the Modified Levene Test, the data is divided into two groups, based on the fitted values. For this model, the number of observations in each group was equal to 5. In this case, the dividing point was the median value of *k* value, the predicted methane generation rate, 0.666 (mean *k* value). The points with *k* value greater than 0.666 were placed in group 1, and the points with *k* value less than the median value were placed in group 2. The absolute deviations of residuals around the medians were calculated for each group. The Modified–Levene test was performed through SAS by using the two-sample t-test. Table 5.21 shows the output of the Modified Levene Test.

Table 5.21 SAS Output of the Final Model Modified Levene Test

The TTEST Procedure

Variable: AbsoluteGroupd_FinalModel

MeanFinalPred_k	Method	Mean	95% CL Mean		Std Dev	95% CL Std Dev	
0.666		0.0511	0.00749	0.0947	0.0351	0.021	0.1009
0.6661		0.0551	0.00126	0.109	0.0434	0.026	0.1246
Diff (1-2)	Pooled	-0.00402	-0.0616	0.0535	0.0395	0.0267	0.0756
Diff (1-2)	Satterthwaite	-0.00402	-0.062	0.054			

Method	Variances	DF	t Value	Pr > |t|
Pooled	Equal	8	-0.16	0.8762
Satterthwaite	Unequal	7.6684	-0.16	0.8763

Equality of Variances				
Method	Num DF	Den DF	F Value	Pr > F
Folded F	4	4	1.53	0.6926

For H_0: Variances of the two groups are equal, the Pr > F = 0.6926.

Since the *p*-value > α = 0.10, we fail to reject the null hypothesis and conclude that the variances in two groups are equal.

Now an analysis is performed by looking for the “Equal” case in T test. For the “Equal” case, Table 5.21 shows that Pr > |t| = 0.8762. This, again, is greater than the value of α = 0.10 (and even when α = 0.05). Therefore, we, again, fail to reject the null hypothesis and conclude that the variance is constant.

Conclusion: The constant error variance assumption is satisfied.

5.3.4 Uncorrelated Residuals

The analysis of a Multi Linear Regression model requires that the errors be uncorrelated or independent from each other. In order to check if the residuals are uncorrelated, a time series plot is used. If an increasing or decreasing trend in the time series plot is identified, it indicates that the errors are correlated. In this research, all the reactors were operated independently from each other, and the *k* values were computed from these reactors.

Therefore, the *k* values were not expected to be correlated and time series plots were not plotted.

5.3.5 Diagnostics (Outlier, Leverage, Variance Inflation)

Leverage values (X-outlier): The x-outliers are identified by performing a visual assessment of the diagonal elements of H, H_{ii}, (also known as the Leverage Values). In order to determine if a specific H_{ii} should be considered large, the following guideline was used: If H_{ii} > 2*hbar* = *2p/n*, then, it is considered large. For these calculations, *p* = number of parameters in the model, and *n* = total number of observations. This model cutoff value (2*p/n*) = (2*4/10) = 0.8. Looking at the values, shown in Table 5.22, it can be seen that Observation #1 has the highest the leverage value of 0.7081, which is lower than this model cutoff value of 0.8. Therefore, it has been concluded that this model has no x-outliers.

Bonferroni Outlier Test (Y-Outlier): The Studentized Deleted Residuals (t_i) are shown in the Table 5.22 as "RStudent". The guideline for the Bonferroni Outlier Test is: If $|t_i| > t(1-\alpha/2n; n-p-1)$, then observation *i* is a y-outlier. This model cutoff values for the Bonferroni Outlier Test were, $t(1-\alpha/2n; n-p-1) = t(0.995; 5) = 4.032$, at $\alpha = 0.1$. Based on the results, shown on table 5.23, there is no y-outlier in this dataset.

Table 5.22 presents the diagnostics to test for outliers, leverage and influence of outliers.

Table 5.22: Final Model Diagnostics to Test for Outliers, Leverage, and Influence of Outliers

Obs	Residual_k2	Cook d_k2	Hat Hii_k2	RStudent_k2	Dffits_k2
1	0.01700	0.23442	0.70810	0.58676	0.91389
2	-0.00562	0.00315	0.38621	-0.12949	-0.10271
3	-0.08345	0.14194	0.15069	-2.39048	-1.00692
4	0.04872	0.09126	0.23228	1.12181	0.61706
5	0.02020	0.05162	0.42648	0.49255	0.42475
6	-0.02763	0.04577	0.30054	-0.61824	-0.40525
7	0.02453	0.11175	0.49171	0.64591	0.63529
8	0.02658	0.11924	0.47559	0.69309	0.66004
9	0.02875	0.05891	0.32895	0.65991	0.46203
10	-0.04908	0.46854	0.49943	-1.50956	-1.50784

Variance Inflation: In order to check for variance inflation, the Variance Inflation factor (VIF) values need to be checked. The decision rule is:

If $\overline{VIF} = \frac{\sum_{k=1}^{p-1}(VIF)_k}{p-1}$ >> 1 and max $(VIF)_k > 10$, then there is serious multicollinearity. Moreover, we need to avoid any model with any $(VIF)_k > 5$.

The VIF values of this model are presented in Table 5.16 The average VIF = (1.95265+1.09405+2.00478)/3 = 1.684, which is not much greater than 1. In addition, none of the individual VIF values is greater than 5.

Conclusion: There is no serious multicollinearity issue in this model.

5.4 Evaluation of the Selected Model

From the above analysis, it has been concluded that all the model assumptions are reasonably satisfied for this model. Therefore, we accept this model as this research selected model, VUMP.

After examining the ANOVA Table, Table 5.17, the following conclusions can be reached:

- Total sum of squares, SSTO**:** This is the sum of explained and unexplained variability (SSR+SSE), and has a degree of freedom n-1. As found from the ANOVA table, SSTO = 0.11484. The model Degree of Freedom = 3.
- Regression sum of squares, SSR: This is the total variability in the methane generation rate that is explained by this model. As found from the ANOVA table, SSR = 0.09947.
- Error sum of squares, SSE: This is the unexplained variability in the model. As found from the ANOVA table, SSE = 0.01537.
- Mean square for regression, MSR: This is the SSR divided by its degrees of freedom. In this model, MSR = 0.03316.

- Mean square for error, MSE: This is the SSE divided by its degree of freedom. In this model, MSE = 0.00256. MSE is an unbiased estimator of the variance (σ^2) of the original random error term, ε_i.
- The F* value: This is a value used to interpret if the regression is significant. It is actually the ratio of MSR to MSE. In case of this model it is 12.94. The fact that the F* value is reasonably greater than 1 indicates that the mean variability of the methane generation rate, explained by the model, is greater than the mean unexplained variability. It also indicates that the regression is significant.
- The Final Model *p*-value = 0.005, which is significant at the 0.10 level (and even when α = 0.05).
- Explained Variability:

As seen from the ANOVA table, the values for the coefficient of determination, R^2 and the Adjusted R^2, R_a^2, are 0.8661 and 0.7992, respectively. Since these two values are not greatly apart, this means that all the variables play a role in explaining the model. Additionally, the R^2 value of 0.8661 means that 86.61% of the variability of *k* value was explained by the predictors in this model.

Conclusion: This study presents a Multiple Linear Regression Model that satisfies all the assumptions of MLR. This model was tested to be strongly significant and it explained 86.61% of the variability of the methane generation rate from the decomposition of synthetic vinasse.

5.5 Validation of the VUMP Model

5.5.1 Estimation of $k_{calculated}$

A hybrid solution of real vinasse mixed with glucose was used to validate the model. The real vinasse was obtained from the White Energy Ethanol Distillery. The vinasse solution had the following composition: COD = 3.171g/L; N = 0.0662g/L; P = 0.2887g/L. The hybrid

vinasse solution was decomposed at 35°C. The VUMP model was used to compute the *k* value.

The following equation represents the VUMP model.

$$k = - 4.96822 + 0.00243COD + 0.01757T + 0.05107(N \times P)$$

where,

k = methane generation rate constant, in terms of first order decomposition constant (day^{-1});

COD = Chemical Oxygen Demand concentration (g/L) = 3.171g/L;

N = Nitrogen concentration (g/L) = 0.0662g/L;

P = Phosphorus concentration (g/L) = 0.2887g/L;

T = Temperature in the mesophilic range (K) = 308 K

Substituting the numerical values into the above equation,

$k_{calculated}$ = 0.452 per day.

5.5.2 Estimation of k_{actual}

The daily methane volume was obtained from the real vinasse hybrid solution, as discussed in the previous section. The methane content reached as high as 71%. The mathematical approach used to estimate k_{actual} was the following:

Methane production was recorded versus time for the real (actual) vinasse formula. Cumulative methane volume was estimated using the following equation:

$$V = L_o(1-e^{-kt}) \qquad (3\text{-}1)$$

where,

V= Cumulative volume of methane per liter of vinasse (mL/L),

L_o = Ultimate methane potential (mL/L) = 475.317 mL/L of vinasse,

k = first-order methane generation rate constant (day^{-1}),

t = time (days).

Rearranging Eq. 3-1 and taking the natural log of both sides gives:

$$\ln(1-V/L_o) = -kt$$

If $\ln(1-V/L_o)$ is plotted vs. time, the negative value of the slope gives k. L_o was estimated from the horizontal asymptote of the plots of $\ln(1-V/L_o)$ vs. time. When the plot did not clearly reach an asymptote, the value of L_o was chosen which gave the largest R^2 value for a regression line fit to $\ln(1-V/L_o)$ vs. time. Figure 5.15 displays the plot of real vinasse data versus time. After these calculations, it was determined that k_{actual} = 0.378/day. The calculated and actual k values agreed fairly well. Figures 5.15, 5.16, and 5.17 display the methane generation pattern exhibited by the anaerobic decomposition of real (actual) vinasse.

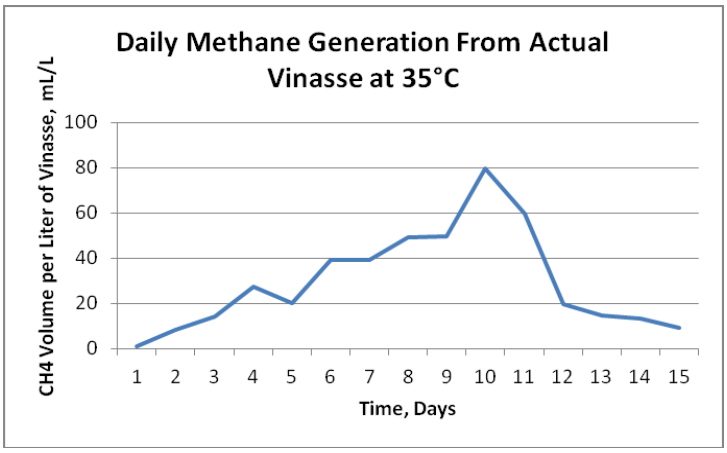

Figure 5.14 Daily Methane Generation from Actual Vinasse at 35°C

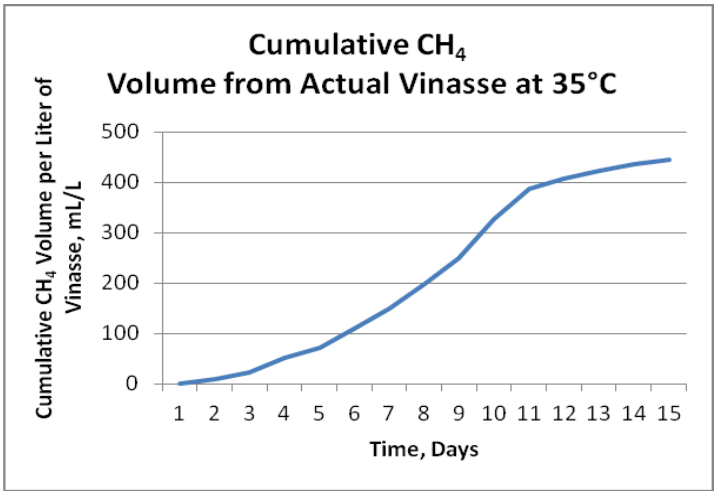

Figure 5.15 Cumulative CH_4 Volume from Actual Vinasse at 35°C

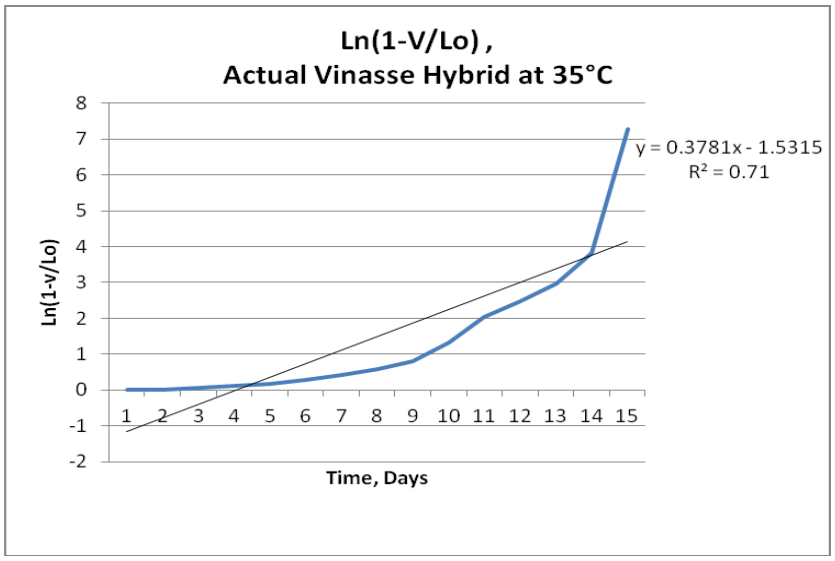

Figure 5.16 Graphical Representation of k_{actual} Determination

CHAPTER 6

CONCLUSIONS AND RECOMMENDATIONS

Currently, treatment solutions that convert industrial wastewater into co-products are important opportunities for recycling valuable substances and generating energy, as well as combating environmental pollution. This work presents a viable treatment solution for ethanol distillery wastewater, as well as the development of a mathematical model for predicting methane generation rates from the anaerobic digestion of vinasse. This model is named VUMP (Vinasse Utilization for Methane Production). The effects of six parameters (temperature, COD, N, P, K, and S) on methane generation in batch-type bioreactors have been studied. Methane generation vs. time has been measured, and used to develop a multiple linear regression model for predicting methane generation as a function of the 6 parameters.

This research has the potential for broad impacts in many countries because it promotes treatment of vinasse, instead of disposed '*in natura'* [as is] on agricultural fields. The model enables methane generation to be estimated from a variety of vinasse compositions. It will be the first such widely applicable model, to our knowledge.

Initially, a strength 2 orthogonal array experimental design (V. Chen, 2011) was used for the laboratory scale setup. The resulting 18 batches, representing 18 synthetic vinasse compositions, to be run at 3 temperatures were then subject to anaerobic decomposition. After collecting the data from each of those 18 batches, 4 of the best methane-producing formulations were repeated at three different temperatures (30, 35, and 40°C). The results from the selected best methane-producing formulations were then used in the development of a multi linear regression equation for estimating the methane generation rate from synthetic vinasse.

6.1 Summary and Conclusions

The results from this research can be summarized as follows:

- Formula #1 at 30°C generated the highest percent of methane, when compared to all the other batches. The high methane volumes associated with Formula #1 may be attributed to the fact that the quantity of ammonia, which had been added to the vinasse solution as the nitrogen source, was within the recommended range. High concentrations of ammonia can inhibit the methanogenic activities. All the constituents in Formula #1 had the minimum values reported by Wilkie et al. (2000). The low quantity of H_3PO_4 resulted in less need for NaOH to keep the pH in the optimum range of 7-8.0, meaning less potential sodium toxicity for microbes. On the other hand, the lower quantities of KOH resulted in no need to decrease the pH with HCl. This reduced potential chloride toxicity for the methanogenic microorganisms. The small quantity of sulfur also meant less potential sulfate toxicity.
- For Formula #4, all batches started generating methane on Day #1. The batch operated at 30°C generated the lowest volume on Day #1 and the 40°C batch generated the most. This indicates a faster start to methane production with higher temperature, which is consistent with increased microbial activity.
- Formula #9, which had the highest quantity of glucose, did not generate exceptionally high volumes of methane. One explanation for these results may be due to the fact that the higher quantity of glucose, added as COD source, enabled the uncontrollable multiplication of several other different microbiological species, which may have reproduced at a faster rate than the methanogens, thus competing for the food and, perhaps, consuming the methanogens. Another reason for the mediocre methane volumes from Formula #9 may be due to the fact that the carboxylic acids, produced by the increased microbiological activities, caused the pH to drop to below the recommended range for the survival of the methanogens.
- The plots from Formula #12 (COD = 75g/L) displayed two, three, and two peaks, when decomposed at 30, 35, and 40°C, respectively. The presence of multiple peaks may be due

to different quantities of the carbon source being consumed at different rates, and, perhaps, due to changes in pH affecting microbial activities.

- The ultimate methane production (asymptotic cumulative value) for Formulas #4, 9, and 12, when decomposed at 35°C, were comparable (only slightly higher) than at 30°C. This is to be expected, since the change in temperature would be anticipated to affect how fast the methane is produced, but not the total quantity produced.
- Using the collected data, a multiple linear regression (MLR) equation for predicting the first-order decay constant, *k,* from vinasse, was developed. The best model was selected using the following model selection algorithms: backward elimination, stepwise regression, and the best subsets. All parameter were significant at α = 0.1. The selected model had an adjusted R^2 of 0.8661. The following equation represents the selected model.

  k = - 4.96822 + 0.00243COD + 0.01757T + 0.05107(N x P)

  where,

  k = methane generation rate constant, in terms of first order decomposition constant (day^{-1});

  COD = Chemical Oxygen Demand concentration (g/L);

  N = Nitrogen concentration (g/L);

  P = Phosphorus concentration (g/L);

  T = Temperature in the mesophilic range (K);

  This model shows that the k values increase with COD, temperature, and the interaction between nitrogen and phosphorus.
- The rate constants are high enough that anaerobic treatment of vinasse seems viable for commercial production of methane, with scaled-up testing.

6.2 Recommendations for Future Studies

Future studies recommendations for estimating the methane generation rate from vinasse decomposition include the following:

- In order to test the VUMP Model's effectiveness in predicting methane generation rates from synthetic vinasse, the validation of this model is recommended. The dataset used for this model validation should originate from the decomposition of varying quantities of COD, N, P, K, S, and temperature.
- Utilize reactors containing automatic pH adjustment devices for the decomposition of vinasse may improve the prediction efficiency of this model.

APPENDIX A

INITIAL EXPERIMENTAL DESIGN

Table A.1 Strength 2 Orthogonal Array

Run	Reactor	Temp	COD	N	P	K	S
1	0	0	0	0	0	0	0
2	1	1	1	1	1	1	0
3	2	2	2	2	2	2	0
4	0	0	1	2	1	2	0
5	1	1	2	0	2	0	0
6	2	2	0	1	0	1	0
7	0	1	0	2	2	1	1
8	1	2	1	0	0	2	1
9	2	0	2	1	1	0	1
10	0	2	2	0	1	1	1
11	1	0	0	1	2	2	1
12	2	1	1	2	0	0	1
13	0	1	2	1	0	2	2
14	1	2	0	2	1	0	2
15	2	0	1	0	2	1	2
16	0	2	1	1	2	0	2
17	1	0	2	2	0	1	2
18	2	1	0	0	1	2	2

Table A.2 Organization of the Initial Experimental Design, Based on the Set Temperature

Temp (°C)	Synthetic Vinasse Composition (g of constituents per L of vinasse)					Run	Reactor label	Period
	COD, $C_6H_{12}O_6$	N, NH_3	P, H_3PO_4	K, KOH	S, $CaSO_4$			
30	2.6	0.06	0.007	0.039	0.034	25	A	1st
30	2.6	0.55	0.7	1.742	0.58	26	B	1st
30	147	0.55	0.09	0.039	0.58	27	C	1st
30	75	1.2	0.09	1.742	0.034	4	A	2nd
30	147	1.2	0.007	0.4	1.47	17	B	2nd
30	75	0.06	0.7	0.4	1.47	15	C	2nd
35	2.6	1.2	0.7	0.4	0.58	7	A	3rd
35	75	0.55	0.09	0.4	0.034	2	B	3rd
35	75	1.2	0.007	0.039	0.58	12	C	3rd
35	147	0.55	0.007	1.742	1.47	13	A	4th
35	147	0.06	0.7	0.039	0.034	5	B	4th
35	2.6	0.06	0.09	1.742	1.47	18	C	4th
40	75	0.55	0.7	0.039	1.47	16	A	5th
40	2.6	1.2	0.09	0.039	1.47	14	B	5th
40	147	1.2	0.7	1.742	0.034	3	C	5th
40	147	0.06	0.09	0.4	0.58	10	A	6th
40	75	0.06	0.007	1.742	0.58	8	B	6th
40	2.6	0.55	0.007	0.4	0.034	6	C	6th
30	Actual Vinasse						A	7th
35	Actual Vinasse						A	8th
40	Actual Vinasse						A	9th

REFERENCES

1. Alex, LK (2008), “Control of Disinfection By-products”; M.Sc. Thesis in Environmental Management, University of Hong Kong, Hong Kong.
2. Almeida, J.R. (1952). “Ação da vinhaça na saúde pública.” *Revista de Agricultura,* Piracicaba, 27 (9-10): 269-74. Brazil.
3. Almeida, V. P. S. (2006). “Acidez orgânica na precipitaçâo e uso do solo no Estado de São Paulo: variabilidade espacial e temporal.” PhD Dissertation, Universidade de São Paulo, USP, São Paulo, Brazil.
4. Afotey, Benjamin (2008). “Statistical approach to the development of a micro scale model for estimating exhaust emissions from light duty gasoline vehicles.” PhD Dissertation, The University of Texas at Arlington, Texas, USA.
5. Ahring, B.K. (1994). “Status on science and application of thermophilic anaerobic digestion.” *Water Science and Technology*, 30 (12), 241-249.
6. Alvarez, David A., Cranor, Walter L., Perkins, Stephanie D., Clark, Randal C., Smith, Steven B. (2008). “Chemical and Toxicologic Assessment of Organic Contaminants in Surface Water Using Passive Samplers.” *J Environ Quality* 37: 1024-1033.
7. Assan, Marco André de Carvalho (2006). “Avaliação do desempenho de um reator biológico de discos rotativos, biodiscos, no tratamento de efluentes da indústria sucroalcooleira.” MS Thesis, Universidade de Ribeirão Preto, São Paulo, Brazil.
8. Athappan, Annaprabha (2008). “Adsorption curve fits for landfill VOCs on bituminous coal based and coconut shell based activated carbon.” M.S. Thesis; The University of Texas at Arlington, Texas, USA.
9. Bach, Morgana (2004), “The role of calcium in and methodologies for overcoming pH excursions for reactivated granular activated carbon”, M Engr. Degree Thesis, University of Florida
10. Basanta, M. V., D. Dourado-Neto, K. Reichardt, O. O. S. Bacchi, J. C. M. Oliveira, P. C. O. Trivelin, L. C. Timm, T. T. Tominaga, V. Correchel, F. A. M. Ca´ ssaro, L. F. Pires, and J. R. de Macedo (2003). “Management effects on nitrogen recovery in a sugarcane crop grown in Brazil.” *Geoderma* 116:235–248.
11. Berton, H., Bill Kovarik and Scott Sklar (1982). “The Forbidden Fuel: Power Alcohol in the Twentieth Century;” New York: Boyd Griffin.
12. Bezerra Viana, A. (2006). “Tratamento Anaeróbico da Vinhaça em Reator UASB, Operado em Temperatura na faixa termofílica (55º C) e submetido ao Aumento Progressivo da Carga Orgânica.” MS Thesis, Engineering School of São Carlos at the University of São Paulo, São Paulo, Brazil.
13. Brunauer, S, Emmett, P.H., Teller, E. (1938), “Adsorption of Gases in Multimolecular Layers”, *J. Am. Chem. Soc.*, *60* (2), pp 309–319.

14. Chan, C. K., Porter, J. F., Li, Y. G., Guo, W., and Chan, C-M. (1999), “The effect of calcination on the microstructures and photocatalytic properties of nano-sized TiO2 powders prepared by vapor hydrolysis.” *J. Am. Ceram. Soc*., 82(3), 566-572.

15. Camhi, J.D. “Tratamento do vinhoto subproduto da destilação de álcool. *Brasil Açucareiro.”* Rio de Janeiro, v.94, n.l, p.18-23, 1979. Brazil.

16. Capel, Paul D., McCarthy, Kathleen A., Barbash, Jack E. (2008). “National, Holistic, Watershed-Scale Approach to Understand the Sources, Transport, and Fate of Agricultural Chemicals.” *J Environ Quality*, 37: 983-993.

17. Chaiprasert, Manus (1996). “Hydrologic Modeling within the GIS Environment.” PhD Dissertation, University of Texas at Arlington, Texas USA.

18. Chan, C. K., Porter, J. F., Li, Y. G., Guo, W., and Chan, C-M. (1999) “The effect of calcination on the microstructures and photocatalytic properties of nano-sized TiO2 powders prepared by vapor hydrolysis.” *J. Am. Ceram. Soc*., 82(3), 566-572.

19. Cheesman, Oliver (2004). “Environmental impacts of sugar production: the cultivation and processing of sugarcane and sugar beet.” CABI Bioscience, Surrey, UK.

20. Coêlho, A.C.D. (2007). “Instruções sobre o tratamento da vinhaça.” In: Reunião dos Profissionais das Indústrias de Açúcar e Álcool do Nordeste, Recife, Brazil.

21. Coelho, M. B. & Peixoto, M. J. C. (1986). “Considerações econômicas sobre aplicação da vinhaça por aspersão em cana-de-açúcar.” In: Congresso Nacional da STAB, 2, Rio de Janeiro, Brazil.

22. Collischonn, Walter et al (2006). “Distributed Hydrological Model for Prevision of Incremental Discharge in the Paranaíba River Basin between Itumbiara and São Simão.” Universidade Federal do Rio Grande do Sul, Rio Grande do Sul, Brazil.

23. Committee on Review and Evaluation of the Army Chemical Stockpile Disposal Program, National Research Council (1999), “Carbon Filtration for Reducing Emissions from Chemical Agent Incineration”, 102p. Commission on Engineering and Technical Systems (CETS), Engineering and Physical Sciences (DEPS).

24. Cortez L. A. and Perez, L.E. (1997). “Experiences on Vinasse Disposal, Part III: Combustion of vinasse -#6 fuel oil emulsions.” *Brazilian Journal of Chemical Engineering*, vol. 14 no. 1, Mar. São Paulo, Brazil.

25. Costa, M. C. G., G. C. Vitti, and H. Cantarella (2003). “Volatilizacao de N-NH3 de fontes nitrogenadas em cana-de-acucar colhida sem despalha e fogo.” *Revista Brasileira de Ciência do Solo*, Viçosa 27:631–637. Brazil.

26. Crosby, E. (2004), Non-published lectures on CE 5347 “Groundwater Hydrology”, University of Texas at Arlington.

27. Davini, Paolo, (2002), “Flue gas treatment by activated carbon obtained from oil-fired fly ash”, *Carbon* Vol. 40, issue 11, September 2002, p. 1973-1979, Italy.

28. De Paula Jr., D.R., Gurgel, M.N.A (2008). “Potentialities of the biodigestion of the vinasse.” http://www.cori.unicamp.br/centenario2008/2007/completos/A09%20-

%20POTENTIALITIES%20OF%20THE%20BIODIGESTION%20OF%20THE%20VINASSE.pdf (Accessed on October, 01, 2009).

29. Dilmore, Robert Michael (2005). “Evaluation of the Kinetics of Biologically Catalyzed Treatment and Regeneration of NOX Scrubbing Process Waters.” PhD Dissertation, University of Pittsburg, Pennsylvania, USA.

30. Dirkse, Martijn H (2007). “Spatial Model Reduction for Transport Phenomena in Environmental and Agricultural Engineering.” PhD Dissertation, Wageningen University, Wageningen, Netherlands.

31. Domagalski, Joseph L., Ator, Scott, Coupe, Richard, McCarthy, Kathleen, Lampe, David, Sandstrom, Mark, Baker, Nancy (2008). “Comparative Study of Transport Processes of Nitrogen, Phosphorus, and Herbicides to Streams in Five Agricultural Basins.” USA, *J Environ Quality*, 37: 1158-1169.

32. Espinoza-Escalante, Froylán M. (2008). "Estudio fisicoquímico y microbiano del proceso de digestión anaerobia de efluentes agroindustriales orientado a la producción de hidrógeno y metano". Tesis de Doctorado; Doctorial Dissertation, Universidad de Guadalajara, Jalisco, Mexico.

33. Fujishima A, Hashimoto K, Watanabe T. (1999). “TiO2 photocatalysis: fundamentals and applications.” Tokyo: BKC, Inc.

34. Gagliardo, P., S. Adham, R. Trussell, A. Olivieri, (1998). “Water repurification via reverse osmosis.” *Desalination* 117, 73.

35. Gluhoi, Andreea Catalina (2005). “Fundamental studies focused on understanding of gold catalysis.” Doctoral Thesis, Leiden University, The Netherlands.

36. Glória, N.A. (1975). “Emprego da vinhaça para fertilização. Piracicaba, CODISTIL, Utilização Agrícola da Vinhaça.” *Brasil Açucareiro*, November, vol. 86, pp. 11-17. Brazil.

37. Goldemberg, J., S.T. Coelho, and P. Guardabassi (2008). “The sustainability of ethanol production from sugarcane.” *Energy Policy*, **36**(6): p. 2086-2097.

38. Gonçalves, Cristiane, “Tratamento físico-químico da vinhaça.” XXVII Congresso Interamericano de Engenharia Sanitária e Ambiental. http://www.cepis.org.pe/bvsaidis/aresidua/i-021.pdf (Accessed on January 03, 2008). Brazil.

39. Gonçalves, Tatiana Diniz (2007). “Geoprocessamento como ferramenta de apoio à gestão dos recursos hídricos subterrâneos do Distrito Federal.” MS Thesis, Universidade de Brasília, Brasília, DF, Brazil.

40. Gunduz, Orhan (2004). “Coupled Flow and Contamination Transport Modeling in Large Watersheds.” PhD Dissertation, Georgia Institute of Technology, Georgia, USA.

41. Gluhoi, Andreea Catalina (2005). “Fundamental studies focused on understanding of gold catalysis.” Doctoral Thesis, Leiden University, Netherlands.

42. Halley, James (2002). “Watershed management and riparian buffer analyses using remotely sensed data.” MS Thesis, Civil Engineering, North Carolina State University, North Carolina, USA.

43. Hugot, Émile (1969). “Sucrerie de canne.’ Vol-2, Ed Dunod; Ingénieur des Arts et Manufactures. Elsevier Publishing Co.: Amsterdam, 1960. Netherlands

44. Hyuk, Jin Oh (2004). “Selective catalytic reduction (SCR) of nitric oxide (NO) with ammonia over vanadia-based and pillared interlayer clay-based.” MS Thesis, Texas A & M University, Texas, USA.

45. Jayaram, V. (2005). “Capture of elemental mercury in a wet membrane plasma enhanced electrostatic precipitator using hydrochloric acid as the reagent gas”. MS Thesis, Ohio University.

46. Karanjekar, R. (2012). "An improved model for predicting methane emissions from landfills based on rainfall, ambient temperature and waste composition". PhD Dissertation, The University of Texas at Arlington, Texas, USA.

47. Khezami, L., Chetouani, A., Taouk, B., Capart, R. (2005), “Production and characterisation of activated carbon from wood components in powder: Cellulose, lignin, xylan”. *Powder Technology*, 157 (1), p.48-56, France.

48. Khatri, Rajesh A. (2005). “In situ infrared study of adsorbed species during catalytic oxidation and carbon dioxide adsorption.” PhD Dissertation, University of Akron, Ohio, USA.

49. Kongara, Veera (2006). “Nonlinear Stability Analysis of Viscous Newtonian and Non-Newtonian Viscous-Elastic Sheets.” MS Thesis, University of Cincinnati, Ohio, USA.

50. Korndorfer, GH and Anderson, DL (1997). “Use and impact of sugar alscohol residues vinasse and filtercake on sugarcane production.” *Sug y Azucar* 92: 26-35.

51. Koziel, J.A., L. Cai, D. Wright, S. Hoff. (2006). “Solid phase microextraction as a novel air sampling technology for improved, GC-Olfactometry-based, assessment of livestock odors.” *Journal of Chromatographic Science*, 44(7), 451-457.

52. Krivanek, CS (1996). “Mercury control technologies for MWC's: The unanswered questions”, *Journal of Hazardous Materials*, Volume 47, Issues 1-3, May 1996, Pages 119-136, Municipal Waste Incineration

53. Lau, Ngai Ting (2006). “Catalytic reduction of sulfur dioxide and nitric oxide. The Institute for Environment and Sustainable Development.” The Hong Kong University of Science and Technology. IENV Conference Paper. Hong Kong.

54. Leitão, Renato (2004). “Robustness of UASB Reactors Treating Sewage Under Tropical Conditions.” PhD Dissertation. Wageningen University, Wageningen, Netherlands.

55. Lima, E., Boddey, R. M., and Do¨bereiner, J. (1987). “Quantification of biological nitrogen fixation associated with sugar cane using a 15N aided nitrogen balance.” *Soil Biol*. *Biochem*. 19, 165–170.

56. Lora, Electo E.S. Dr. (2007). "Análise termodinâmica de projetos de cogeração na indústria açucareira e a sua relação com a eficiência em caldeiras". Universidade Federal de Itajubá. II GERA: Workshop de Gestão de Energia e Resíduos na Agroindústria**;** Universidade de São Paulo**,** Brazil.

57. Lu, Qiuli (2006), "Adsorption of Phenolics on Activated Carbon – Impact of Pore Size Distribution", PhD Dissertation, University of Cincinnati, Department of Civil and Environmental Engineering.

58. Luksenberg, J.M., Sá, A., Durso, M.N. (1980). "Processo para a producao de alcool combustivel, sem vinhoto. Relatorio Descritivo da patente de invenção." Dyna Engenharia S.A., São Paulo, Brazil.

59. Magpantay, Gibert Merle (2008). "Photocatalytic Oxidation of Ethanol Using Macroporous Titania." MS Thesis, Louisiana State University, Louisiana, USA.

60. Maness PC, Smolinski S, Blake DM, Huang Z, Wolfrum EJ, Jacoby WA. (1999). "Bactericidal activity of photocatalytic TiO2 reaction: toward an understanding of its killing mechanism." *Appl Environ Microbiol* 65(9):4094–4098.

61. March, Daniel Jackson (2001). "Pollutant Monitoring of Effluent Credit Trading Programs For Agricultural Nonpoint Source Control." MS Thesis, Virginia Polytechnic Institute and State University, Virginia, USA.

62. Marmur, Amit (2006). "Air-quality modeling and source-apportionment of fine particulate matter: implications and applications in time-series health." PhD Dissertation, Georgia Tech University, Georgia, USA.

63. Martinez, Felipe A. (2001), "Polyurethane foam based packing media for biofilters removing volatile organic compounds from contaminated air", MS Thesis, Louisiana State University.

64. Matam, Santhosh Kumar (2005). "On the nature of different Fe sites on Fe-containing micro and mesoporous materials and their catalytic role in the abatement of nitrogen oxides from exhaust gases." PhD Dissertation, Humboldt University, Berlin, Germany.

65. Mistry, Reena (2008). "Characterisation and Applications of CO2-Expanded Solvents." PhD Dissertation, University of Leicester, Leicester, UK.

66. Mochida, I., Korai, Y., Shirahama,M., Kawano, S., Hada, T., Seo, Y., Yoshikawa, M., Yasutake, A. (2000), "Removal of SO_x and NO_x over activated carbon fibers", *Carbon*, 38 (2), p.227-239, Japan.

67. NOBRE, C.A.; MATTOS, L.F.; DERECZYNSKI, C.P.; TARASOVA, T.A. & TROSNIKOV, I.V. Overview of atmospheric conditions during the smoke, clouds and radiation- Brazil (SCAR-B) field experiment. *Journal of Geophysical Research D: Atmospheres*, v. 103, n. 24, p. 31, 809, 31, 820, Dec. 27 1998.

68. Ochoa, Marilyn Viloria (2006). "Analysis of Drilling Fluid Rheology and Tool Joint Effect to Reduce Errors in Hydraulic Calculations." PhD Dissertation, Texas A & M University, Texas, USA.

69. Orlando Filho, J.; Zambello, Jr., E.; Agujaro, R. & Rossetto, A. J. (1983). “Efeito da aplicação prolongada da vinhaça nas propriedades químicas dos solos com cana-deaçúcar.” Estudo exploratório. STAB, *Açúcar*, *Álcool e Subprodutos*, 1(6):28-33. Brazil.

70. Ozdemir, Ekrem (2004), “Chemistry of the adsorption of carbon dioxide by Argonne premium coals and a model to simulate CO_2 sequestration in coal seams”. PhD Dissertation, University of Pittsburgh.

71. Patel, Nikhil (2007). “Studies on the combustion and gasification of concentrated distillery effluent.” PhD Dissertation, Indian Institute of Science, Bangalore, India.

72. Pera Titus, Marc (2007). “Preparation, characterization and modeling of zeolite NaA membranes for the pervaporation dehydration of alcohol mixtures.” PhD Dissertation, UB, Univeritat de Barcelona, Catalonia, Spain.

73. Polack, J.A.; Day, D.F. and Cho, Y.K. (1981). “Gasohol from Sugarcane Stillage Disposition.” *Audubon Sugar Institute*, Louisiana State University, September, p. 47.

74. Porter, J. F., Li, Y. G., and Chan, C. K. (1999). “The effect of calcination on the microstructural characteristics and photoreactivity of Degussa P-25 TiO2.” *J. Materials Science*, 34(7), 1523-1532.

75. Rebouças, A. C. ; Batista, R. P. ; Hassuda, S. ; Cunha, R. C. A. & Poppe, L. M. N. (1986). “Efeitos da infiltração de vinhoto de cana no aquífero de Bauru.” In: *Cong. Brasileiro de Águas Subterrâneas*, SP, pp.184-193. Brazil.

76. Redda, Michael Abraha (2008). “Studies of the performance, stability and reliability of various configurations of the activated sludge process at full-scale municipal wastewater treatment plants.” PhD Dissertation, The University of Texas at Arlington, Texas, USA.

77. Ribas, M.M.F. (2006). “Tratamento de vinhaca em reator anaerobic operado em batelada sequencial contend biomassa imobilizada sob condicoes termofilicas e mesofilicas.” PhD Dissertation, Escola de Engenharia de São Carlos, São Paulo, Brazil.

78. Rivera, E.C., Costa, A.C., Atala, D.I.P., Maugeri, F., Maciel, M.R.W., Maciel Filho, R. (2006). “Evaluation of optimization techniques for parameter estimation: Application to ethanol fermentation considering the effect of temperature.” *Process Biochemistry* 41, 1682-1687.

79. Rosenberk, Ranjith Samuel (2008). “Life cycle assessment of bio-material stabilized expansive soils.” MS Thesis, The University of Texas at Arlington, Texas, USA.

80. Rousseau, Alain N, Quilbé Renaud, Villeneuve Jean-Pierre (2005). “Information technologies in a wider perspective: integrating management functions across the urban–rural interface.” *Environmental Modeling & Software* Volume 20, Issue 4, Pages 443-455.

81. Ro, K.S., Mcconnell, L.L., Johnson, M.H., Hunt, P.G., Parker, D. (2008), Livestock air treatment using PVA-coated powdered activated carbon biofilter. Applied Engineering in Agriculture. 24(6):791-798.

82. Rocha, Mateus H. (2009). "Uso da análise do ciclo de vida para a comparação do desempenho ambiental de quatro alternativas para tratamento da vinhaça". Dissertação de Mestrado; Master of Science Degree Thesis, Universidade Federal de Itajubá, Minas Gerais, Brazil.

83. Saikkonen, Kelly (2006); "Technical and Economic Feasibility of Upgrading Dairy Manure-Derived Biogas for Natural Gas Pipeline", Master of Science Degree Thesis, (2006)Cornell University, USA.

84. Salomon, Karina Ribeiro (2007). "Avaliação Técnico-Econômica e Ambiental da Utilização do Biogás Proveniente da Biodigestão da Vinhaça em Tecnologias para Geração de Eletricidade". Tese de Doutorado; Doctorial Dissertation, Universidade Federal de Itajubá, Minas Gerais, Brazil.

85. Sánchez B., Coronado J.M., Candal R., Portela R., Teje-dor I., Anderson M.A., Tompkins D., Lee T. (2006). “Preparation of TiO2 Coatings on PET Monoliths for the Photocatalytic Elimination of Trichloroethylene in the Gas Phase.” *Appl*. *Catal. B.* 66 (3-4), 295-301.

86. Sattler, Melanie, Ph.D., P.E. (2011). "Anaerobic Processes for Waste Treatment and Energy Generation". Iniversity of Texas at Arlington, Texas, USA.

87. Schroeder, B. L., Robinson, J. B., Wallace, M., and Turner, P. E. T. (1994). “Soil acidification: Occurrence and effects in the South African sugar industry.” *Proc. S. Afr*. *Sugar Technol*. *Assoc*. 70–74.

88. Singh-Jutla, Antarpreet, (2006). “Hydrological Modeling of Reconstructed Watersheds using a System Dynamics Approach.” MS Thesis, University of Saskatchewan, Saskatchewan, Canada.

89. Silva, Mellissa A. S. da, Griebeler, Nori P., Borges, Lino C. (2007)."Use of stillage and its impact on soil properties and groundwater." Rev. *Bras*. *eng*. *agríc*. *Ambient*, vol.11, no.1. Brazil.

90. Silva, G. M. A. & Orlando Filho, J. (1981). “Caracterização da composição química dos diferentes tipos de vinhaça no Brasil.” Bol. Tec. *Planalsucar*, 3(8):5-22. Brazil.

91. Somy, A. *et al* (2009), “Adsorption of carbon dioxide using impregnated activated carbon promoted by Zinc.” *International Journal of Greenhouse Gas Control,* 3 (3), p.249-254.

92. Taraba, J.L., Heaton, L. M., Ilvento, T. W. (2001), “Water quality in Kentucky: using activated carbon filters to treat home drinking water”, Agricultural Engineering Department, IP 6, Issued: 9-90, Revised.

93. Tauk, S. M. (1987). “Efeito de doses cumulativas de vinhaça em algumas propriedades do solo sob cerrado e do solo de culturas do milho e cana-de-açúcar no

município de Corumbataí, SP." PhD Dissertation, Instituto de Biociências, Universidade Estadual Paulista, São Paulo, Brazil.

94. Teixeira, C. M. L. L.; Morales, E**. (**2006**). "**Microalga como matéria-prima para a produção de biodiesel. In: I Congresso da Rede Brasileira de Tecnologia de Biodiesel." 2006, Brasília, DF: MCT/ABIPT, p.91-96. Brazil.

95. Tekin, T.; Bayramoglu, M., (2001). "Exergy and structural analysis of raw juice production and steam-power units of a sugar production plant." *Energy*, 26, 287-297.

96. Thwaites, M. W., McEnaney, B., Botha, F., D., McNeese, B. E., Sumner, M. B. (2006), "Synthesis and characterization of activated pitch-based carbon fibers". University of Kentucky , Center for Applied Energy Research and Ashland Carbon Fibers Division, Ashland, KY.

97. Turner, PE, Meyer, JH and King AC (2002). "Field Evaluation of concentrate molasses stillage as a nutrient source for sugarcane in Swaziland." *Proc S Afr Sug Technol Assc* 76:61-69. South Africa.

98. Tseng, R.L. (2006), **"**Mesopore control of high surface area NaOH-activated carbon"**,** *Journal of Colloid And Interface Science*, 303 (2), p.494-502, Taiwan.

99. Van Greunen, Larey-Marie (2006). "Selection of air pollution control technologies for power plants, gasification and refining processes." MS Thesis, University of Pretoria, Gauteng, South Africa.

100. Vazoller, R.F. (1997). "Microbial aspects of thermophilic anaerobic biodigestion of vinasse." *Novel Trends in Biological Wastewater.* 527-532.

101. Vogel, Jason R., Majewski, Michael S., Capel, Paul D. (2008). "Pesticides in Rain in Four Agricultural Watersheds in the United States." *J Environ Quality*, 37: 1101-1115.

102. Voinov, A., Fitz, C., Boumans, R., and Constanza, R. (2004). "Modular ecosystems modeling." *Environmental Modeling and Software*, 19:285-304.

103. Viana, A.B. (2006). "Tratamento termofilico da vinhaca em reator UASB." 60p. MS Thesis, Universidade de São Paulo – Escola de Engenharia de São Carlos. São Paulo, Brazil.

104. Wald, Matthew L. (2006). "Corn Power Put to the Test- New York Times." The New Your Times- Breaking News, Workd News & Multimedia. 7 Feb. 2006. 11. Aug 2009 http://www.nytimes.com/2006/02/07/science/07fuel.html (Accessed on August 2009).

105. Walker, John Thomas (2005). "Atmospheric chemistry and air/surface exchange of ammonia in an agricultural region of the southeast United States." PhD Dissertation, North Carolina State University, North Carolina. USA.

106. Wilkie, A. C., Riedesel, K.J., Owens, J.M. (2000). "Stillage characterization and anaerobic treatment off ethanol stillage from conventional and cellulosic feedstocks." *Biomass and Bioenergy*, 19, p. 63 - 102.

107. Yang, Jiun-Chan (2007). “Nanoporous zeolite and solid-state electrochemical devices for nitrogen-oxide sensing.” PhD Dissertation, Ohio State University, Ohio. USA.

.

BIOGRAPHICAL INFORMATION

Lucina Márcia-Affonso-de-Mello Kuusisto earned her bachelor's degree in Chemical Engineering from the Universidade Federal de Pernambuco, Brazil. As a Chemical Engineering Intern, she acquired practical training in an ethanol distillery, in Jaboatão, Brazil. Later, Márcia attended Texas Tech University, from where she earned her Master of Science degree. The focus of her master's degree coursework was in Water Resources Engineering. She considers Water Resources Engineering a very fascinating field. Manufacturing engineering logistics, renewable energy, and environmental health are other fields of interest to her. After earning her PhD, Márcia intends to work with the scientific community of Brazil and the United States.